

ACTIVATED CARBON PRODUCTION FROM PRETREATED AND FERMENTED
AGRICULTURAL RESIDUES

by

HACER YILDIRIM

BS. in Environmental Engineering, Kocaeli University, 2008

Submitted to the Institute of Environmental Sciences in partial fulfillment of
the requirements for the degree of
Master of Science
in
Environmental Technology

Boğaziçi University

2016

ACKNOWLEDGEMENTS

First of all, I would like to express my deepest gratitude to my thesis supervisor, Assoc. Prof. Dr. Nilgün Cılız, for her guidance, valuable comments, encouragement, and support throughout the study. I am grateful to have the chance to work with her.

I am very grateful to my thesis committee members, Prof. Dr. Ferhan Çeçen and Assoc. Prof. Dr. Moiz Elnkave, sparing their valuable time for commenting on my thesis.

The financial support for this study was provided by The Scientific and Technological Research Council of Turkey (Project No: 110Y261) and Boğaziçi University Scientific Research Projects Support (Project No: 7182) and is appreciated.

I would like to thank my dear friend, Başak Daylan for her unlimited support and presence in the complete process. Her help allowed me to overcome the challenges of the experimental path of the study. I am very thankful to my friends, Lalehan Salar and Merve Harmankaya for their friendship and patience against my complaints during my study. I also wish to express my special thanks to my colleagues from Boğaziçi University Sustainable Development and Cleaner Production Center for their support and friendship.

Last but not least, I want to express my sincere gratefulness to my family for their endless support, understand and encouragement. Their support, motivation, faith and love guided me my entire life and through this process.

ACTIVATED CARBON PRODUCTION FROM PRETREATED AND FERMENTED AGRICULTURAL RESIDUES

All forms of lignocellulosic biomass consist of three major chemical components: cellulose, hemicellulose and lignin. The remaining lignin from bioethanol production can be utilized as a feedstock for green chemicals. The purpose of this study was to produce activated carbon from pretreated and fermented agricultural residues and to investigate the influence of different process conditions such as feedstock type, impregnation ratio, and carbonization temperature on the pore structure of the products. This is the first study that investigated the production of activated carbon as a high value-added product from lignin-rich residues generated from bioethanol processes.

The first step in the experimental path of the study was the recovery of lignin-rich biomass samples. Four samples were prepared from ethanol production wastes; the first one was from the pretreatment of corn stover, the second one was from pretreatment of wheat straw, the third one was from fermentation of corn stover, and the fourth one was from fermentation of wheat straw. The second step was the chemical characterization of feedstocks. In the third step, feedstocks were impregnated with 30%, 40% and 50% (w/w) H_3PO_4 and then carbonized with a rate of $20^\circ\text{C}/\text{min}$ to carbonization temperatures of 400°C , 500°C , 600°C and 700°C . The N_2 adsorption/desorption capacities of products were compared according to their specific surface area and pore volume by applying the Brunauer-Emmett-Teller (BET) equation.

The results demonstrated that the best way to produce activated carbon from lignin-rich residue was using pretreated wheat-based lignin, which was impregnated with 40% H_3PO_4 concentration and carbonized at 700°C . In addition, both pretreated corn and fermented wheat-based products, which were impregnated with 50% H_3PO_4 and carbonized at 500°C , had quite well developed specific surface area. Interestingly, mesoporous structures dominate in H_3PO_4 -impregnated lignocellulosic material-based activated carbon. Therefore, these carbons are ideal for the adsorption of large molecules and decolorization.

TARIMSAL ATIKLARIN ÖN ARITIMI VE FERMENTASYONU SONUCU OLUŞAN PROSES KALINTISINDAN AKTİF KARBON ÜRETİMİ

Doğal biyokütlede bulunan başlıca bileşikler selüloz, hemiselüloz ve lignindir. Lignoselülozik biyokütleden biyoetanol üretimi sonucu elde edilen proses kalıntısı potansiyel lignin kaynağı olarak görülmektedir. Bu çalışmanın amacı, seçilen tarımsal atıklardan (mısır sapı/püskülü ve buğday samanı) laboratuvar ölçekli biyoetanol üretimi sonucu oluşan lignince zengin proses kalıntısından piroliz yöntemi ile aktif karbon üretiminde hammadde, impregnasyon oranı ve karbonizasyon sıcaklığı gibi farklı proses şartlarının ürün fiziksel özelliklerine etkisinin araştırılmasıdır.

Çalışmanın deneysel kısmının ilk kademesinde, lignince zengin proses kalıntısından ligninin ekstraksiyonu gerçekleştirilmiştir. Çalışmada, mısır sapı/püskülünün ön arıtımı sonrası elde edilen lignin, buğday samanının ön arıtımı sonrası elde edilen lignin, mısır sapı/püskülünün fermentasyonu sonrası elde edilen lignin ve buğday samanının fermentasyonu sonrası elde edilen lignin olmak üzere dört farklı hammadde kullanılmıştır. Deneysel çalışmaların ikinci kademesinde, belirlenen hammaddelerden farklı kimyasal aktivasyon koşulları (kütlece %30, %40 ve %50 H_3PO_4) ve farklı karbonizasyon sıcaklıklarında (400°C, 500°C, 600°C ve 700°C) aktif karbon üretimi gerçekleştirilmiştir. Üretilen aktif karbon numuneleri azot gazı adsorpsiyonu ile karakterize edilerek Brunauer-Emmett-Teller (BET) spesifik yüzey alanları ve gözenek hacimleri açısından karşılaştırılmış ve en uygun şartlar belirlenmiştir.

Çalışmanın sonucunda buğday samanının ön arıtımı sonucu ekstrakte edilen lignin kullanılarak kütlece %50 emdirme oranı ve 700°C karbonizasyon sıcaklığında elde edilen aktif karbonun en geniş yüzey alanı ve gözenek hacmine sahip olduğu görülmüştür. Bununla birlikte, mısır sapı/püskülünün ön arıtımı ve buğday samanının fermentasyonu sonrası ekstrakte edilen lignin kullanılarak üretilen aktif karbonlar için en uygun şartlar kütlece %50 H_3PO_4 emdirme oranı ve 500°C karbonizasyon sıcaklığı olarak belirlenmiştir.

Bu çalışma, tarımsal atıklardan biyoetanol üretimi sırasında ortaya çıkan lignince zengin kalıntılardan aktif karbon üretilerek, yan ürünlerin değerli kimyasal olarak değerlendirilmesini araştıran ilk çalışma olmuştur. Üretilen aktif karbonların mezopor hacimlerinin mikropor hacimlerine göre daha yüksek olduğu gözlenmiş ve bu ürünlerin büyük moleküllü kirleticilerin adsorpsiyonu ve renk giderimi için uygun olduğu sonucuna ulaşılmıştır.

TABLE OF CONTENTS

ACKNOWLEDGEMENTS	iii
ABSTRACT	iv
ÖZET	v
TABLE OF CONTENTS	vii
LIST OF FIGURES	x
LIST OF TABLES	xiii
LIST OF SYMBOLS/ABBREVIATIONS	xvi
1. INTRODUCTION	1
2. LITERATURE REVIEW	3
2.1. Agricultural Residues	3
2.1.1. Potential Agricultural Residues for Bioethanol Production	3
2.1.2. Chemical Structure and the Basic Components of Lignin	5
2.1.3. Lignin Based Products in Certain Industries	7
2.2. Biomass Pyrolysis as a Recovery Technology	8
2.3. Activated Carbon	10
2.3.1. Classification of Activated Carbon	11
2.3.2. Application of Activated Carbon	12
2.3.3. Production of Activated Carbon	13
2.3.3.1. Chemical activation	14
2.3.3.2. Physical activation	15
2.4. Adsorption	16
2.4.1. Factors Influencing Adsorption	17
2.4.2. Gas Adsorption Phenomena and Standard Isotherms	18
2.4.2.1. Brunauer, Emmett and Teller (BET) theory	19
2.5. Summary of the Previous Studies Performed for Producing Activated Carbon	21
3. MATERIALS AND METHODS	26
3.1. Main Steps of the Study	26

3.2.	The Selected Feedstocks	28
3.3.	Characterization of Raw Feedstock	29
3.3.1.	Preparation of Biomass Sample	30
3.3.2.	Proximate Analysis of Raw Feedstocks	30
3.3.2.1.	Determination of total solids	30
3.3.2.2.	Determination of ash	31
3.3.2.3.	Determination of extractives	32
3.3.3.	Wet Chemical Analysis of Feedstock	34
3.3.3.1.	Determination of acid insoluble and acid soluble lignin content	34
3.4.	Feedstock Preparation for Activated Carbon Production	36
3.4.1.	Preparation of Pretreated Based Feedstock	36
3.4.2.	Preparation of Fermented Based Feedstock	39
3.5.	Characterization of the Processed Feedstocks	40
3.5.1.	Thermogravimetric Analysis of Processed Feedstocks	41
3.6.	Production of Activated Carbon Samples	41
3.7.	The characterization of the produced activated carbon	45
3.7.1.	Char Yield and Chemical Recovery Value of Produced Activated Carbon	45
3.7.2.	Determination of the pH	46
3.7.3.	Brunauer-Emmett-Teller (BET) Surface Area of Products	46
3.7.4.	Pore Analysis by Adsorption/Desorption	47
4.	RESULTS AND DISCUSSION	48
4.1.	Feedstock Characterization	48
4.1.1.	Proximate Analysis of Feedstocks	48
4.1.1.1.	Raw lignocellulosic materials	48
4.1.1.2.	Lignin-rich residue generated from pretreatment	49
4.1.1.3.	Lignin-rich residue generated from fermentation	50
4.1.2.	Determination of Extractives	51
4.1.3.	Determination of Lignin Content of Feedstocks	52
4.1.3.1.	Raw lignocellulosic materials	52
4.1.3.2.	Lignin-rich residue generated from pretreatment	52
4.1.3.3.	Lignin-rich residue generated from fermentation	53
4.2.	Thermogravimetric Analysis of Proceeded Feedstocks	55
4.2.1.	TGA Analysis of Pretreated Feedstocks	55

4.2.2. TGA Analysis of Fermented Feedstocks	57
4.3. The Effect of Different Process Conditions on Yield and Chemical Recovery	59
4.4. pH of Produced Activated Carbon	66
4.5. Ash Content of Produced Activated Carbon	69
4.6. The Influence of Different Process Conditions on the BET Surface Area	70
4.6.1. PC-Based Activated Carbon	71
4.6.2. PW-Based Activated Carbon	73
4.6.3. FC-Based Activated Carbon	74
4.6.4. FW-Based Activated Carbon	76
4.7. Influence of Different Process Conditions on Pore Volume	77
5. CONCLUSIONS	82
REFERENCES	87

LIST OF FIGURES

Figure 2.1. Generic diagram of fuel ethanol production from lignocellulosic biomass	5
Figure 2.2. Schematic diagram for lignin distribution in biomass	6
Figure 2.3. Schematic representation of the pore network of a carbon adsorbent	11
Figure 2.4. Classification of activated carbons in terms of physical properties	12
Figure 2.5. Five main types of adsorption isotherms	19
Figure 2.6. Linear forms for graphical representation of BET equation	21
Figure 3.1. General scheme for the characterization of the raw feedstocks	29
Figure 3.2. Corn stover and wheat straw before and after milling	30
Figure 3.3. Soxhlet extraction set up for extractive determination	33
Figure 3.4. The schematic representation of the two-stage delignification process	37
Figure 3.5. Lignin precipitation from black liquor	39
Figure 3.6. The lignin rich-residue obtained from filtration	39
Figure 3.7. Residue separation after SSF	40
Figure 3.8. PC, PW, FC, and FW samples used for activated carbon production	40
Figure 3.9. General scheme for the characterization of the processed feedstocks	41

Figure 3.10. General scheme for production of activated carbon	43
Figure 3.11. Experimental set-up for carbonization	44
Figure 3.12. Activated carbon produced from lignin rich-residue	45
Figure 3.13. The types of adsorption-desorption hysteresis loops	47
Figure 4.1. Typical Thermogravimetric Analysis diagram of PC samples	55
Figure 4.2. Typical Thermogravimetric Analysis diagram of PW samples	56
Figure 4.3. Typical Thermogravimetric Analysis diagram of lignin-rich residue from FC samples	57
Figure 4.4. Typical Thermogravimetric Analysis diagram of lignin-rich residue from FW samples	58
Figure 4.5. The effect of process conditions on yield for PC-based activated carbon	60
Figure 4.6. The effect of process conditions on C.R. for PC-based activated carbon	61
Figure 4.7. The effect of process conditions on yield for PW-based activated carbon	62
Figure 4.8. The effect of process conditions on C.R. for PW-based activated carbon	62
Figure 4.9. The effect of process conditions on yield ratio for FC-based product	63
Figure 4.10. The effect of process conditions on C.R. ratio for FC-based product	64
Figure 4.11. The effect of process conditions on yield ratio for FW-based product	65
Figure 4.12. The effect of process conditions on C.R. ratio for FW-based product	65

Figure 4.13. The effect of process conditions on pH ratio for PC-based product	68
Figure 4.14. The effect of process conditions on pH ratio for PW-based product	68
Figure 4.15. The effect of process conditions on pH ratio for FC-based product	68
Figure 4.16. The effect of process conditions on pH ratio for FW-based product	69
Figure 4.17. An example to multi-point BET of produced activated carbon	71
Figure 4.18. The effect of process conditions on BET surface area for PC-based product	73
Figure 4.19. The effect of process conditions on BET surface area for PW-based product	74
Figure 4.20. The effect of process conditions on BET surface area for FC-based product	75
Figure 4.21. The effect of process conditions on BET surface area for FW-based product	77
Figure 4.22. N ₂ adsorption/desorption isotherms of sample PC5	79
Figure 4.23. N ₂ adsorption/desorption isotherms of sample PW10	80
Figure 4.24. N ₂ adsorption/desorption isotherms of sample FW5	81

LIST OF TABLES

Table 2.1. Quantities of agricultural waste available for bioethanol production	4
Table 2.2. Chemical structures of three primary monomers of lignocellulosic biomass	7
Table 2.3. Possible products from lignin transformations	8
Table 3.1. Methodology of the project (Project No. ÇAYDAG-110Y261)	27
Table 3.2. The content of mixtures for first pretreatment step	37
Table 3.3. The content of mixtures for second pretreatment step	38
Table 3.4. Experimental conditions for activated carbon production	44
Table 4.1. Proximate analysis of raw corn stover	49
Table 4.2. Proximate analysis of raw wheat straw	49
Table 4.3. Proximate analysis of PC residue	50
Table 4.4. Proximate analysis of PW residue	50
Table 4.5. Proximate analysis of FC residue	50
Table 4.6. Proximate analysis of FW residue	50
Table 4.7. Extractive content of corn stover samples	51
Table 4.8. Extractive content of wheat straw samples	51

Table 4.9. Lignin content of raw corn stover samples	52
Table 4.10. Lignin content of raw wheat straw	52
Table 4.11. Lignin content of PC residue	52
Table 4.12. Lignin content of PW residue	53
Table 4.13. Lignin content of FC residue	53
Table 4.14. Lignin content of FW residue	53
Table 4.15. Characteristics of all feedstocks	54
Table 4.16. Temperature range and weight loss of PC samples	56
Table 4.17. Temperature range and weight loss PW samples	57
Table 4.18. Temperature range and weight loss of lignin-rich residue from FC samples	58
Table 4.19. Temperature range and weight loss of of lignin-rich residue FW samples	59
Table 4.20. Yields and C.R. ratios for PC-based activated carbon	60
Table 4.21. Yields and C.R ratios for PW-based activated carbon	61
Table 4.22. Yields and C.R ratios for FC-based activated carbon	63
Table 4.23. Yields and C.R ratios for FW-based activated carbon	64
Table 4.24. pH values of the activated carbon samples	67
Table 4.25. Ash content of produced activated carbon samples	70

Table 4.26. BET surface areas for PC-based activated carbon samples	72
Table 4.27. BET surface areas of PW-based activated carbon	74
Table 4.28. BET surface areas of FC-based samples	75
Table 4.29. BET surface areas of FW-based samples	76
Table 4.30. Porosity analysis for produced activated carbon	78

LIST OF SYMBOLS/ABBREVIATIONS

Symbol	Explanation	Units
AIL	Acid insoluble lignin	%
AIR	Acid insoluble residue	%
ASL	Acid soluble lignin	%
ASTM	American Society for Testing and Materials	
BET	Brunauer-Emmett-Teller	
BTX	Benzene, toluene, and xylene	
CO	Carbon monoxide	
CO ₂	Carbon dioxide	
C ₂ H ₆	Ethane	
(C ₅ H ₈ O ₄) _m	Hemicellulose	
(C ₆ H ₁₀ O ₅) _x	Cellulose	
[C ₉ H ₁₀ O ₃ .(OCH ₃) _{0.9-1.7}] _n	Lignin	
C.R.	Chemical recovery	
Dp	Average pore diameter	nm
DTG	Derivative thermogravimetry	
EAC	Extruded activated carbon	EAC
Ext.	Extractive Content	%
FC	The lignin residue derived from the fermented corn stover	
FW	The lignin residue derived from the fermented wheat straw	
GAC	Granular activated carbon	
h	Hour	h
H ₂	Hydrogen	
H ₂ SO ₄	Sulphuric acid	%
H ₃ PO ₄	Phosphoric acid	%
I.R.	Impregnation ratio	%

IUPAC	International Union of Pure and Applied Chemistry	
KOH	Potassium hydroxide	
LAP	Laboratory analytical procedure	
mL	Milliliter	
Mtons	Million tones	
NaOH	Sodium hydroxide	%
N ₂	Nitrogen gas	mL/min
NaOH	Sodium hydroxide	%
NREL	National renewable energy laboratory	
ODW	Oven dried weight	g
PAC	Powdered activated carbon	PAC
PC	The lignin residue derived from the pretreated corn stover	
PW	The lignin residue derived from the pretreated wheat straw	
RC	Raw corn stover	
RW	Raw wheat straw	
S _{BET}	BET surface area	m ² /g
S _{micro}	Micropore area	m ² /g
TGA	Thermogravimetric analysis	
TS	Total solids	%
V _{meso}	Mesopore volume	cm ³ /g
V _{micro}	Micropore volume	mm ³ /g
VS	Volatile solids	%
V _T	Total pore volume	cm ³ /g
(v/v)	Volume/volume	
(w/w)	Weight/weight	%
ZnCl ₂	Zinc chloride	ZnCl ₂

1. INTRODUCTION

Production of renewable fuels holds remarkable potential to meet the current energy demand of the world. The transportation sector is 95% dependent on fossil fuel and responsible for 61% of the world oil consumption. Furthermore, demand for oil will increase by around 0.8% each year until 2035 (BP Energy Outlook 2035, 2015). Oil consumption for transportation is a significant contributor to greenhouse gas emissions, accounting for about 23% of global carbon dioxide (CO₂) emissions (IEA, 2013). In this context, depleting natural resources, growing environmental awareness and economic considerations are the major driving forces to produce biofuels, especially bioethanol from renewable resources such as lignocellulosic materials as a potential alternative to petroleum-derived transportation fuel.

Ethanol, used in the production of transport fuels, is one of the products obtained from biomass. After cellulose and hemicellulose, lignin is considered to be the most abundant natural polymer present on Earth and is found in the range of 25-35% (w/w) in dry wood (Foyle et al., 2007). During ethanol production, cellulose and hemicellulose turn to ethanol, but lignin is removed from the system as a waste in large quantities. In order to meet the goal to replace 30% of fossil fuels by biofuels by 2030, about 227 cubic hectometer (hm³) of bioethanol will be needed, which would generate around 225 million tones (Mtons) of lignin (Cotana et al., 2014). Therefore, development of value-added products from lignin is considered of utmost importance in order to achieve sustainable economy and to reduce carbon footprint. Since environmental considerations have been one of the most important factors affecting the potential market for lignin-based products, lignin transformation technologies have been progressing. Although there are a number of studies on alternative products from lignin residue, there is still room for improvement, and it is necessary to develop the production methodologies with respect to lignin utilization. These technologies are based on the recovery of valuable chemicals from lignin and their potential application in biorefinery operations.

The aim of this study was to produce activated carbon from lignin-rich residue and to investigate the influence of different process conditions such as feedstock type, impregnation ratio, and carbonization temperature on the pore structure of the products. For this purpose,

experiments were conducted in a horizontal pyrolysis furnace to produce activated carbon from different types of feedstocks derived from lignin-rich corn stover and wheat straw residues subjected to dilute acid/steam pretreatment processes, and saccharification and fermentation processes. The products were analyzed for the values of specific surface area, pore structure, yield and chemical recovery in order to evaluate process performances. The material and methods used in this study are explained in detail in Section 3. The results are discussed in Section 4.

2. LITERATURE REVIEW

The literature review has been divided into four main sections: agricultural residues, pyrolysis of biomass, activated carbon and adsorption.

2.1. Agricultural Residues

2.1.1. Potential Agricultural Residues for Bioethanol Production

Agricultural residues are potentially major contributors of resources for energy and material production. Depending on their properties, they are used in different branches of the food, forestry, construction, energy, medicine and chemical industries (Dalla Marta et al., 2014). Only a small portion of globally produced agricultural residues is used as animal feed, the rest is removed from the field by burning or disposed of as waste, a common practice all over the world (Gupta and Verma, 2015). They do not have food value like energy crops as well. Hence, lignocellulosic biomass has been projected to be one of the main resources for economically attractive bioethanol production.

The world bioethanol production in 2008 was about 66 billion liters. It has grown to 88 billion liters in 2013 and it was expected to reach 90 billion liters in 2014 (Gupta and Verma, 2015). Kim and Dale (2004) reported that 491 billion liters of bioethanol can be produced from crop residues and waste crops per year, about five times higher than the actual world bioethanol production. The most favorable agricultural residues for bioethanol production are rice straw, corn stover, wheat straw and baggase due to their availability throughout the year (Sarkar et al., 2012). Turkey is an agricultural country and thus it has important forestry potential. In Turkey, corn stover and wheat straw are the most abundant agrowastes compared to other major wastes. Worldwide production of these agricultural residues is presented in Table 2.1.

Table 2.1. Quantities of agricultural waste available for bioethanol production (Sarkar et al., 2012; Başçetinçelik et al., 2005).

Agricultural Waste, million tons	Africa	Asia	Europe	America	Oceania	Turkey
Rice Straw	20.9	667.6	3.9	37.2	1.7	0.18
Wheat straw	5.34	145.20	132.59	62.64	8.57	3.5
Corn stover	0	33.90	28.61	140.86	0.24	4.13
Bagasse	11.73	74.88	0.01	87.62	6.49	-

The process of bioethanol production from lignocellulosic materials consists of several steps: milling, pretreatment, enzymatic hydrolysis, fermentation with yeast and distillation (Figure 2.1). The pretreatment is the initial process for separation of free cellulose from residues. Under pretreatment process, the lignocellulosic matrix breaks down to reduce the degree of crystallinity of the cellulose and increase the part of amorphous cellulose. This form of cellulose is the most suitable form for enzymatic hydrolysis. After pretreatment, cellulose is hydrolyzed to fermentable sugars including glucose, xylose, arabinose, galactose and mannose by enzymes. Fermentation of the saccharified biomass can be performed with diverse microorganisms. Yeast strains were developed for fermentation of both sugars, glucose and xylose. The product is recovered from fermentation broth via distillation. Lignin rich residue remains a residual by product (Kahr et al., 2013).

In bioethanol production process, lignin restricts hydrolysis by enzymes and the affinity between lignin and cellulose prevents affecting enzyme accessibility to the cellulose. In order to enhance this situation, lignin can be removed from the process after hydrolysis. Each ethanol production process has lignin as a residue since it is presented in all lignocellulosic biomass and thus it is used as a co-product of lignocellulosic bioethanol industries or as a feedstock in production of value-added products.

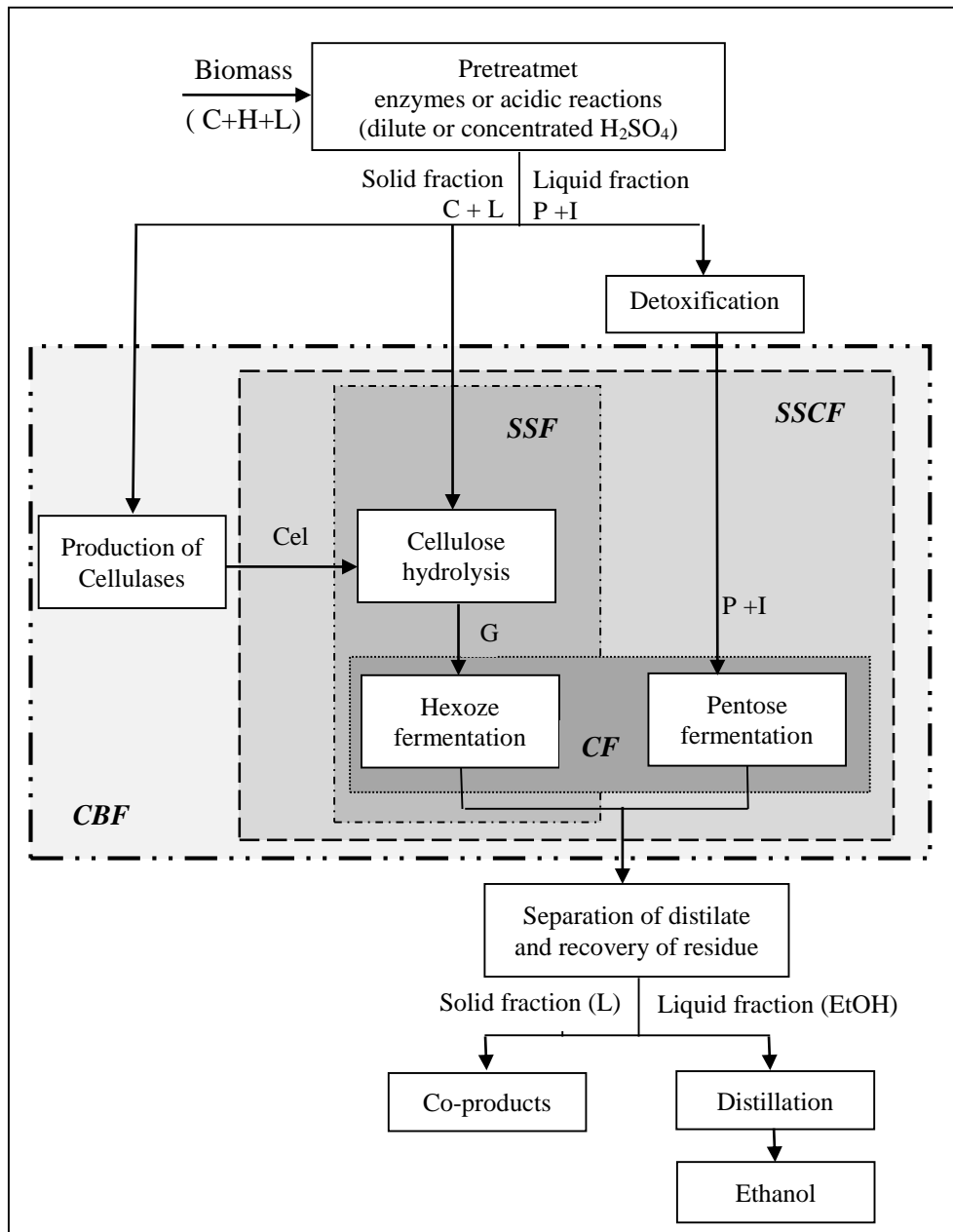


Figure 2.1. Generic diagram of fuel ethanol production from lignocellulosic biomass (Cardona and Sanchez, 2007).

CF, co-fermentation; CBP, consolidated bioprocessing. Main stream components: C, cellulose; H, hemicellulose; L, lignin; Cel, cellulases; G, glucose; P, pentoses; I, inhibitors.

2.1.2. Chemical Structure and the Basic Components of Lignin

The chemical structure and major organic components in biomass are extremely important in the development of processes for producing derived fuels and chemicals. Lignocellulosic biomass is mostly cell wall material that is composed of three principal

components: cellulose, hemicellulose, and lignin. Cellulose ($C_6H_{10}O_5$)_x is the predominant polymer within the range 35-50% (w/w). Hemicellulose ($C_5H_8O_4$)_m is found within the range 20-35% (w/w) in lignocellulosic biomass. Lignin [$C_9H_{10}O_3(OCH_3)_{0.9-1.7}$]_n is the second most abundant natural polymer after cellulose and the largest renewable source of aromatics on earth (Mansouri et al., 2011). The lignin contents on a dry basis in both softwoods and hardwoods generally range from 20% to 40% by weight and from 10% to 40% by weight in various herbaceous species, such as bagasse, corncobs, peanut shells, rice hulls and straws. As seen in Figure 2.2, the cell wall is comprised of several layers in which lignin concentration systematically decreases from the outer layers including middle lamella (ML) and primary wall (P), to the inner layers including secondary wall, S1, S2, and S3. The thicknesses of the layers are approximately 0.1 mm for S1 and S3, and 0.6 mm for S2 (Azadi et al., 2013).

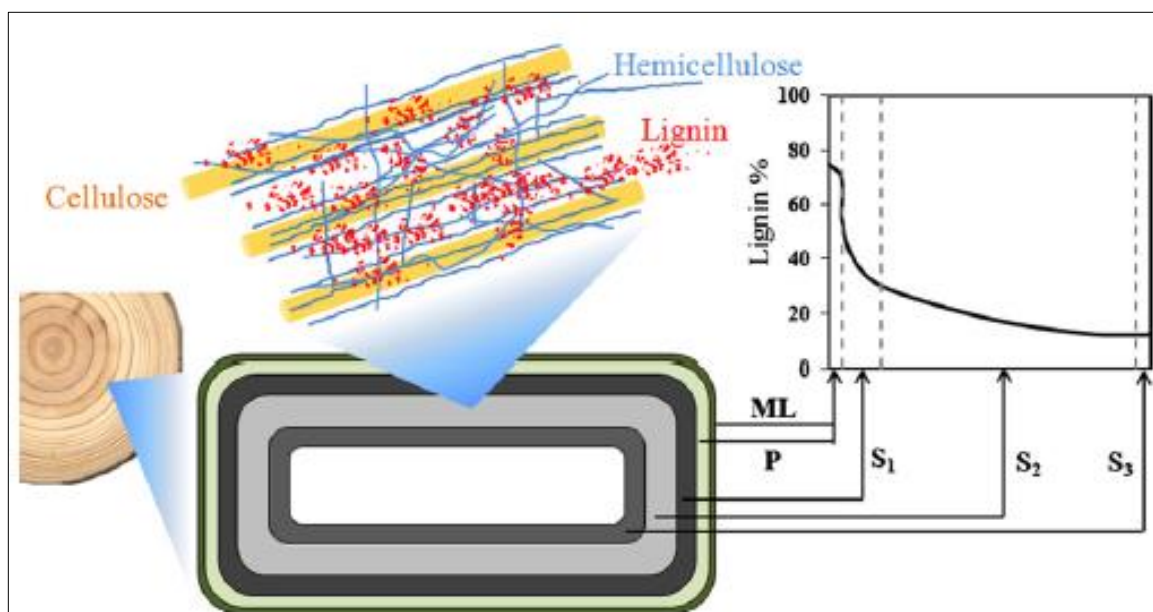
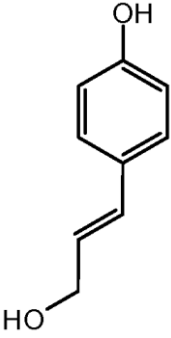
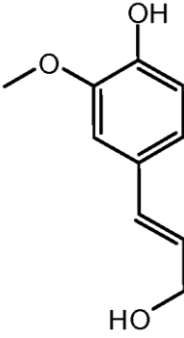
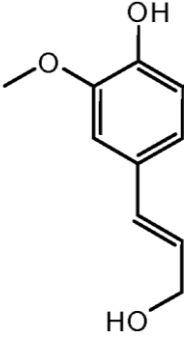


Figure 2.2. Schematic diagram for lignin distribution in biomass (Azadi et al., 2013).

Lignin is a heterogeneous polymer with a three-dimensional structure: p-hydroxyphenyl (H), guaiacyl (G), and syringyl (S) alcohols as shown in Table 2.2. The compositional variations in these units depend upon the type of biomass feedstocks like hardwood, softwood, and herbaceous biomass (Jung et. al, 2015; Azadi et al, 2013). As listed in Table 2.2, corn stover lignin and wheat straw lignin contain all of three monolignol units in

significant amounts which are 4%, 35%, and 61% of corn lignin, and 5%, 49%, and 46% of wheat lignin, respectively (Buranov and Mazza, 2008).

Table 2.2. Chemical structures of three primary monomers of lignocellulosic biomass (Buranov and Mazza, 2008).

	p-hydroxyphenyl (H)	Guaiacyl (G)	Syringyl (S)
Phenylpropane unit			
Corn stover lignin, %	4	35	61
Wheat straw lignin, %	5	49	46

2.1.3. Lignin Based Products in Certain Industries

Until now, most commercial lignin has been supplied from paper and pulp industry with an annual production capacity between 40 and 50 Mtons, but the residues from bioethanol production processes could be an additional potential source. In order to meet the goal to replace 30% of fossil fuels by biofuels by 2030, about 227 hm³ of bioethanol will be needed, which would generate around 225 Mtons of lignin (Cotana et al., 2014). Currently, much of the residual lignin produced by the certain industries is often used just for power generation. However, there are some other marginal applications such as an adhesive or tanning agent with the small-scale applications and large scale economic values. The opportunities that arise from utilizing lignin fit into three categories which are;

- heat, fuel and syngas as a carbon sources,
- macromolecules like carbon fiber, polymer modifiers, adhesives and resins,
- aromatics and miscellaneous monomers like BTX (benzene, toluene, and xylene), chemicals, and phenol (Holladay et al., 2007).

An initial list of possible lignin transformation technologies and their products has been summarized in Table 2.3. Among those applications, aromatics commodities that are derived from lignin such as BTX, phenol, and vanillin, are expected to offer a significant market potential with an estimated market value of over \$130 billion. Moreover, pyrolysis technology has drawn attention to opportunities available for converting lignin into these high value-added products (Jung et al., 2015).

Table 2.3. Possible products from lignin transformations (Gosselink et al., 2004; Holladay et al., 2007).

Technology	Value-added product
Pyrolysis	Activated carbon, acetic acid, phenol, substituted phenols, methane
Fast thermolysis	Acetylene, ethylene
Alkali fusion	Phenolic acids
Enzymatic oxidation	Oxidized lignin for paints and coatings
Microbial conversion	Vanilic and ferulic acids
Oxidative	Vanillin, dimethylsulfide
Hydrolysis	Phenol, substituted phenols
Hydrogenation	Phenol, cresols, substituted phenols

Coals and lignocellulosic materials are commonly used as the starting material for preparing activated carbon. As lignin with its considerably similar molecular structure to coal has a high carbon content, it is an ideal precursor and interesting material to utilize in the production of activated carbon via pyrolysis (Suhas and Carrott, 2007).

2.2. Biomass Pyrolysis as a Recovery Technology

Biomass pyrolysis can be described as the thermal conversion of organic materials without oxygen resulting in the breakdown of these organic materials into their various components. These processes were utilized for the commercial production of a wide range of fuels, solvents, chemicals, and other products from biomass feedstocks. Yield of products generated from biomass pyrolysis can be maximized as gases, vapors and tar components, and a carbon rich solid residue.

Each component of lignocellulosic (cellulose, hemicelluloses and lignin) biomass is pyrolysed at different rates by different mechanisms and pathways. The pyrolysis for production of fuel and chemical is divided into three main processes which are conventional (slow), fast and flash. The difference between them are the process conditions which involves the solid residence times, heating rate, particle size and temperature. Conventional pyrolysis consists of the slow, irreversible, thermal decomposition of the organic components in biomass. Slow pyrolysis has traditionally been used for the production of charcoal. Short residence time pyrolysis (fast, flash, rapid, and ultrapyrolysis) of biomass at moderate temperatures has generally been used to obtain high yield of liquid products. Fast pyrolysis is characterized by high heating rates and rapid quenching of the liquid products to terminate the secondary conversion of the products.

Depending on the volatile content and the pyrolysis temperature, the char fraction contains inorganic materials ashed to varying degrees and carbonaceous residues produced from thermal decomposition of the organic components. It constitutes approximately 20-25 % of yield and it is desirable product for producing activated carbon. The liquid fraction is a complex mixture of water and organic chemicals, oxygenated aliphatic and aromatic compounds. For highly cellulosic biomass feedstocks, the liquid fraction usually contains acids, alcohols, aldehydes, ketones, esters, heterocyclic derivatives and phenolic compounds. The tars contain native resins, intermediate carbohydrates, phenols, aromatics, aldehydes, their condensation products and other derivatives. Tar comprises approximately 60-65% of the products. The pyrolysis gas mainly contains CO_2 , CO , CH_4 , H_2 , C_2H_6 , C_2H_4 , minor amounts of higher gaseous organics and water vapor constituting 20-25% of the total products of pyrolysis (Agrawal and Cluskey 1983; Klass, 1998).

Yields are also often influenced by how the feedstock is prepared and fed to the pyrolysis reactor. If the feed has been shredded into smaller particles, the lower amounts of solid and liquid products and the higher amounts of gases generated (Kiran, 1998). If the purpose is to maximize the liquid product yield, process conditions are selected as low temperature, high heating rate and short gas residence time. For high char yield, low temperature and low heating rate are required. In order to have a high yield of gaseous product, high temperature, low heating rate and long gas residence time should be applied (Yaman, 2004).

2.3. Activated Carbon

Activated carbon is a porous carbonaceous adsorbent that exhibit a high degree of porosity and an extended inter-particulate surface area. Activated carbon is used to adsorb a variety of organic molecules such as aromatics, phenolics, hydrocarbons, ketons, esters, alcohols or soluble organic dyes that cause taste and odor, color, mutagenity and toxicity.

Carbon is the major constituent of activated carbons and is present to the extent of 85 to 95% (Bansal and Goyal, 2005). It also contains small amounts of different heteroatoms like oxygen, hydrogen, nitrogen and sulphur. The oxygen content of an activated carbon can vary, however, depending on the type of the source raw material and the conditions of the activation process. Moreover, it contains some ashes derived from the raw material. The amount of ash ranges from 1% to 12%. The ash content increases the hydrophilicity of activated carbon. If the ash content is high, powdered activated carbon (PAC) is more effective because PAC is more likely to stay inside the reactor rather than sticking on reactor walls for water treatment (Aktaş, 1999). The elemental composition of a typical activated carbon has been found to be 88% C, 0.5% H, 0.5% N, 1.0% S, and 6 to 7% O, with the balance representing inorganic ash constituents (Bansal and Goyal, 2005). It has a high adsorptive surface area of 500-1500 m²/g, while the pore volume ranges between 0.7 and 1.8 cm³/g (Pontius, 1990). The porous structure is perhaps the main physical property in characterization of an activated carbon. According to the International Union of Pure and Applied Chemistry (IUPAC), the pore sizes of the activated carbon have been categorized as follows:

- Micropores (< 2 nm diameter)
- Mesopores (2-50 nm diameter)
- Macropores (> 50 nm diameter)

This classification is based on the width (w), which represents the distance between the walls of a slit-shaped pore or the radius of a cylindrical pore.

Schematic representation of the pore network of a carbon adsorbent is shown in Figure 2.3. Each of these three groups of pores has its specific function in the process of adsorption on activated carbon.

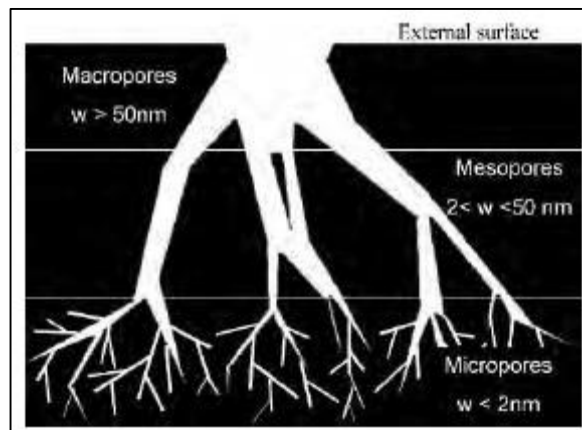


Figure 2.3. Schematic representation of the pore network of a carbon adsorbent (Bandoz, 2006).

2.3.1. Classification of Activated Carbon

Activated carbons are complex products, which are difficult to classify on the basis of their behavior, surface characteristics and preparation methods. However, some broad classification is made for general purpose based on their physical characteristics. The selection of the most suitable type of activated carbon for a specific application depends on the physical and chemical properties of the substances to be adsorbed. There are three forms of activated carbon (Figure 2.4):

- *Powdered Activated Carbon (PAC)*: PAC is defined as the activated carbon being retained on an 80-mesh sieve (0.177 mm) according to ASTM Standard. It presents large external surface area and the rate of adsorption is very high. It has been used in both liquid and gas phase applications and it might be useful in both drinking water and wastewater treatment (Çeçen and Aktaş, 2011).

- *Granular Activated Carbon (GAC)*: GAC has a relatively larger particle size and a smaller surface area compared to PAC. According to ASTM Standard, it has been designated with a mesh sieve of 50 (0.297 mm). GACs are used for water treatment as an advanced treatment system, deodorization and separation of components. These carbons are preferred for adsorption of gases and vapors as their rate of diffusion are faster (Dury, 2009).

- *Extruded activated carbon (EAC)*: EAC is extruded and cylindrical shaped with diameters from 0.8 to 5mm. These are mainly used for gas phase applications because of their low-pressure drop, high mechanical strength and low dust content (Dury, 2009).



Figure 2.4. Classification of activated carbons in terms of physical properties.

2.3.2. Application of Activated Carbon

Activated carbon is commonly used in various application areas, but especially in environmental field. With the rising awareness of environmental pollution at the beginning of the twentieth century, activated carbon is very often used in the removal of various organic and inorganic pollutants from surface water, groundwater and wastewater. When activated carbon is used in drinking water treatment, the main aim is usually the removal of taste and odor. However, more than 800 specific organic and inorganic chemicals have been found in various drinking water and adsorption by activated carbon is one of the major methods to control or remove them for standard values. Moreover, it might be utilized in remediation of groundwater for drinking purpose (Çeçen and Aktaş, 2011).

GAC filtration and PAC membranes are mainly utilized to remove dissolved and recalcitrant organic matter in tertiary treatment of municipal wastewater treatment. In addition, activated carbon is most commonly used in industrial wastewater treatment. It can be placed after physicochemical treatment steps such as coagulation/flocculation or filtration. In addition, it can be used before biological treatment to remove toxic matters.

However, activated carbon is mainly conducted as an advanced treatment system to remove refractory organics in advanced treatment systems (Çeçen and Aktaş, 2011).

Aside from environmental pollution control, adsorption on activated carbon is mainly used in chemical and petroleum industries, separation, catalysis, energy storage, batteries, fuel cells, nuclear power stations, pharmaceutical and others. In food industries, activated carbon can be used for decolourization, deodorization and taste removal purposes. In medicine field, it is useful for harmful chemical and drug adsorption purpose. In gas cleaning applications, activated carbon is used for air filters and air conditioning purpose. It has also been used in the purification of flue gases like emerging gases from incinerator, and sulfur compounds from gas stream. In mineral industry, for example, activated carbon has been used for gold recovery from leached liquors (Yahya et al., 2015).

Various industrial sectors use lignocellulosic activated carbon in operations such as chemical processes, petroleum refining, wastewater treatment, air pollution treatment and volatile organic compounds (VOC) adsorption (Cagnon et al., 2009; Suhas and Carrot, 2007; Ioannidou and Zabaniotou, 2007). In addition, lignocellulosic activated carbon is used for gas phase applications, such as for separation, deodorization, purification, storage and catalysis (Tsai et al., 1998). According to Nor et al. (2013), air pollutant removal studies with lignocellulosic activated carbon have not been applied widely in the industry. The potential of lignocellulosic activated carbon can be developed more using various types of chemicals or catalyst via impregnation. Chemical impregnation gives greater sorption capacity of gases if the functional group of the chemical is suitable for gas adsorption.

2.3.3. Production of Activated Carbon

In practice, commercial activated carbons are produced from materials with a high carbon content and a low inorganic content such as coal, lignite, wood, lignocellulosic materials, and petroleum-based residues. The quality of the produced activated carbon is considerably influenced by the raw material. Selection of the appropriate raw material is based on the following criteria (Bandosz, 2006):

- Possibility of yielding a good activated carbon in terms of adsorption capacity, high density and hardness.
- Low inorganic matter. The adsorption capacity is measured per mass unit, and since inorganic materials are non-porous, their presence reduces the adsorption capacity.
- Availability and cost. As with any other product, the price of raw material affects the final cost, so high availability is important to ensure stable prices.

Due to the rich carbon content of lignin, lignocellulosic biomass is a good option to be used as precursor in activated carbon production. In literature, activated carbon with high adsorption capacity has been produced from numerous sources of lignocellulosic biomass, such as corncobs (Bagheri and Abedi, 2009), maize cobs (Ketcha et al., 2012), straw lignin (Jin et al., 2010), brewers spent grain (Musatto et al., 2010), coconut shell (Hu et al., 2001), apricot stones (Girgis, 1998), pine wood (Wu and Zhang, 2012), lignin rich residue recovering bioethanol production from banana plants (Anaya et al., 2011) and other lignocellulosic materials. Moreover, two basic production methods, which are chemical and physical activation, have been used in the production of activated carbon as mentioned below.

2.3.3.1. Chemical Activation. In chemical activation, the raw material is firstly impregnated with a given chemical agent. Several activating agents have been reported for the chemical activation process: phosphoric acid (H_3PO_4), zinc chloride ($ZnCl_2$) and alkaline metal compounds. H_3PO_4 and $ZnCl_2$ are usually used for the activation of lignocellulosic materials which have not been previously carbonized; while, alkaline metal compounds like KOH and NaOH, are usually used for activation of coal precursors (Çuhadar, 2005). Following, impregnated sample is pyrolyzed at high temperature of 400-1000°C under N_2 flow in order to produce activated carbon (Hayashi et al., 2000). As a result of the pyrolysis process, a much richer carbon content material is produced, and once the chemical agent is eliminated after the heat treatment, the porosity is highly developed.

The major factor in chemical activation is the degree of impregnation. When the degree of impregnation is further raised, the number of larger diameter pores increases and the volume of the smallest pores decreases (Balci, 1992).

An important advantage of chemical activation is that the process normally takes place at a lower temperature and for a shorter time than those used in physical activation. In addition, higher surface area can be obtained in chemical activation. Moreover, the yield of carbon in chemical activation is usually higher than that of physical activation because the chemical agents have dehydrogenation properties that inhibit formation of tar and reduce the production of other volatile products. However, chemical activation process requires an important washing step to protect the chemical properties of the activated carbon, to eliminate congestion of pores by activating agents and the corrosiveness of the chemical activation process (Balci, 1992).

H₃PO₄ is commonly utilized due to economic and environmental reasons since it requires relatively low activation temperature and it can be removed easily at the end of the process (Mussatto et al., 2010). When ZnCl₂ is used as an activating agent, the activated carbon samples must be rinsed with other chemicals like HCl in order to remove them from chemical agents. However, in the case of H₃PO₄, there is no need for other chemicals. As a result, the hot distilled water is the only solution used for washing of the produced activated carbons in the final step (Yağsi, 2004).

2.3.3.2. Physical activation. Physical activation, generally called “partial gasification”, occurs in two steps that are carbonization and activation of carbonized intermediate product with gaseous agents.

Carbonization. The main aim of the carbonization step is to reduce the volatile content of the source material in order to convert it to a suitable form for activation. During the phase of the carbonization, the carbon content of the product attains a value of about 80%. Carbonization of lignocellulosic material starts above 170°C and it is nearly completed around 500-600°C. In the production of charcoal, it is desirable to carry out pyrolysis sufficiently quickly, in order to reduce the time of contact of the carbon formed with decomposition products (Balci, 1992).

Activation of Carbonized Intermediate Product with Gaseous Agents. The most common activation agents are steam, carbon dioxide and oxygen (air). The activation step is generally conducted at temperatures between 800°C and 1100°C. The active oxygen in the activating

agent burns away the more reactive portion of the carbon, depending on the gaseous agent employed. The main factors that influence the rates of the reactions of carbon with carbon dioxide, steam and oxygen are:

- the concentration of active sites on the carbon surface,
- the crystallinity and structure of carbon,
- the presence of inorganic impurities,
- the diffusion of reactive gases to active sites (Balci, 1992).

Generally, carbonization and activation steps are carried out separately, but recently there is an increasing tendency to conduct the two processes together.

2.4. Adsorption

Adsorption is recognized as a significant phenomenon in natural, physical, chemical and biological process. Sorption on solids has become a widely used operation in environmental field. Because of the large surface areas per unit weight, most common industrial adsorbents are activated carbon, silica gel and alumina.

Adsorption is the process of accumulating substances that are in solution on a suitable interface (Metcalf and Eddy, 1991). It occurs between two phases such as liquid and liquid, gas and liquid, gas and a solid or liquid and a solid. The molecule being concentrated or adsorbed at the interface is called an adsorbate, and the material being used as the adsorbing phase is adsorbent (Pontius, 1990; Çeçen and Aktaş, 2011). Adsorption is a case in which matter is extracted from one phase and concentrated at the second phase surface. Such surface reactions must occur through the active forces within the phase or surface boundaries. These forces cause characteristic boundary energies. Adsorption is different from absorption, a process through which a substance, originally present in one phase, is removed from that phase by dissolution in another, which is typically a liquid as opposed to the accumulation at the interface as in the case of adsorption (Weber, 1972).

Depending upon the nature of the forces involved, the adsorption is of three types: physical or van der Waals adsorption, chemical adsorption and exchange adsorption. The

basis of distinction is the nature of the bonding between the molecule and the surface. When bonding is by weak van der Waals forces, this phenomenon is called physical adsorption. This type of adsorption is observed at low temperature and characterized by a relatively low adsorption energy. In case of chemical adsorption, there are much stronger forces between the molecules, so it is rarely reversible. It is predominant at higher temperature compared to physical adsorption because chemical reactions progress more quickly at higher temperature. The bond formed between the adsorbate and the adsorbent is essentially a chemical bond and is thus much stronger than in physical adsorption. The third one, which is called exchange adsorption, refers to electrical attraction between the molecules because of opposite charge of the surface. Ion exchange is an exchange adsorption phenomenon (Aktaş, 1999).

2.4.1. Factors Influencing Adsorption

Adsorption is directly related with specific surface area of the adsorbent, pore size distribution, as well as the properties of the adsorbate, pH, and temperature, as mention below.

The extent of adsorption depends directly upon the specific surface area of the adsorbent within the pores that are accessible to the adsorbate. It is the available part of the total surface area for adsorption. A relatively large volume of micropores generally corresponds to a large surface area and a large adsorption capacity for small molecules, whereas a large volume of macropores is generally directly correlated to capacity for large molecules (Pontius, 1990). Both molecular size and adsorbent particle size have important effects on the rate of adsorption. Large molecules are adsorbed better than smaller molecules by activated carbon. In addition, the grade of solubility of the solute is important factor for adsorption. In the case of high solubility, the solute-solvent bonds are stronger than the attractive forces between the solute and adsorbent. Polarity of the adsorbate is another factor that affects adsorption. A polar solute is more easily adsorbed by a polar adsorbent, whereas a nonpolar solute is rather adsorbed on a nonpolar adsorbent. Activated carbon adsorbs nonpolar molecules better than polar molecules.

Other major factors that affect adsorption are pH and temperature. Generally, adsorption is increased at pH ranges where the species have no any charge. Many organics form negative ions at high pH, positive ions at low pH, and natural species at intermediate pH ranges. Adsorption of many organic pollutants in liquid are increased by decreasing pH because of neutralization of negative charges at the carbon surface at low pH values (Çeçen and Aktaş, 2011). Adsorption reactions are normally exothermic, thus when temperature is decreased adsorption extent generally increases.

2.4.2. Gas Adsorption Phenomena and Standard Isotherms

As assessment of adsorption kinetics is an important criterion in evaluating the adsorption equilibrium condition, adsorption kinetics should be determined experimentally to drive the equilibrium time at which no change in concentration of the substrate could be detected. If reaction is reversible, it is a critical time that the rate of the forward reaction (adsorption) equals the rate of the reverse reaction (desorption). When this condition is present, equilibrium has been attained and no further change in the concentration of the reactants and products will occur.

One of the most important characteristics of an adsorbent is the quantity of adsorbate that it can accumulate. The relation between the quantity of adsorbed (q) and the equilibrium concentration of adsorbate in solution (C) at the constant temperature (T) is called the adsorption isotherm at T , as shown Equation 2.1 (Chiou, 2002). The amount of adsorbed material per unit weight of adsorbent increases with increasing concentration, but not in direct proportion (Aktaş, 1999).

$$q = q(C) \text{ at } T \quad (3.2)$$

Where;

q = the quantity of adsorbed,

C = the equilibrium concentration of adsorbate in solution,

T = the constant temperature.

The more important adsorption isotherms are the Langmuir, the Freundlich, the Temkin, the Brunauer-Emmett-Teller (BET), and the Dubinin equations. The first three isotherm equations are very important for chemisorption, although the Langmuir and Freundlich isotherms are equally important for physisorption. The BET equation and Dubinin equations are most important for analysis of the physical adsorption of gases and vapors on porous carbons (Bansal and Goyal, 2005). Brunauer (1945), grouped the isotherms into five principle types shown in Figure 2.6. Type I isotherm is characterized by Langmuir-type adsorption. It indicates a microporous adsorbent. Type II is perhaps most common for physical adsorption and it is most frequently encountered when adsorption occurs on powders with pore diameters larger than micropores. Type III isotherms are observed when the adsorbate interaction with an adsorbed layer is greater than the interaction with the adsorbent surface and it signifies a relatively weak gas-solid interactions. Type IV occurs on porous adsorbents possessing pores mainly in the mesopore range. The slope increases at higher pressures as it is true for the Type II, the knee generally occurs near the completion of the first monolayer. Type V isotherms result from small adsorbate-adsorbent interaction potentials similar to the Type III isotherms (Çuhadar, 2005).

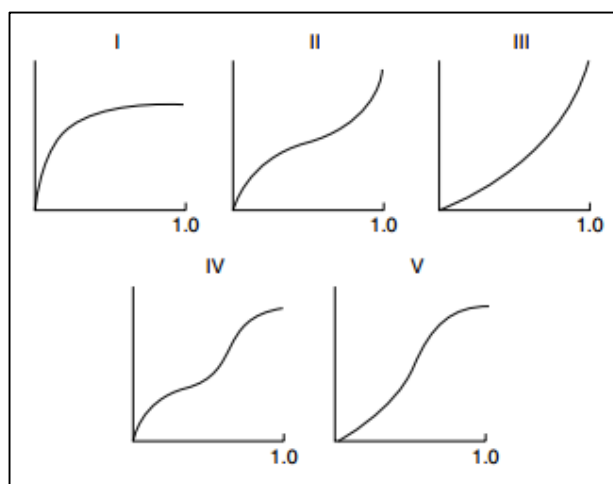


Figure 2.5. Five main types of adsorption isotherms (Çuhadar, 2005).

2.4.2.1. Brunauer, Emmett and Teller (BET) theory. The BET theory continues to be almost universally used because of its simplicity, and its ability to accommodate each of the five isotherm types. BET isotherm was put forward by Brunauer, Emmett and Teller. The Langmuir model is that an adsorbate accumulates in a monolayer, whereas the BET model accommodates multilayer. The fundamental assumption for BET model is that a number of

layers of adsorbate molecules form at the surface and that the Langmuir equation applies to each layer. A further assumption is that the surface is homogeneous and different layers of molecules do not interact. Each adsorbed molecule in the monolayer is assumed to be an adsorption site for the second layer of molecules, and so on as the relative pressure increases, until bulk condensation occurs (Brunauer, 1945).

In the region of relative pressures near the completion of monolayer, the BET theory and experimental isotherms do agree very well leading to a powerful and extremely useful method for the estimation of surface areas of various materials including activated carbon, coal and coal chars. The BET equation takes the following simplified form;

$$q_e = \frac{BCq_{\max}}{(C_s - C)[1 + (B-1)(C_s/C)]} \quad (2.2)$$

Where;

C = the measured concentration in solution at equilibrium

q_{\max} = the number of moles of solute adsorbed per unit weight of adsorbent in forming a complete monolayer on the surface

q_e = the number of moles of solute adsorbed per unit weight at concentration C

B = the constant expressive of the energy of interaction with the surface

C_s = the saturation coefficient of the solute

The linearized form of the BET equation was given in Equation 2.3 and the linear form is illustrated in Figure 2.7.

$$\frac{C_e}{(C_s - C_e)} = \frac{1}{(Bq_{\max})} + \left(\frac{B-1}{Bq_{\max}}\right)\left(\frac{C_e}{C_s}\right) \quad (2.3)$$

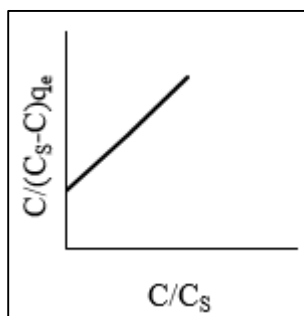


Figure 2.6. Linear forms for graphical representation of BET equation.

The BET equation usually gives a good representation of the frequently appearing Type II and IV isotherms within the range of relative pressures 0.05-0.3, and this range is generally used in practice for measurement of the surface area. At higher relative pressures, the BET equation is usually inaccurate because of capillary condensation effect, while at P/P_0 values below about 0.05, the amount of adsorbed gas is too small to be measured with sufficient accuracy. A poorer description is obtained for the type I, III and V isotherms, but in practice, they too are often analyzed by the BET method. Using BET it is possible to measure pores down to 10 nm.

2.5. Summary of the Previous Studies Performed for Producing Activated Carbon

In most of the published work, the composition of lignocellulosic materials is not specified and there is no attempt to relate the adsorptive properties to the amount of lignin or cellulose present. Nevertheless, there are some results pointing out that lignin is the main component responsible for adsorption by wood and other lignocellulosic materials.

The effect of process variables such as carbonization time, temperature, particle size, chemical agents, and impregnation ratio in the chemical activation and carbonization was reported by a certain amount of work carried out on the production of activated carbon from lignin-derived precursors. A summary of some relevant studies was given below.

Gonzalez-Serrano et al. (2004) used H_3PO_4 as activating agent. Activated carbon samples were prepared from pyrolysis of the H_3PO_4 impregnated lignin. The impregnation ratio H_3PO_4 /lignin was 2 and the activation temperature around $450^\circ C$ was recommended as

the best combination of operating conditions to prepare activated carbon for aqueous phase applications. It was found that increasing the temperature of activation from 350°C to 450°C increased the surface area from 1000 m²/g to 1500 m²/g.

Anaya et al. (2011) produced activated carbon from biomass originated in ethanol production from banana plants. They performed experiments with three different biomasses, (1) biomass produced during acid hydrolysis of the banana fruit, (2) biomass obtained from the enzymatic hydrolysis of the banana tree pseudostem, and (3) raw banana tree pseudostem. Samples were impregnated with a H₃PO₄ solution with a concentration of 80% and 85% weight during 4 hours (h). After that, they were carbonized at 450°C for 1 h. The recalcitrant biomass produced during the acid hydrolysis of the banana fruit is not suitable due to its high ash content. Contrarily, the other two-biomass samples, the one produced during an enzymatic hydrolysis of the banana tree pseudostem and the raw banana tree pseudostem, gave good results when they were activated with H₃PO₄.

Ahmadpour et al. (1995) produced activated carbon from bituminous coal through chemical activation using KOH and ZnCl₂ as the activating agent. The highest surface area of activated carbon samples from bituminous coal was found 925 m²/g with 1 h KOH activation at 700°C, and 865 m²/g through 1 h ZnCl₂ activation at 500°C. They have argued that the most important parameter in chemical activation of coal with both of the chemical agents was the impregnation ratio. In addition, carbonization temperature had a high effect on pore volume evolution. Increasing the carbonization temperature enhanced surface area and pore volumes of activated carbon impregnated with KOH whereas it destroyed carbon structure in the ZnCl₂.

Lozano-Castello et al. (2001) produced activated carbon samples from Spanish anthracite by using KOH. In this study, the activation agent/coal r was found to be the most important parameter in chemical activation. As the ratio of activation agent to coal ratio reached a maximum ratio 4:1, micropore volume and BET surface area increased to 1.45 cm³/g and 3290 m²/g, respectively. In addition, it was concluded that an acid washing step after carbonization could be avoided because the results were not very different from those obtained with water washing.

Girgis et al. (1998) carbonized H_3PO_4 impregnated apricot stones at 300°C, 400°C and 500°C. In their study, they used 20%, 30%, 40% and 50% phosphoric acid by weight. The highest BET surface area was obtained from the sample which was impregnated with 30% H_3PO_4 and carbonized at 500°C. They observed that, as the temperature increased, the BET surface area increased from 700 m^2/g up to 1400 m^2/g .

Girgis et al. (2002) obtained activated carbon from date pits by using H_3PO_4 . The raw material was impregnated with increasing concentrations of H_3PO_4 (30-70% w/w) followed by pyrolysis at 300°C, 500°C and 700°C. The best porosity development was found at 700°C with 50% H_3PO_4 (w/w) impregnated sample having 945 m^2/g of BET surface area.

Hu et al. (2001) prepared activated carbons from ZnCl_2 impregnated coconut shells by pyrolysis under nitrogen flow until temperature reached 800°C. They investigated the effect of impregnation ratio between 0.25 and 3. As a result, the BET surface area increased with increasing ratio of ZnCl_2 from 0.25 to two and reached a maximum BET surface area of 2450 m^2/g . It was indicated that as the impregnation ratio was higher than 2, many micropores were enlarged to mesopores.

Fierro et al. (2007) used kraft lignin to produce activated carbon via chemical activation with KOH and NaOH for 0.4 to 4 h and carbonization at 400-700°C. The resultant activated carbon samples were characterized in terms of BET surface area, total, micro and mesopore volumes, average pore width, carbon yield and packing density. They showed that an optimal activation temperature existed at 700°C. It was shown that KOH led to the most microporous materials, having surface areas and micropore volumes typically 1.5 and 1.2 times higher than those obtained with NaOH. The maximum surface areas were obtained as 3100 and 2400 m^2/g for KOH and NaOH, respectively and micropore volumes was 1.5 and 1 cm^3/g for KOH and NaOH, respectively. The total pore volume presented a maximum above which the micropores became less and less abundant. Since the carbon yield decreased while the density rises, the lignin is still converted into carbon, but into a less and less porous one at high hydroxide/lignin ratios. Again, an optimum impregnation ratio was 3.

Bagheri and Abedi (2009) prepared activated carbon by chemical activation of corn with H_3PO_4 . The effect of different parameters, such as particle size, method of mixing, ratio

of chemical to corn cobs, activation time and activation temperature, on weight loss and BET surface area of the produced activated carbons was discussed. As a result, BET surface area was higher for smaller particle sizes therefore the surface area and micropore volume were more developed. Moreover, BET surface area increased with an increasing chemical to corn ratio. The maximum surface area of 1200 m²/g was observed at 550°C for 1 h at an impregnation ratio of 1:1.

Wu and Zhang (2012) developed activated carbon samples from pinewood with the activating agent recycling simultaneously. Chemical activation using ZnCl₂ was carried out with 1:1 (w/w) impregnation ratio. Carbonization was performed about 6 h at 400-800°C. They obtained that optimal temperature for producing activated carbon was 500°C to reach the maximum surface area of 1350 m²/g.

Tay et al. (2009) prepared activated carbon samples from the pyrolysis of soybean oil cake at 600°C and 800°C by chemical activation with K₂CO₃ and KOH. The influence of temperature and type of chemical reagents on the porosity development was investigated. K₂CO₃ was found more effective than KOH as a chemical reagent under identical conditions in terms of both porosity development and yields of the activated carbons. The maximum surface area of 1352 m²/g was obtained at 800°C with K₂CO₃ activation which lied in the range of commercial activated carbons. As a result, the yields of the activated carbons produced by chemical activation were lower than those of biochars for all carbonization temperatures.

Ketcha et al. (2012) used maize cobs as the precursors for activated carbon production. Carbonization of raw materials was done at 500°C for 1 h under nitrogen flow. Chemical activation was performed by use of five different ZnCl₂ concentrations that are 1 g, 2 g, and 3 g of solid ZnCl₂ for 1 h and 10% solution of ZnCl₂ for 1 h and 24 h. The sample activated with 1 g solid ZnCl₂ had the maximum BET surface area of 701.68 m²/g, which are higher than of the commercial sample of which the specific surface area. The experimental results indicated that this method of preparation of chars was easy, economic and activated carbon obtained particularly from the hard part of the cob has very significant physicochemical and structural properties.

Musatto et al. (2010) prepared activated carbon from brewer's spent grain lignin by chemical activation with H_3PO_4 solutions with 1, 2, 3 (w/w) impregnation ratio during 1 h at room temperature. It was followed by carbonization with activation temperature ranging from 300°C to 600°C for 2 h. They obtained an activated carbon presented the best product, having BET surface area of $692 \text{ m}^2/\text{g}$, with impregnation ratio of 3 at 600°C .

Hayashi et al. (2000) investigated the influence of carbonization and activating reagent on the pore structure of the activated carbon. They produced activated carbon from lignin by chemical activation with ZnCl_2 , H_3PO_4 and some alkali compounds like K_2CO_3 , KOH , and NaOH . It was found that the best products were obtained at the carbonization temperature of 600°C in both ZnCl_2 and H_3PO_4 . On the other hand, in alkali metal activation, it was found that the maximum surface area was obtained at the carbonization temperature of 800°C .

Jin et al. (2010) produced activated carbon samples from straw lignin by means of activation with K_2CO_3 and KOH (40% aqueous solution) with the ratio ranging from 0.8 to 2.4 at 16 h. It was followed by carbonization in a flow of nitrogen at $500\text{-}900^\circ\text{C}$ for 1 h with a heating rate of $20^\circ\text{C}/\text{min}$. The activated carbon prepared by K_2CO_3 was permitted to obtain the highest BET surface area of $1104 \text{ m}^2/\text{g}$ for the material carbonized at 800°C with 2:1 (w/w) impregnation ratio.

Further, Zanzi et al. (2002) noted that higher lignin content resulted in higher char yield in their study on the pyrolysis of agricultural residues at high temperature. Gonzalez et al. (2003) reached a similar result in their study on the pyrolysis of cherry stones, and they suggested that lignin was the main source of char formation, while hemicellulose and cellulose are the volatile fractions.

3. MATERIALS AND METHODS

3.1. Main Steps of the Study

This study was conducted within the scope of TÜBİTAK 1001 project (Project No. ÇAYDAG-110Y261, Bioethanol production from agricultural wastes for waste minimization and carbon budget analysis) and Boğaziçi University Scientific Research Projects (Project No. 13Y00P2, By-product utilization opportunities from pretreatment and fermentation processes of selected agricultural residues). The aim of these projects is production of bioethanol from agricultural residues by optimizing the pretreatment conditions and fermentation process to increase ethanol yield (Daylan, 2016) as well as activated carbon production from residue of bioethanol production (this thesis). The experimental path of these projects was divided into five main steps as shown in Table 3.1. This thesis contains first (characterization of feedstock) and fourth (activated carbon production from lignin rich residue) steps of these projects.

During the experiments, commercial reagents such as H_3PO_4 and H_2SO_4 with a purity of $\geq 98\%$ were provided from Sigma-Aldrich. Stock H_2SO_4 solution (72% w/w) and H_3PO_4 solution (30%, 40%, and 50% (w/w)) were prepared and dissolved by the ultrasonic sonication water bath (Bandelin Sonarex) in order to obtain homogenous solution. Stock solutions were stored in amber glass bottles and protected from sunlight to prevent decomposition. Deionize water (DI) used in all experiments was supplied by the deionized water system (Labconco waterpro). The autoclavable automatic pipettors (Axygen), ranging from 0.2 to 10.00 mL were used for addition of chemicals and sampling. All glassware were rinsed with tap and DI water and dried in a laboratory oven (Nüve FN500) before use.

Table 3.1. Methodology of the project (Project No. ÇAYDAG-110Y261).

PART I Characterization of Feedstock	PART II Optimization of Dilute Sulfuric Acid/Steam Pretreatment Process	PART III Optimization of Fermentation Process	PART IV Activated carbon production from lignin rich residue	PART V Life Cycle Assessment and Environmental Life Cycle Cost Analysis
<ul style="list-style-type: none"> • Determination of total solids • Determination of ash • Determination of extractives • Determination of starch • Determination of protein • Determination of acid insoluble and acid soluble lignin • Determination of structural carbohydrate (<i>celluloses and hemicellulose sugars</i>) 	<ul style="list-style-type: none"> • Feedstock substrate and chemical preparation • Parr reactor applications for optimization process conditions (<i>temperature, acid load, time</i>) • Analyzing of the sample for monomeric sugar, total sugar (<i>monosaccharides and oligosaccharide</i>) and byproducts by HPLC 	<ul style="list-style-type: none"> • Measurement of cellulase activity of enzyme • Optimization of the hydrolysis of lignocellulosic biomass (SAC) (<i>hydrolysis temperature</i>) • Inoculum Preparation • Optimization of the SSF process (<i>feedstock and yeast type, fermentation temperature, enzyme load versus ethanol yield</i>) • Optimization of the fermentation process by bioreactor application (<i>comparison of SHCF and SSCF</i>) 	<ul style="list-style-type: none"> • Recovery of lignin-rich residues (<i>two-stage delignification</i>) • Optimization of chemical activation process (<i>acid ratio</i>) • Optimization of carbonization process (<i>feedstock type and temperature</i>) • Characterization of produced activated carbons (N₂ adsorption /desorption capacities) 	<ul style="list-style-type: none"> • Definition of goal and scope, FU and system boundry • LCI Analysis • Application of LCA and ELCC through GaBi Software • Life Cycle Impact Assessment (<i>classification, characterization, normalization</i>)

During the feedstock characterization, the wet chemistry, proximate and thermogravimetric analyses were performed to obtain information about the physical, chemical and thermal characteristics of the selected feedstocks. The compositional analysis of the selected feedstock is an essential step to evaluate the efficiency of the production processes designed to convert these feedstocks to activated carbon. The aim of the thermogravimetric analysis was also to optimize the experimental variables and conditions to produce high quality activated carbon samples that are consistent with the literature. Besides these four types of feedstock, raw corn stover (RC) and wheat straw (RW) were also analyzed to understand the efficiency of delignification process performed to the lignin residues generated from pretreatment and bioethanol fermentation processes.

Following by the feedstock characterization and delignification process, activated carbon was produced via chemical activation and carbonization. Chemical activation was selected as the production process since it is usually carried out at lower temperatures compared to physical activation. The production at lower temperatures promotes the development of both more suitable surface area and porous structure in activated carbon. After the production of activated carbon samples from different types of lignin-rich residues, the physical and textural properties of products such as conversion yield, chemical recovery, pH value, ash content, total surface area and pore volume were compared to assess the effect of activating agent concentration and carbonization temperature on production process.

3.2. The Selected Feedstocks

During this study, corn stover and wheat straw samples, supplied from the Marmara Region and Black Sea Region of Turkey, were used as feedstock to produce activated carbon. Biomass samples were stored in a cold room, at 4°C before experimental works. In experimental research, four types of feedstocks were used to produce activated carbon samples, which are:

- The lignin residue derived from the pretreated corn stover; PC
- The lignin residue derived from the pretreated wheat straw; PW
- The lignin residue derived from the fermented corn stover; FC
- The lignin residue derived from the fermented wheat straw; FW

3.3. Characterization of Raw Feedstock

Figure 3.1 shows the stages of proximate and wet chemical analyses used for the characterization of raw feedstocks.

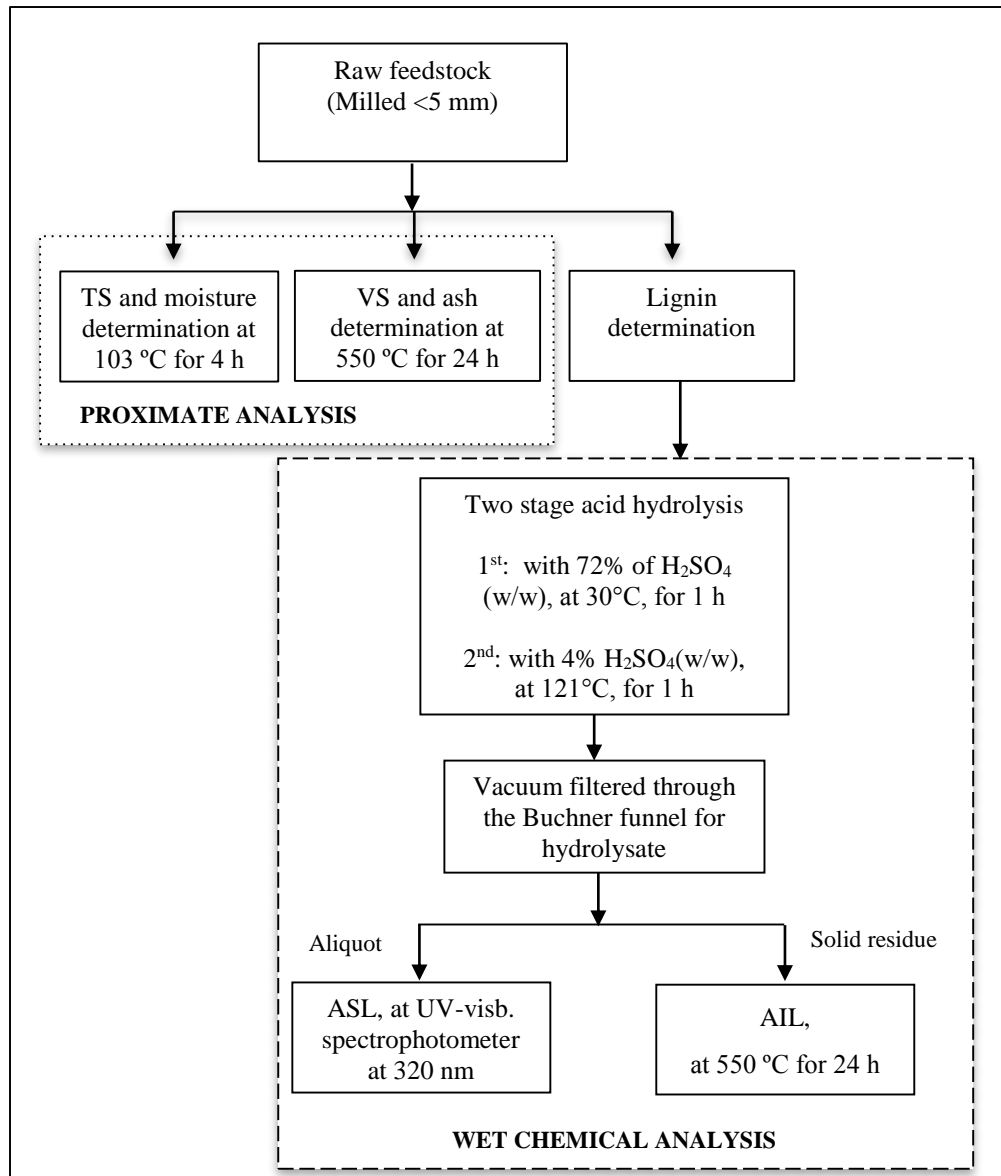


Figure 3.1. General scheme for the characterization of the raw feedstocks.

3.3.1. Preparation of Biomass Sample

Biomass samples were prepared according to National Renewable Energy Laboratory (NREL), “Laboratory Analytical Procedure (LAP) Preparation of Samples for Compositional Analysis” (Hames et al., 2008). The biomass sample was dried in an oven at 45°C for 24 to 48 h. This method may be used for very wet biomass samples that have a risk for microbial growth during drying, wet pretreated biomass, or when ambient humidity does not allow the sample to moisture content below 10% (Hames et al., 2008). After drying, material was milled by a laboratory knife-mill (Tetra Laboratory cutting mill), equipped with a sieve with an equivalent pore size of below 5 mm (Figure 3.2). The milled samples were stored inside sealed plastic bags and stored at 4°C for short term application.



Figure 3.2. Corn stover and wheat straw before and after milling

3.3.2. Proximate Analysis of Raw Feedstocks

3.3.2.1. Determination of total solids. The total solid (TS) content of raw material was determined by NREL, LAP- Determination of Total Solids in Biomass and Total Dissolved Solids in Liquid Process Samples (Sluiter et al., 2008). According to this procedure, crucibles were incinerated for over 4 h at 550°C in a muffle furnace (Protherm PLF 110/8),

cooled inside a desiccator and weighted using Denver Instrument analytical balance. A certain amount of biomass was placed into crucibles and the weight was recorded. The crucibles with biomass were placed inside the oven at 105°C for about 4 h, left to cool inside a desiccator and then weighted. The percentage of TS was calculated by Equation 3.1:

$$\%TS = \left(\frac{W_3 - W_1}{W_2} \right) * 100 \quad (3.1)$$

Where;

TS = the total solid content of sample, %

W₁ = the weight of dry crucible, g

W₂ = the weight of sample as received, g

W₃ = the weight of dry sample and crucible, g

3.3.2.2. Determination of ash. The ash content was determined by placing the crucibles obtained from TS determination in the muffle furnace at 550°C, for 24 h. The crucibles were left to cool inside a desiccator and then their weight was recorded (Sluiter et al., 2008a). The ash content was calculated by Equation 3.2 and Equation 3.3:

$$ODW_{\text{sample}} = \left(\frac{W_2 * \%TS}{100} \right) \quad (3.2)$$

Where;

ODW = the oven dried weight of sample, g

W₂ = the weight of sample as received, g

TS = the total solid content of sample, %

$$\% \text{ Ash} = \left(\frac{W_4 - W_1}{ODW_{\text{sample}}} \right) * 100 \quad (3.3)$$

Where;

Ash = the ash content of the sample, %

- W_1 = the weight of dry crucible, g
 W_4 = the weight of dry sample and crucible, g
ODW = the oven dried weight of sample, g

3.3.2.3. Determination of extractives. Before the structural component analysis of lignocellulosic raw materials, it is required to remove non-structural material from biomass to prevent interference with later analytical steps. The raw biomass was analyzed for extractives using the LAP- Determination of Extractives in Biomass (Sluiter et al., 2008b). A two-step soxhlet extraction process was applied to remove water-soluble and ethanol soluble materials. Water-soluble materials may include inorganic material, non-structural sugars, and nitrogenous material, among others. Ethanol soluble material includes chlorophyll, waxes, or other minor components.

In the soxhlet extraction process, a certain amount of biomass sample was placed to a tarred extraction thimble and inserted into a soxhlet extraction tube, which was connected to a receiving flask in a heating mantel below, and a condenser above, as shown in Figure 3.3. Firstly, water extraction was carried out by adding 190 mL of deionized water into the receiving flask at 90°C. The extraction was run for about 16-24 h and soxhlet tube refluxed 4-5 times per h. After water extraction, the receiving flasks containing the water residue were removed and replaced by a new flask containing 190 mL of ethanol to remove ethanol soluble materials. The following extraction was carried out in similar procedure to the water extraction, but the temperature was set to 75°C. When soxhlet extraction was complete, the extracted solids were filtered into cellulose filter paper in a Buchner funnel. The solids were washed with 100 mL of ethanol, filtered using vacuum filtration, air dried and weighted.

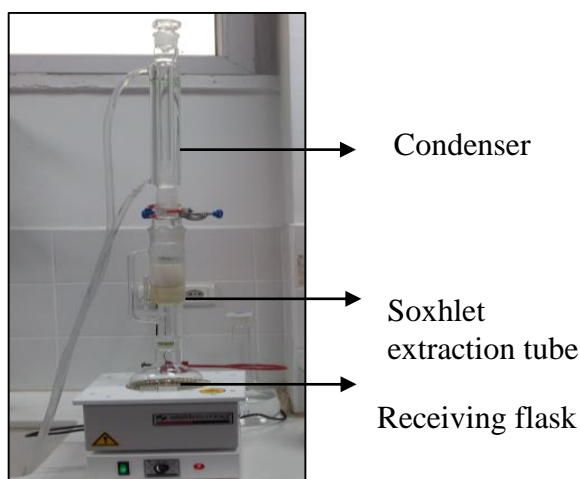


Figure 3.3. Soxhlet extraction set up for extractive determination.

The water and ethanol extraction residues evaporated by a Heidolph Laborata 4000 rotary evaporator equipped with water baths at 60°C in case of water extractives, and 40°C in case of ethanol extractives. The percentage of extractives was calculated by Equation 3.4 and Equation 3.5.

$$\text{ODW}_{\text{sample}} = \left(\frac{W_s * \%TS}{100} \right) \quad (3.4)$$

Where;

ODW = the oven dried weight of sample, g

W_s = the weight of sample as received, g

TS = the total solid content of sample, %

$$\% \text{ Ext.} = \frac{(W_{\text{flask+extractives}} - W_{\text{flask}})}{\text{ODW}_{\text{sample}}} * 100 \quad (3.5)$$

Where;

Ext. = the percentage of extractives of the sample, %

W_{flask} = the weight of the receiving flasks, g

W_{ext} = the weight of the extractives, g

ODW = the oven dried weight of sample, g

3.3.3. Wet Chemical Analysis of Feedstock

The wet chemical analysis method is widely used for determination of lignin and structural carbohydrate content of lignocellulosic feedstocks which use a two-step sulfuric acid hydrolysis process to fractionate biomass for gravimetric and instrumental analyses and provide consistent information about biomass composition. This method has worked well with wood, herbaceous feedstocks and crop residues to compare the potential feedstocks for value added chemical production, and to measure the efficiency of biomass-to-renewable chemical conversion processes (Xu et. al. 2013). The data obtained from compositional analyses can be used to evaluate the techno-economic studies of conversion processes calculating the mass balance and process yields. These results affect the optimization of process configuration, reactor design, and process performance. During this study, only lignin was determined since it is the only component that affects activated carbon production.

3.3.3.1. Determination of acid insoluble and acid soluble lignin content. Lignin content in lignocellulosic raw materials was determined by NREL laboratory procedure, “LAP-Determination of Structural Carbohydrates and Lignin in Biomass” (Sluiter et al., 2011). According to this procedure, a two-step acid hydrolysis was carried out. In the first step, approximately 300 mg of extracted free biomass was added into the tarred pressure tube and its weight was recorded. 3 mL of 72% sulfuric acid was then added to each pressure tubes. After brief mixing, the tubes were put into the water bath at 30°C, for an h and mixed at every five minutes. In the second step, the acid was diluted to 4% by adding 84 mL of deionized water into the pressure tube and then they were autoclaved for one h at 121°C.

The part of acid insoluble lignin was determined using the sample resultant from the last step of dilute acid hydrolysis. After the application of two-step acid hydrolysis process, the autoclaved hydrolysate was vacuum filtered through the Buchner funnel. The aliquot was used for the determination of acid-soluble lignin (ASL) and the residue above the filter paper was used for acid-insoluble lignin (AIL) determination. The acid insoluble residue (AIR) was placed into a crucible, dried at 105°C for 4 h, and weighted. Then the crucibles were put inside the muffle furnace, at 550°C for 24 h, cooled inside a desiccator, and weighted for the ash content. The percentage of AIL was calculated by Equation 3.6 and Equation 3.7. Ciliz

et al. (2015) estimated the protein content of corn stover and wheat straw as 5.25% and 2.4%, respectively.

$$\% \text{ AIR} = \frac{(W_{\text{crucible+AIR}} - W_{\text{crucible}})}{\text{ODW}_{\text{sample}}} * 100 \quad (3.6)$$

Where;

- AIR = the percentage of acid-insoluble residue, %
 ODW = the oven dried weight of raw material, g
 W_{AIR} = the amount of acid-insoluble residue, g
 W_{crucible} = the weight of the crucible, g

$$\% \text{ AIL} = \frac{(W_{\text{crucible+AIR}} - W_{\text{crucible}}) - (W_{\text{crucible+ash}} - W_{\text{crucible}}) - W_{\text{protein}}}{\text{ODW}_{\text{sample}}} * 100 \quad (3.7)$$

Where;

- AIL = the percentage of acid-insoluble lignin, %
 W_{AIR} = the amount of the acid-insoluble residue, g
 W_{ash} = the amount of ash, g
 W_{protein} = the amount of protein present in the acid insoluble residue, g
 ODW = the oven dried weight of raw material, g

Aliquots of the filtrates from the hydrolysate liquors were analyzed for acid-soluble lignin determination within 6 h of the acid hydrolysis. DI water was used as a blank and the measurements were performed by the UV-160A Shimadzu UV Visible Spectrophotometer at 320 nm. If necessary, the samples should be diluted to have an absorbance in the range 0.7-1.0. The percentage of ASL was determined by Equation 3.8. The total lignin content in biomass was the sum of the AIL and ASL (Equation 3.9).

$$\% \text{ ASL} = \frac{(\text{UV}_{\text{abs}} * V_{\text{filtrate}} * D)}{\epsilon * \text{ODW}_{\text{sample}}} * 100 \quad (3.8)$$

Where;

- ASL = the percentage of acid soluble lignin, %

UV_{abs} = the average absorbance for the sample at 320 nm

V_{filtrate} = the volume of filtrate, g

D = the dilution ratio

ε = the absorptivity of biomass at 320 nm

$$\text{Lignin} = \text{AIL} + \text{ASL} \quad (3.9)$$

Where;

Lignin = the percentage of total lignin, %

AIL = the percentage of acid insoluble lignin, %

ASL = the percentage of acid soluble lignin, %

3.4. Feedstock Preparation for Activated Carbon Production

3.4.1. Preparation of Pretreated Based Feedstock

The corn stover and wheat straw samples were obtained by a sequential process of dilute-acid hydrolysis and alkali pretreatment which is a typical lignocellulosic biomass pretreatment for bioethanol process. Two-stage pretreatment was applied for a successful delignification process to remove lignin from the pretreated feedstocks (Minu et. al., 2012; Jung et al., 2015). Figure 3.4 shows the schematic representation of delignification process.

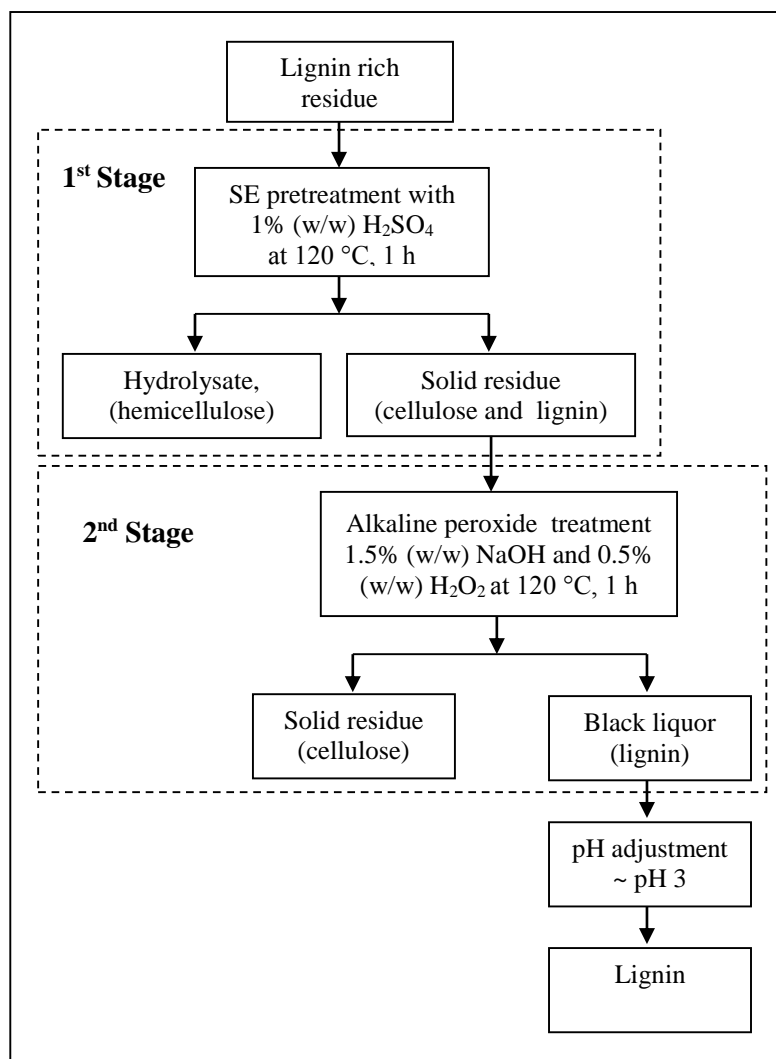


Figure 3.4. The schematic representation of the two-stage delignification process.

Table 3.2. The content of mixtures for first pretreatment step.

Mixture	Percentage, % (w/w)
H ₂ SO ₄	1
Total solid	10
Water	92

In the first step, the sample was treated by dilute acid at 120 °C for 1 h; using 1% (w/w) H₂SO₄. The content of mixtures as a percentage (w/w) for this step was shown in Table 3.2. During the dilute acid hydrolysis, the hemicellulose was solubilized in the form of monomeric sugars into the hydrolysate, but the cellulose and lignin remained in the solid residue.

In the following step, the resulting residue was then subjected to the delignification process at 120 °C for 1 h using alkaline peroxide, which was a mixture of 1.5% (w/w) NaOH and 0.5% (w/w) H₂O₂. The content of mixtures as percentage (w/w) for the delignification step was shown in Table 3.3.

Table 3.3. The content of mixtures for second pretreatment step.

Mixture	Percentage, % (w/w)
NaOH	1.5
H ₂ O ₂	0.5
Total solid	10
Water	88.5

After second step, the mixture was filtered by Buchner funnel to separate the black liquor (lignin rich residue) and solid residue that contains cellulose. The black liquor was taken in a beaker and the initial pH of the black liquor was between 10 and 13. The final pH value of the black liquor was adjusted to 3 from 10 using 2% (v/v) H₂SO₄ to remove lignin. After adjusting the pH to the desired value (~pH 3), the beaker was kept undisturbed for settling of the flocs formed by the addition of acid. Figure 3.5 showed the lignin precipitation from black liquor via pH adjustment. After complete precipitation, the content of beaker was filtered using a vacuum filtration unit (Figure 3.6). The precipitates (PC and PW samples) were then air-dried overnight followed by oven drying at 105 °C for 24 h to remove the moisture content and obtain a constant weight. PC and PW samples were stored at 4°C for short term application.



Figure 3.5. Lignin precipitation from black liquor.



Figure 3.6. The lignin rich-residue obtained from filtration.

3.4.2. Preparation of Fermented Based Feedstock

After simultaneous saccharification and fermentation (SSF) of corn stover and wheat straw, lignin-rich residues were obtained as a byproduct. Lignin rich residue generated from fermentation process was centrifuged (Hettich Rotina 380 Centrifuge) for 10 minutes at 6000 rpm to separate solid part from aliquot (Figure 3.7). Since this residue also contains yeast culture, it should be sterilized in the autoclave (Selecta Presoclave-2) for 15 minutes at 121°C followed by oven drying at 105 °C for 4 h. The FC and FW samples were separated by the same sequential process of dilute-acid hydrolysis and alkali pretreatment applied to PC and

PW samples. PC, PW, FC, and FW samples used for activated carbon production were shown in Figure 3.9.



Figure 3.7. Residue separation after SSF.



Figure 3.8. PC, PW, FC, and FW samples used for activated carbon production.

3.5. Characterization of the Processed Feedstocks

The lignin rich residues obtained from pretreatment and fermentation were physically and chemically characterized using the same procedures (the proximate and wet chemical analyses) given in Section 3.2. The thermogravimetric analysis (TGA) was also used to evaluate the weight loss of feedstocks with respect to temperature and time, and to compare thermal decomposition behavior of feedstocks. Figure 3.9 shows the general scheme for characterization of the processed feedstocks.

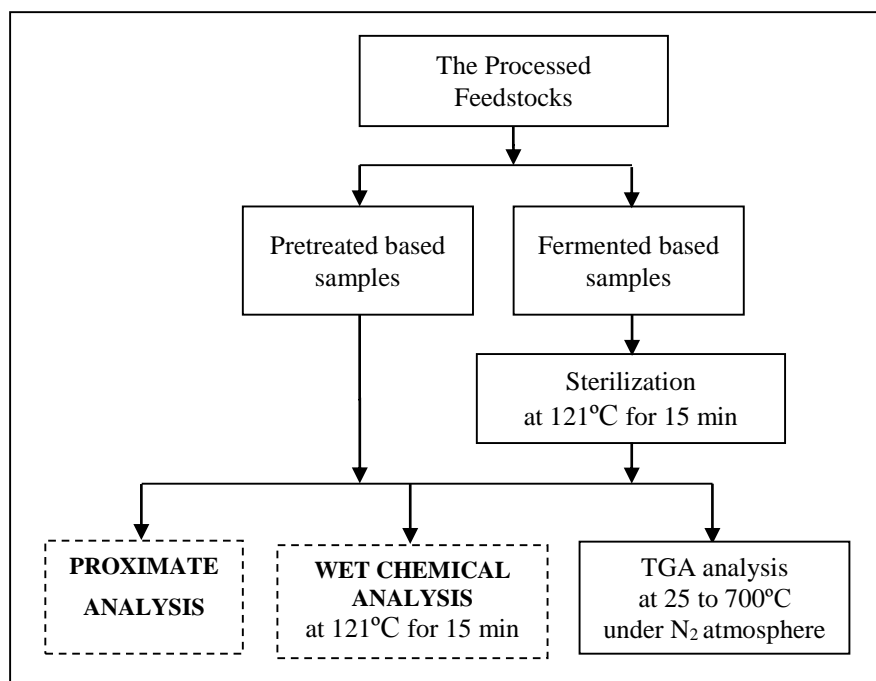


Figure 3.9. General scheme for the characterization of the processed feedstocks.

3.5.1. Thermogravimetric Analysis of Processed Feedstocks

TGA experiments were measured in Gebze Technical University. TGA was performed using Mettler Toledo TGA/SDTA 851 Instrument. Approximately 5-6 mg of samples was placed in a pan of the TGA microbalance, which was enough to fill the pan because of the low density of the ground feedstocks. The measurements were conducted at a constant purge flow rate of 40 mL/min in N₂ atmosphere. The samples were held at 25 °C for 1 min and heated to 695°C at a rate of 20°C/min. Residual weight of the sample and the derivative weight values with respect to time and temperature (differential thermogravimetric analysis, DTG) were recorded using TGA software.

3.6. Production of Activated Carbon Samples

In this study, chemical activation and carbonization methods were used to produce activated carbon from lignin-rich residues obtained from dilute acid/steam pretreatment processes, and saccharification and fermentation process. The main steps used in the production of activated carbon from PC, PW, FC and FW were presented in Figure 3.10.

Throughout the experiments, the effect of activating agent concentration on the physical properties of products was investigated. In the chemical activation process, H₃PO₄ solution was employed as an impregnation reagent. The lignin rich residues were treated with 30%, 40%, and 50% H₃PO₄ solutions (w/w) at 25°C for 24 h to compare the effect of chemical concentration on process efficiency. For the impregnation of 1 g residue, 2 mL H₃PO₄ solution was added to achieve a homogenized mixture that provides contacting all particles with the acid solution (Yağşı, 2004). After impregnation, solution was filtered to remove the residual acid. Subsequently, the impregnated samples were air dried at room temperature for 3 days.

The impregnation ratio (I.R.) of H₃PO₄ solution was calculated from the following equation:

$$\text{I.R.} = \left(\frac{W_2 - W_1}{W_1} \right) \quad (3.10)$$

Where;

I.R. = the impregnation ratio of the feedstock, %

W₁ = the weight of lignin residue , g

W₂ = the weight of lignin residue after impregnation, g

After the application of chemical activation, dried samples were ready for the carbonization experiments. Carbonization experiments were carried out in a horizontal “Protherm PTF/12/38/250” furnace with an inside diameter of 50 mm and a length of 60 cm. To ensure an inert atmosphere, N₂ gas was passed horizontally throughout the furnace. The inlet and outlet of ceramic tube were connected with ceramic fittings to avoid both the escape of N₂ from the system and the entrance of air to the furnace. A flow meter was connected to inlet of furnace to measure the N₂ flow rate passing through the system. All experiments were performed under the fume hood. Experimental set up used in carbonization is shown in Figure 3.11. Experimental conditions in production of activated carbon samples are presented in Table 3.4.

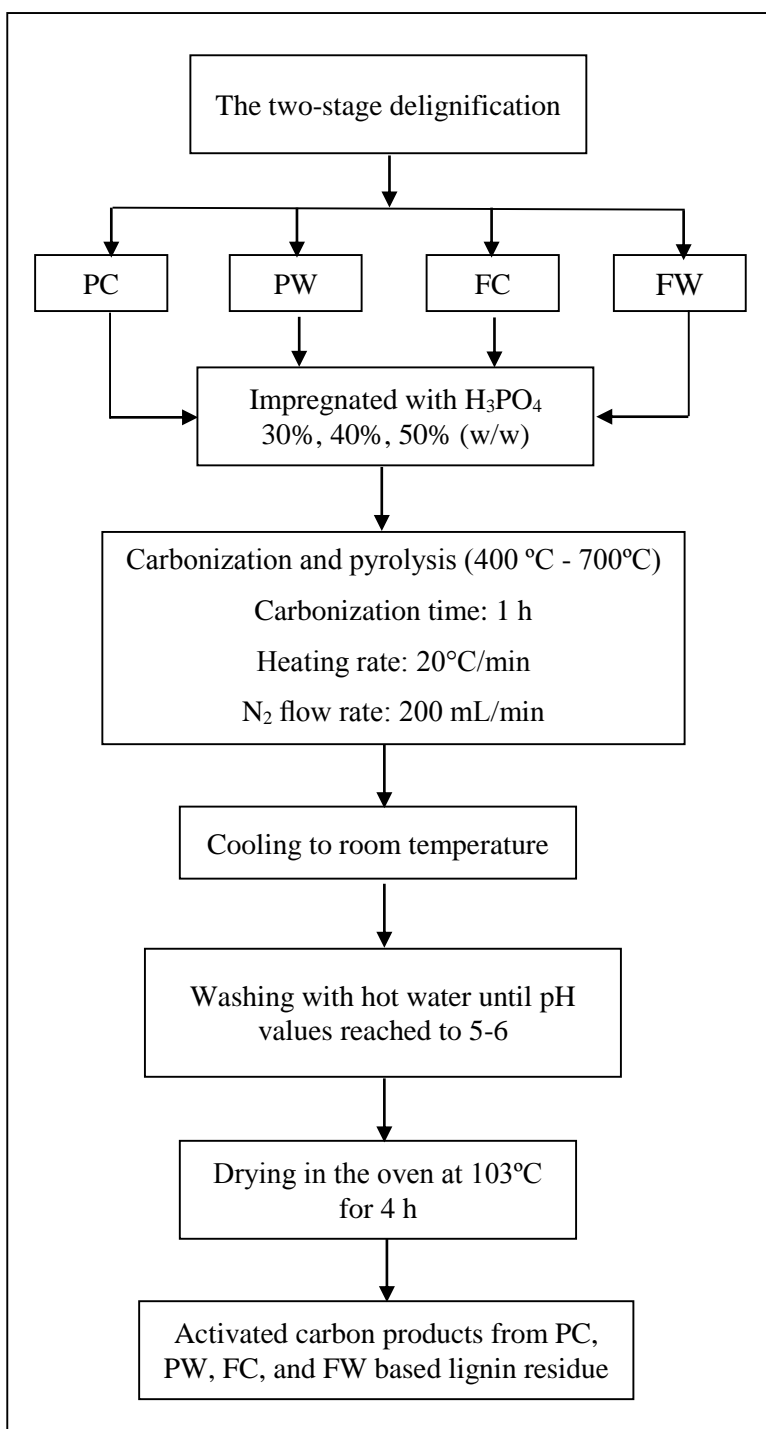


Figure 3.10. General scheme for production of activated carbon.



Figure 3.11. Experimental set-up for carbonization.

Table 3.4. Experimental conditions for activated carbon production.

Fixed parameters	Heating rate, °C/min	20			
	N ₂ flow rate, mL/min	200			
	Carbonization time, h	1			
Variable parameters	Type of feedstock	PC	PW	FC	FW
	Carbonization temperature, °C	400	500	600	700
	H ₃ PO ₄ concentration, % (w/w)	30	40	50	

Samples were put inside the horizontal furnace and the N₂ flow was started to purge the air in the ceramic tube for 5 minutes. After purging, the furnace was started to heat till the selected carbonization temperature was achieved. Carbonization time was measured from the point when the selected temperature was reached. After 1 h of carbonization time, the furnace was cooled down to room temperature. When the product was taken from the furnace to a flask, distilled water was added to prevent interaction with the air. Finally, the product was washed several times with hot water to remove H₃PO₄ until the pH values reached to 5-6 and the washed product was dried at 103°C. The product, shown in Figure 3.12, was stored at room temperature until the physical characterization experiments.



Figure 3.12. Activated carbon produced from lignin rich-residue.

3.7. The characterization of the produced activated carbon

In order to investigate the influence of on the physical and textural characteristics of the activated carbon samples, the basic parameters such as yield, chemical recovery, pH value, ash content and the adsorption capacities of the products were compared.

3.7.1. Char Yield and Chemical Recovery Value of Produced Activated Carbon

Char yield and chemical recovery value were regarded as the indicator of the efficiency of the chemical activation process (Musatto et al., 2010). The product yield has been calculated by dividing the amount of char (after washing to remove H_3PO_4) to the initial mass of sample prior to the impregnation. The conversion yield was estimated taking into account equation (3.11) (Fierro et al., 2007):

$$\%Yield = \left(\frac{W_f}{W_i} \right) * 100 \quad (3.11)$$

Where;

Yield = the percentage of product yield, %

W_f = the final weight of dry sample, g

W_i = the initial weight of dry sample, g

The chemical recovery value was estimated by the equation (3.12) (Musatto et. al., 2010):

$$C.R. = \left(\frac{W_{pi} - W_{pf}}{W_c} \right) * 100 \quad (3.12)$$

Where;

C.R. = the chemical recovery, %

W_{pi} = the weight of product before washing, g

W_{pf} = the weight of product after washing, g

W_c = the weight of chemical agent used, g

3.7.2. Determination of the pH

0.05 g of activated carbon was mixed with 50 mL DI water at a temperature of 25°C to determine the pH of the solution. After agitation, the pH of each sample was measured (P Selecta pH 2005 pH meter).

3.7.3. Brunauer-Emmett-Teller (BET) Surface Area of Products

N₂ adsorption/desorption experiments were carried out TUBITAK Marmara Research Center. The adsorption isotherm of N₂ for the produced activated carbon was measured at 77°K by the constant volume adsorption apparatus (Quanthachrome Nova 4000E). Before measuring the isotherm, the activated carbon was heated at 150°C for 16 h with vacuum to clean its surface. The surface area of the activated carbon was calculated by the BET method using the adsorption isotherm of N₂. While the micropore volume was calculated from the amount adsorbed N₂ gas at relative pressure of 0.1 (P/P₀) the mesopore volume was calculated by subtracting the amount adsorbed N₂ at a relative pressure range of 0.1 to 0.95 (P/P₀).

In this study, the specific surface area was calculated by applying BET equation. The BET area is determined by the measurement of gas adsorbed (typically N₂) at a given pressure. The application of carbonization to an impregnated material further accelerates thermal degradation and the volatilization process. This process leads to pore development and increases the surface area (Gratuito et al., 2008). BET surface areas of the samples can

be obtained from the plot of $P/V(P_0-P)$ versus P/P_0 plot, in the relative pressure range of 0-0.2, shown in Figure 4.17 as an example.

3.7.4. Pore Analysis by Adsorption/Desorption

Gregg and Sing (1982) found that there are four types of hysteresis loops which were correlated with various pore shapes for adsorption-desorption isotherms. The hysteresis part of the isotherms contains information about the mesopores. Figure 3.13 showed the classification for the four types of hysteresis (Gregg and Sing, 1982). It is commonly found that the branches of the adsorption and desorption graph are not parallel over the whole pressure range which is called as hysteresis for porous solids. To get information about the porous texture of the adsorbent, the view of the hysteresis loops were compared with the adsorption-desorption isotherm view obtained at this study.

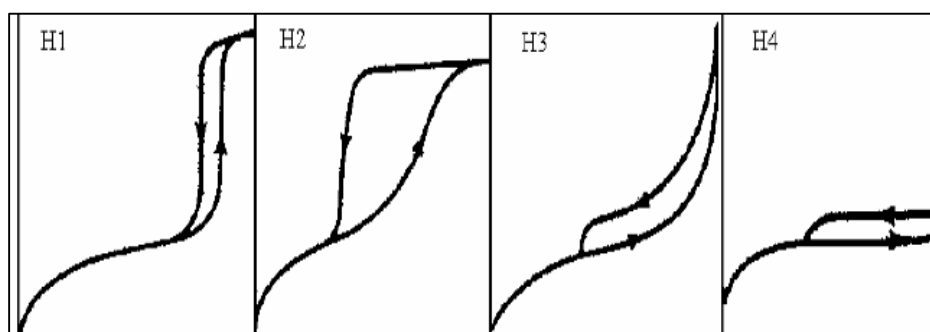


Figure 3.13. The types of adsorption-desorption hysteresis loops (Gregg and Sing, 1982).

4. RESULTS AND DISCUSSION

During this study, the impacts of different feedstock types on production of activated carbon were evaluated at different conditions, such as the impregnation ratio and carbonization temperature. For this purpose, a laboratory-scale pyrolysis system was utilized.

4.1. Feedstock Characterization

Chemical characterization of the feedstock is a prerequisite to optimize the production of activated carbon. It has been shown that there is a relationship between the adsorptive properties and the composition of lignocellulosic materials (Suhas and Carrot, 2007). For instance, raw materials containing a certain amount of inorganic substances result in a reduction in the adsorption capacity since inorganic materials have a non-porous structure. The features of lignocellulosic biomass differ by the production location (geographic area) and conditions such as climate, harvest period, soil type, and fertilization practices (Templeton et al., 2009; Xu et al., 2013). The composition of the feedstocks can be used to evaluate the efficiency of corn stover and wheat straw to produce activated carbon via pyrolysis because it affects the optimization of process configuration, reactor design, and process performance (Templeton et al., 2010). In addition, it affects product specifications and product yield. For this purpose, the characterization of raw lignocellulosic feedstocks was considered for activated carbon production in terms of total solid, moisture, volatile solid, ash and lignin contents. In addition to PC, PW, FC and FW samples, RC and RW were also characterized to understand the effect of the delignification process on lignin residues generated from pretreatment and bioethanol fermentation processes.

4.1.1. Proximate Analysis of Feedstocks

4.1.1.1. Raw lignocellulosic materials. Three parallel samples were used to determine the proximate analyses of raw corn stover and wheat straw which are shown in Tables 4.1 and 4.2, respectively.

The total, ash and volatile solids (VS) contents of corn stover were determined as 92.61%, 8.5% and 84.05%, respectively. The raw wheat straw samples had a lower ash content (4.9%) compared to corn stover samples, and the VS content was measured as 88.44%.

Table 4.1. Proximate analysis of raw corn stover.

Parameter, %	Sample 1	Sample 2	Sample 3	Average
TS	92.52	92.35	92.79	92.61
Moisture	7.48	7.65	7.21	7.45
Ash	5.99	8.30	11.21	8.50
VS	86.53	84.05	81.58	84.05

Table 4.2. Proximate analysis of raw wheat straw.

Parameter, %	Sample 1	Sample 2	Sample 3	Average
TS	95.25	95.56	92.21	93.34
Moisture	4.75	4.44	7.79	5.66
Ash	4.39	5.28	5.02	4.90
VS	87.86	90.28	87.19	88.44

4.1.1.2. Lignin-rich residue generated from pretreatment. The feedstocks obtained from the acid hydrolysis process had a viscous structure relative to the raw lignocellulosic materials. The proximate analyses of PC and PW are summarized in Table 4.3 and Table 4.4, respectively.

The lignin contents of both the pretreated corn and wheat-based lignin residues decreased by 27% compared to the raw lignocellulosic materials. As the lignin flocs formed by the addition of an acid solution had a more viscous structure relative to the raw material, the moisture content of the lignin-rich residue increased in pretreated samples. The ash contents of pretreated corn and wheat-based residues increased by 20% and 66%, respectively, compared to raw materials because of diluted acid pretreatment reactions. According to Anaya et al. (2011), the high ash content of a sample restricts its use as an activated carbon precursor, but the sample having an ash content value lower than 10% can be used as feedstock in activated carbon production.

Table 4.3. Proximate analysis of PC residue.

Parameter, %	Sample 1	Sample 2	Sample 3	Average
TS	67.13	67.46	68.72	67.77
Moisture	32.87	32.54	31.28	32.23
Ash	11.06	10.11	9.19	10.12
VS	56.07	57.35	59.53	57.65

Table 4.4. Proximate analysis of PW residue.

Parameter, %	Sample 1	Sample 2	Sample 3	Average
TS	67.35	66.07	66.23	66.55
Moisture	32.65	33.93	33.77	33.45
Ash	10.02	8.21	8.77	9.00
VS	57.33	57.86	57.46	57.85

4.1.1.3. Lignin-rich residue generated from fermentation. After sterilization and delignification, the lignin-rich fermentation residue had a compact structure relative to the pretreated samples. Proximate analyses of FC and FW were summarized in Table 4.5 and Table 4.6, respectively.

Table 4.5. Proximate analysis of FC residue.

Parameter, %	Sample 1	Sample 2	Sample 3	Average
TS	84.15	78.71	80.11	80.99
Moisture	15.85	21.29	19.89	19.01
Ash	10.16	9.47	11.42	10.35
VS	73.99	69.24	68.69	70.64

Table 4.6. Proximate analysis of FW residue.

Parameter, %	Sample 1	Sample 2	Sample 3	Average
TS	83.06	82.35	78.18	81.19
Moisture	16.94	17.65	21.82	18.80
Ash	7.12	7.48	7.42	7.34
VS	75.94	74.87	70.76	73.85

The TS contents of both FC and FW samples decreased by 13% compared to the TS contents of raw lignocellulosic materials. The ash content of corn-based fermented lignin residue was higher than that of the wheat-based fermented lignin residue. FC and FW

samples have high VS contents – 70.64% and 73.85%, respectively. The VS content plays a vital role in estimating the approximate tar content of feedstocks, which is volatile and results in a dramatic weight loss at carbonization temperatures (Hu et al., 2001).

4.1.2. Determination of Extractives

Before the lignin determination, non-structural materials should be removed from the biomass since they interfere with subsequent analysis. During experiments, three lignocellulosic batch samples were sequentially extracted with water and then ethanol. The percentages of water soluble and ethanol soluble extractives in raw corn stover and wheat straw are given in Tables 4.7 and 4.8, respectively.

Table 4.7. Extractive content of corn stover samples.

Parameter, %	Sample 1	Sample 2	Sample 3	Average
Water Extractives	15.86	18.54	19.76	18.05
Ethanol Extractives	4.58	3.31	5.65	4.51
Extractives	20.44	21.84	25.41	22.56

The raw corn stover samples contained a higher amount of extractives (22.56%) than the raw wheat straw samples (20.15%). Since acid hydrolysis and fermentation processes were performed on the extractive-free biomass, there was no need to determine the extractive contents of the pretreated and fermented lignin residues used as activated carbon precursors.

Table 4.8. Extractive content of wheat straw samples.

Parameter, %	Sample 1	Sample 2	Sample 3	Average
Water Extractives	18.76	15.66	14.56	16.32
Ethanol Extractives	3.13	4.59	3.77	3.83
Extractives	21.88	20.25	18.33	20.15

4.1.3. Determination of Lignin Content of Feedstocks

4.1.3.1. Raw lignocellulosic materials. The percentage of acid soluble lignin, acid insoluble lignin and total lignin in corn stover and wheat straw samples are given in Table 4.9 and Table 4.10. The lignin content of wheat straw samples (23.18%) was higher than for corn stover samples (14.60%) by 9.42 %.

Table 4.9. Lignin content of raw corn stover samples.

Parameter, %	Sample 1	Sample 2	Sample 3	Average
ASL	1.33	1.23	0.83	1.13
AIR	25.98	23.65	26.75	25.46
AIL	17.01	17.70	15.07	16.60
Extractive-free lignin	18.34	18.93	15.90	17.72
Lignin in biomass	14.60	15.17	11.86	14.60

Table 4.10. Lignin content of raw wheat straw.

Parameter, %	Sample 1	Sample 2	Sample 3	Average
ASL	1.13	1.29	1.24	1.22
AIR	23.42	24.19	27.46	25.02
AIL	20.91	19.63	25.33	21.96
Extractive-free lignin	22.04	20.92	26.58	23.18
Lignin in biomass	17.22	17.77	21.70	23.18

4.1.3.2. Lignin-rich residue generated from pretreatment. The percentages of lignin contents in PC and PW residues are given in Table 4.11 and Table 4.12.

Table 4.11. Lignin content of PC residue.

Parameter, %	Sample 1	Sample 2	Sample 3	Average
ASL	1.39	1.17	1.25	1.27
AIL	67.93	75.18	71.6	71.57
Lignin in Biomass	69.32	76.35	72.85	72.84

Table 4.12. Lignin content of PW residue.

Parameter, %	Sample 1	Sample 2	Sample 3	Average
ASL	1.44	1.46	1.27	1.39
AIL	73.88	70.62	70.75	71.75
Lignin in Biomass	75.32	72.08	72.02	73.14

The lignin content of PC residue was five times higher than that of raw corn stover. Further, relative to raw wheat straw, the lignin content of the PW residue increased approximately three fold. The results show that the delignification process has been very effective for pretreated feedstocks.

4.1.3.3. Lignin-rich residue generated from fermentation. The percentages of lignin content in FC and FW residues are given in Table 4.13 and Table 4.14.

Table 4.13. Lignin content of FC residue.

Analyse	Sample 1	Sample 2	Sample 3	Average
ASL, %	1.61	1.46	1.58	1.55
AIL, %	45.96	46.81	46.55	46.44
Lignin in Biomass, %	47.57	48.27	48.13	47.99

The lignin content of the FC residue was found to be three times higher than that of raw corn stover. Additionally, the lignin content of the FW feedstocks was about two and a half times greater than that of raw wheat straw. The results show that the delignification process has also been effective for fermented feedstocks.

Table 4.14. Lignin content of FW residue.

Analyse	Sample 1	Sample 2	Sample 3	Average
ASL, %	1.74	1.87	1.46	1.69
AIL, %	60.49	50.17	57.64	56.10
Lignin in Biomass, %	62.23	52.04	59.10	57.79

In summary, the characterization data for corn and wheat-based feedstocks as a whole are given in Table 4.15.

Table 4.15. Characteristics of all feedstocks.

Feedstock	TS, %	Moisture, %	Ash, %	VS, %	Lignin, %
RC: Raw corn stover	92.61	7.45	8.50	84.05	14.60
PC: Pretreated corn stover residue	67.77	32.23	10.12	57.65	72.84
FC: Fermented corn stover residue	80.99	19.01	10.35	70.64	47.99
RW: Raw wheat straw	93.34	5.66	4.90	88.44	23.18
PW: Pretreated wheat straw residue	66.55	33.45	9.00	57.85	73.14
FW: Fermented wheat straw residue	81.19	18.80	7.34	73.85	57.79

The TS contents of raw corn stover and wheat straw were measured as 92.61% and 93.34%, respectively. Zhu et al. (2010) found the TS content of corn stover and wheat straw to be 94.7% and 93.0%, which are comparable with this study. The ash content of RC samples (8.50%) was higher than literature values, which are in the range of 3.8 to 8.0%. The ash content of WR samples (5.66%) was within the range of literature values, which varied from 1.3 to 8.30%. In contrast, the lignin content of RC samples was similar to literature values (6 to 22%), while the observed lignin content for RW samples was higher than literature values (12 to 18%) (Foyle et al., 2007; Wolfrum and Sluiter, 2009; Singh et al., 2011; Huijgen et al., 2012; Liu et al., 2012).

As seen in Table 4.15, the PC, PW, FC, and FW samples have high lignin contents – 72.84%, 73.14%, 47.99%, and 57.79%, respectively. Since this is the first study investigating the production of activated carbon as a value-added product from lignin-rich residues generated from bioethanol processes, no previously published research about lignin-rich residues obtained from pretreatment and bioethanol fermentation processes exists. However, Orfao et al. (1999) showed that lignin was the main component responsible for most of the char production, and similarly, Zanzi et al. (2002) noted that a high char yield can be observed when biomass has a high lignin content. In addition, Yorgun and Yıldız (2015), argued that the low ash content (below 10%) of biomass resources makes them good starting materials for the production of activated carbon, which matches ash values found in this study. The results of these analyses showed that the feedstocks originated from corn stover and wheat straw samples were appropriate for activated carbon production.

4.2. Thermogravimetric Analysis of Proceeded Feedstocks

In this study, TGA results were used to monitor the course of the carbonization stages, and the results helped to choose different carbonization temperatures in the selection of the experimental conditions. Under identical experimental conditions, TGA experiments were carried out to obtain information in terms of yields of acid impregnated samples.

4.2.1. TGA Analysis of Pretreated Feedstocks

During thermal degradation, PC has three distinct stages of weight loss. Figure 4.1 shows the three stages of the thermal decomposition behavior of PC. A small amount of weight loss was observed from 25°C to 193°C due to the release of moisture. Following the first stage, there was negligible weight loss (<0.5%) in the temperature range of 193 to 251°C, whereas there was significant weight loss from 251 to 425°C due to the release of volatiles. A low amount of weight loss was observed in the last stage from 455 to 700°C (Table 4.16). The profile suggests that the weight loss could be described by the VS content of PC samples. In the carbonization process, the tar content was a predominant product of devolatilization, indicated by a significant weight loss (64% by weight) in the temperature in the range of 251°C to 425°C. This can be seen in the derivative thermogravimetry (DTG) curve when a sharp peak was observed at 355°C related to the pyrolysis of volatiles. TGA results showed that the char yield of PC samples could be above 30% after the active pyrolysis stage.

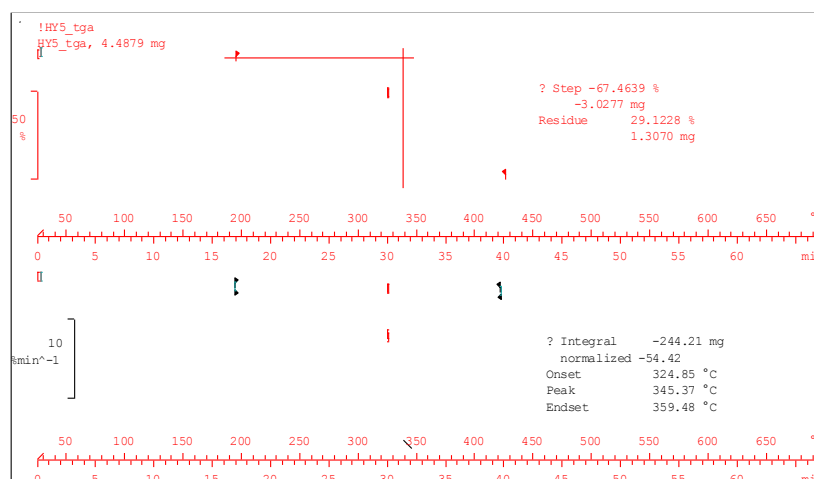


Figure 4.1. Typical Thermogravimetric Analysis diagram of PC samples.

Table 4.16. Temperature range and weight loss of PC samples.

Stage	Temperature, °C	Weight Loss, wt %
I	25	100
	193	96.50
II	251	94.02
	425	29.50
III	455	29.50
	695	5.25

A typical TGA plot of PW in N₂ atmosphere is shown in Figure 4.2. The first stage ranged from 25 to 182°C because of dehydration. Following the first stage, there was negligible weight loss (<0.5%) in the temperature range of 182 to 273°C. After this step, a sharper drop in the mass of PW was observed from 97.47% to 35.95% in the second stage, referred to active pyrolysis, at 273 to 383°C. In the active pyrolysis stage, the pyrolysis of VS was obtained at 362°C when a sharp peak occurred in the DTG curve, which is similar to PC samples. The third stage, called as passive pyrolysis zone, ranged from about 383 to 700°C, and the char yield of PW samples could be above 30% after active pyrolysis stage.

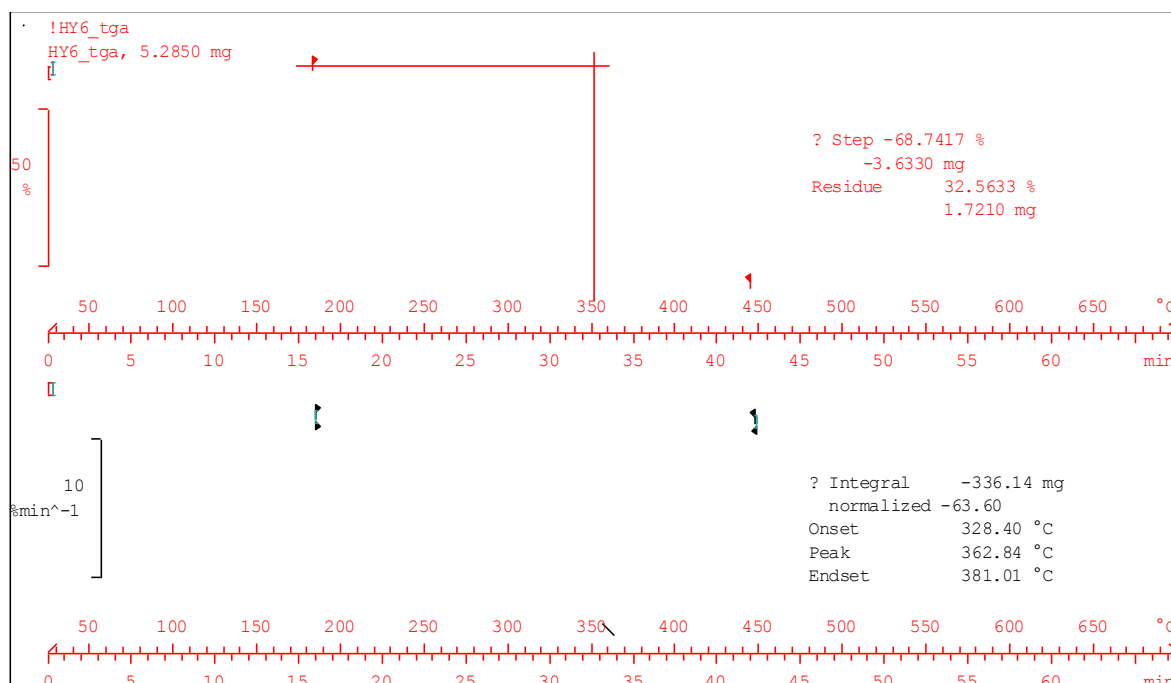


Figure 4.2. Typical Thermogravimetric Analysis diagram of PW samples.

Table 4.17. Temperature range and weight loss PW samples.

Stage	Temperature, °C	Weight Loss, wt %
I	25	100
	182	98.42
II	273	97.47
	383	35.95
III	383	35.95
	695	25.16

4.2.2. TGA Analysis of Fermented Feedstocks

The TGA result and DTG curves of FC samples are shown in Figure 4.3. However, the TGA result of FC samples was very different from the TGA results of PC, PW and FW samples since the transition of the pyrolysis stage was not clear, as seen in Figure 4.3. The low amount of weight loss at low temperatures can be attributed to the release of moisture; however, the weight loss increased gradually between 215 and 520°C. There are two small peaks in the DTG curves; the first one was observed at 170°C, and the second one appeared at 530°C.

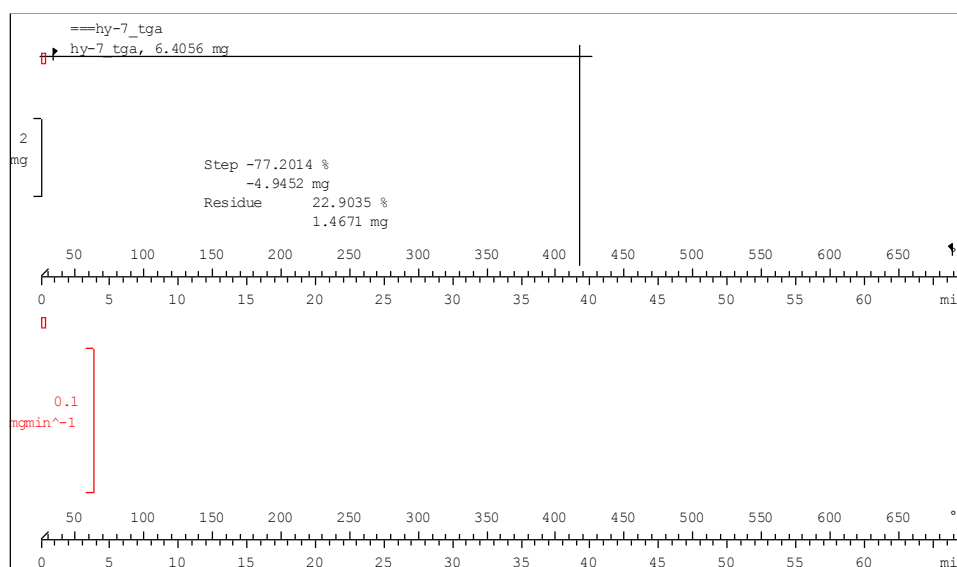


Figure 4.3. Typical Thermogravimetric Analysis diagram of lignin-rich residue from FC samples.

Table 4.18. Temperature range and weight loss of lignin-rich residue from FC samples.

Stage	Temperature, °C	Weight Loss, wt %
I	25	100
	140	95.60
II	215	85.02
	520	46.24
III	520	46.24
	695	21.70

The weight loss (TG) and DTG curves of FW samples are shown in Figure 4.4. The first stage of weight loss ranged from 25°C to approximately 160°C (Table 4.19), which was clearly distinct from the other stages of weight loss because of the moisture content of the sample. The second phase started at roughly 235°C, and the volatile tar was a predominant product by 42% weight loss since there was only one observable peak in the derivative plot region with a temperature range of 235 to 350°C. However, after the second stage, there was a continuous and slow rate of weight loss between 350 and 700°C. Given the slow rate of weight loss, this third stage represented the passive pyrolysis zone. As a result, the product yield of FC samples could be approximately 30-40%.

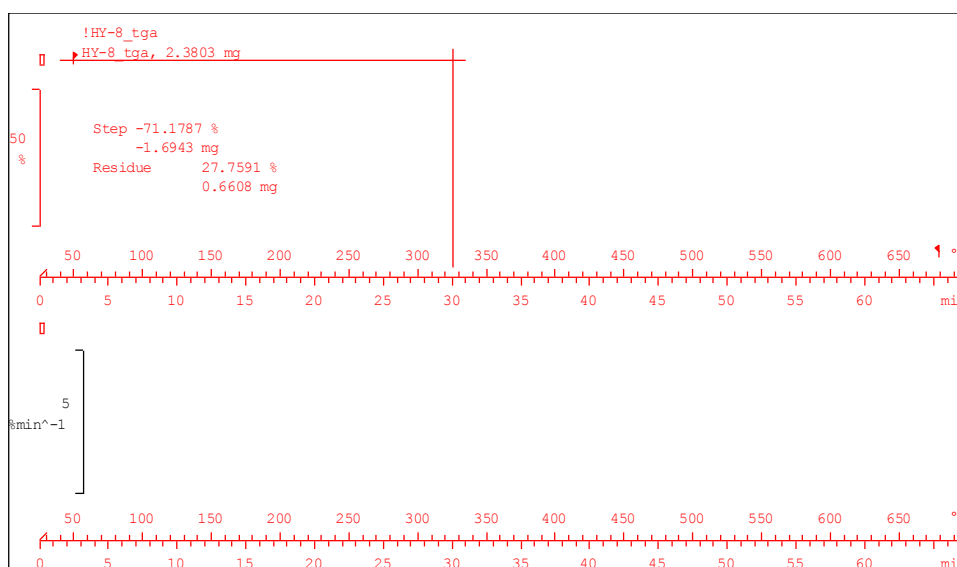


Figure 4.4. Typical Thermogravimetric Analysis diagram of lignin-rich residue from FW samples.

Table 4.19. Temperature range and weight loss of of lignin-rich residue FW samples.

Stage	Temperature, °C	Weight Loss, wt %
I	25	100
	162	97.18
II	235	92.63
	350	50.90
III	350	50.90
	695	26.94

4.3. The Effect of Different Process Conditions on Yield and Chemical Recovery

For production of activated carbon from different types of lignin-rich residues, H_3PO_4 was used as an activating agent in the impregnation step. Solutions of 30%, 40% and 50% H_3PO_4 (w/w) were mixed with feedstocks in the ratio of 2 mL acid per 1 g sample and carbonized at temperatures of 400°C, 500°C, 600°C and 700°C, as mentioned in Section 3.5. At H_3PO_4 concentration of 30%, 40%, and 50%, the impregnation ratios were about 1.5, 1.7, and 1.8, respectively. Thus, ten different activated carbon samples were obtained for each type of feedstock labelled as PC, PW, FC, and FW.

Product yield and chemical recovery (C.R.) are important measures for the feasibility of preparing activated carbon from a given precursor. According to Guo and Rockstraw (2007), significant product yield differences can be observed depending on the origins of the feedstocks. In addition to the origin of the feedstocks, temperature and impregnation ratio used during the carbonization stage are also factors that affect the char yield. Thus, the effects of impregnation ratio and temperature on product yield and chemical recovery were estimated for each activated carbon sample.

The carbon yield and chemical recovery values of activated carbon produced from PC, PW, FC, and FW based residues were given in four tables – from Table 4.20 to Table 4.23. In addition, the effect of carbonization temperature and H_3PO_4 concentration on the yield of PC, PW, FC, and FW are shown more clearly in Figure 4.5, Figure 4.7, Figure 4.9 and Figure 4.11, respectively. Moreover, the graphs, which represented the change of chemical recovery according to the impregnation ratio and the temperature, were given in Figure 4.6, Figure 4.8, Figure 4.10, and Figure 4.12, respectively.

In PC residues, the yields of char impregnated with H_3PO_4 dramatically decreased between the temperatures of 400°C and 700°C. In addition, activation with a lower H_3PO_4 impregnation ratio resulted in a higher yield range. The yield of sample PC1 (impregnated with 40% H_3PO_4 and carbonized at 400°C) found as 37.63% (w/w) was significantly higher than that of the others samples, as shown in Figure 4.5. For this type of lignin-rich residue, the chemical recovery ratios decreased with increasing temperature and impregnation ratio. As can be seen Figure 4.6, the H_3PO_4 recovery rate decreased when the temperature raised to 700°C from 400°C for all impregnation ratios. However, the decline ratios of products impregnated with 50% H_3PO_4 were lower relative to other concentrations at temperatures between 400°C and 700°C. As a result, the 50% H_3PO_4 concentration was the most suitable activation ratio to produce PC-based activated carbons.

Table 4.20. Yields and C.R. ratios for PC-based activated carbon.

Sample No	Temperature, °C	H_3PO_4 , %	Yield, %	CR, %
PC1	400	40	37.63	64.21
PC2		50	34.44	60.12
PC3	500	30	36.81	61.45
PC4		40	34.13	56.8
PC5		50	34.72	55.13
PC6	600	30	31.50	59.41
PC7		40	30.97	42.25
PC8		50	27.26	40.36
PC9	700	30	21.56	35.6
PW10		40	20.18	36.94

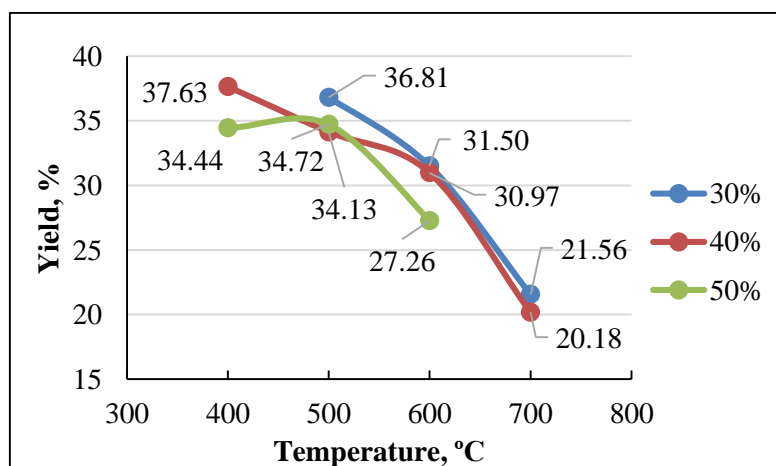


Figure 4.5. The effect of process conditions on yield for PC-based activated carbon.

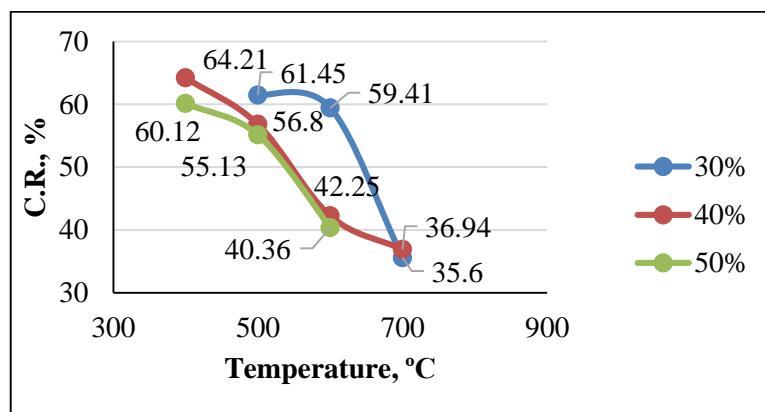


Figure 4.6. The effect of process conditions on C.R. for PC-based activated carbon.

The effect of carbonization temperature and H₃PO₄ concentration on yield and chemical recovery for PW residues had similar results with the PC residue based production process. As the carbonization temperature increased from 400°C to 700°C, the char yield decreased from 38.44% to 28.38% at 50% H₃PO₄ concentration, as seen in Figure 4.7. The yield rate of activated carbons impregnated with 40% H₃PO₄ decreased from 41.91% to 29.40%. Products impregnated with 30% H₃PO₄ had the maximum yield rates. As can be seen in Figure 4.8, the H₃PO₄ recovery rate dramatically decreased when the temperature increased from 400°C to 700°C at each impregnation ratio.

Table 4.21. Yields and C.R ratios for PW-based activated carbon.

Sample No	Temperature, °C	H ₃ PO ₄ conc., %	Yield, %	CR, %
PW1	400	40	41.91	64.80
PW2		50	38.44	49.15
PW3	500	30	34.18	56.21
PW4		40	33.24	49.27
PW5		50	28.38	44.85
PW6	600	30	31.70	44.19
PW7		40	29.25	39.83
PW8		50	28.50	25.77
PW9	700	30	33.66	37.15
PW10		40	29.40	35.93

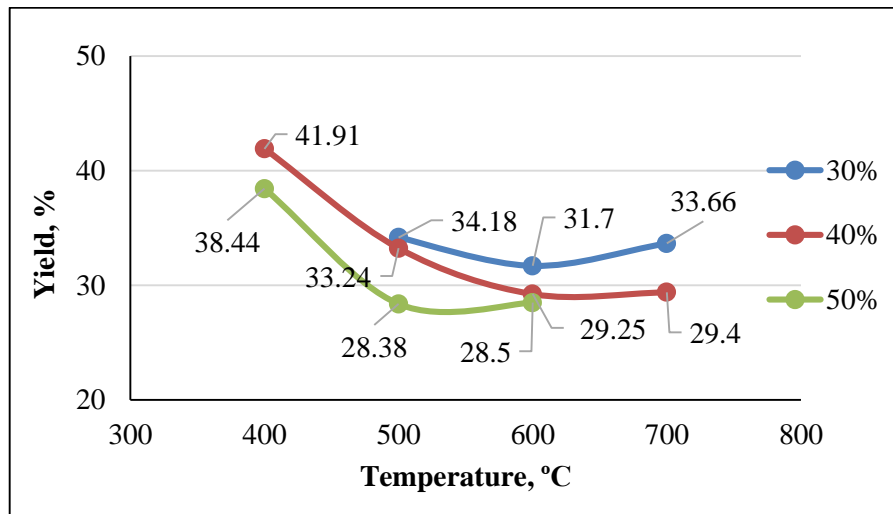


Figure 4.7. The effect of process conditions on yield for PW-based activated carbon.

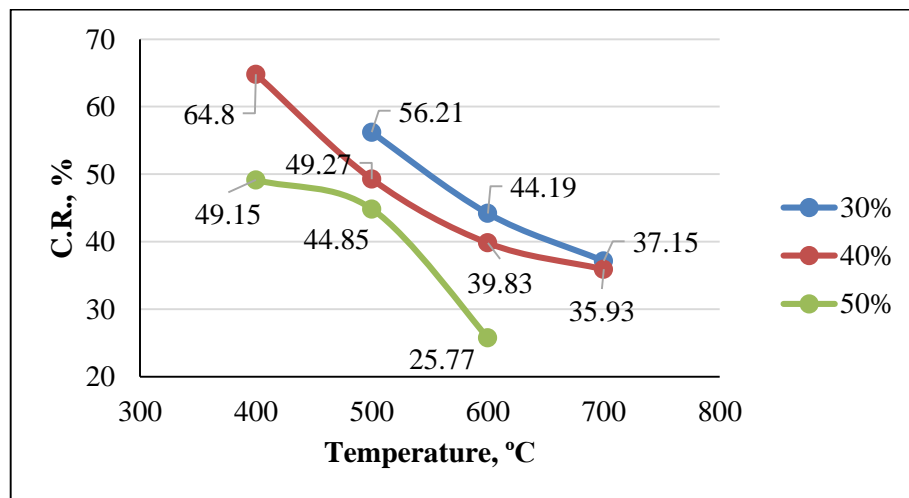


Figure 4.8. The effect of process conditions on C.R. for PW-based activated carbon.

In FC and FW-based activated carbon, yield and C.R. ratios again decreased with increasing temperature as shown in Figures 4.9 and 4.10 and Figures 4.11 and 4.12, respectively. In addition, a lower impregnation ratio resulted in a higher amount of char yield and C.R. ratio.

Table 4.22. Yields and C.R ratios for FC-based activated carbon.

Sample No	Temperature, °C	H ₃ PO ₄ conc., %	Yield, %	CR, %
FC1	400	40	41.12	40.79
FC2		50	41.79	41.37
FC3	500	30	42.20	51.16
FC4		40	40.17	44.06
FC5		50	37.24	39.27
FC6	600	30	38.25	48.25
FC7		40	36.33	42.14
FC8		50	25.14	36.15
FC9	700	30	26.25	37.24
FC10		40	11.12	35.67

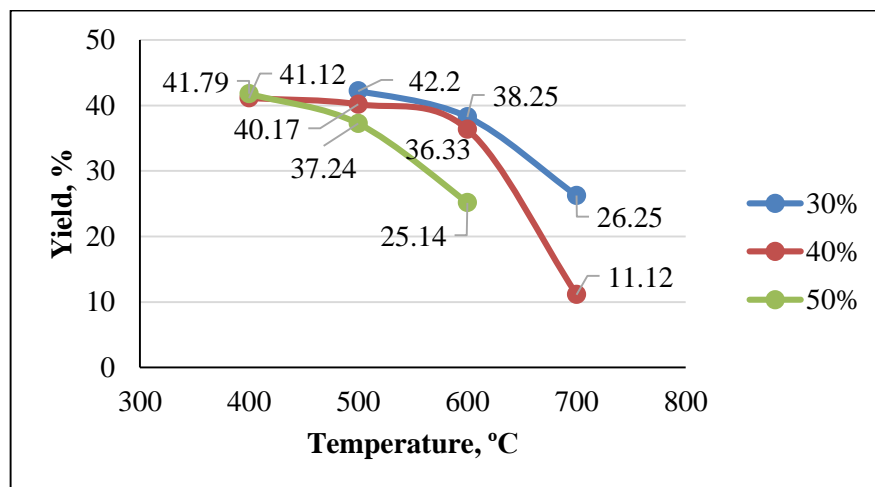


Figure 4.9. The effect of process conditions on yield ratio for FC-based product.

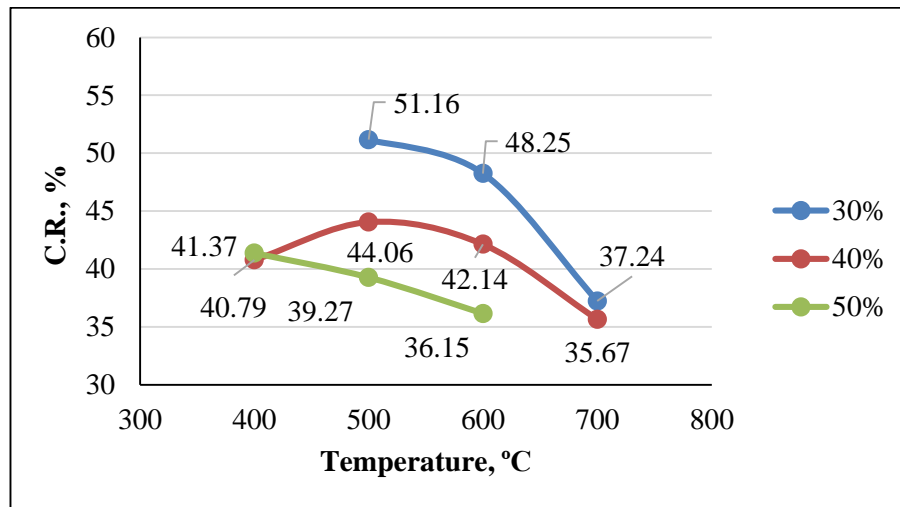


Figure 4.10. The effect of process conditions on C.R. ratio for FC-based product.

Table 4.23. Yields and C.R ratios for FW-based activated carbon.

Sample No	Temperature, °C	H ₃ PO ₄ conc., %	Yield. %	CR. %
FW1	400	40	40.20	52.14
FW2		50	39.25	41.31
FW3	500	30	39.28	50.82
FW4		40	40.67	48.78
FW5		50	35.71	39.86
FW6	600	30	41.38	49.29
FW7		40	29.80	41.97
FW8		50	29.15	31.73
FW9	700	30	17.47	32.22
FW10		50	21.15	34.52

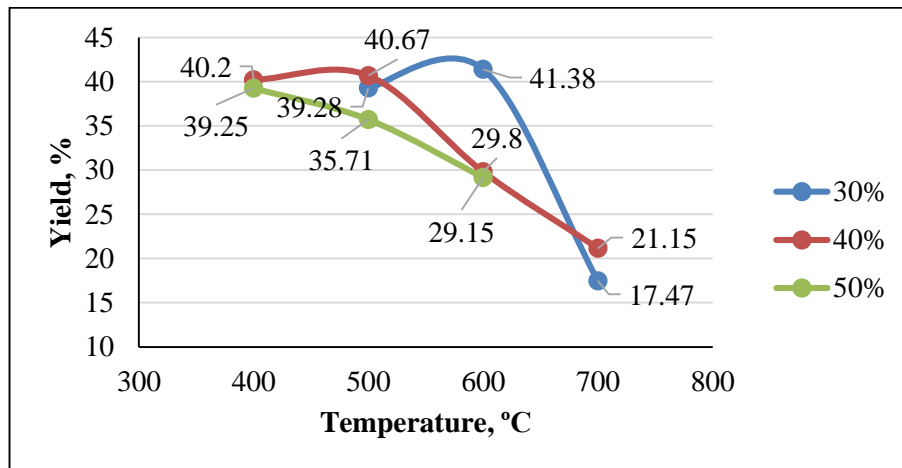


Figure 4.11. The effect of process conditions on yield ratio for FW-based product.

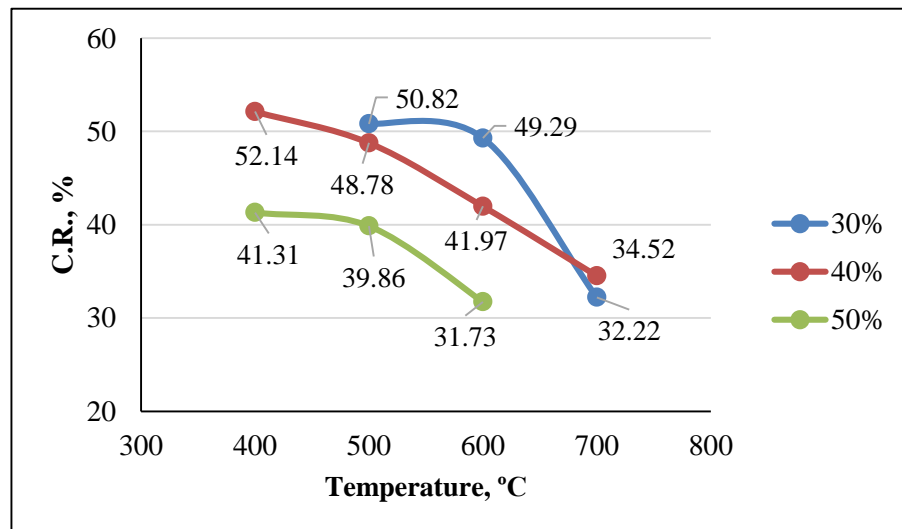


Figure 4.12. The effect of process conditions on C.R. ratio for FW-based product.

For all types of feedstock, the yield of activated carbon decreased with increasing activation temperature, as the weight loss rate increased due to the large amount of volatiles that can be easily released at higher temperatures. In addition, at each carbonization temperature, the activated carbon yields decreased with increasing impregnation ratio. The H_3PO_4 reacted with the char and volatile matter and diffused quickly out of the surfaces of particles during the process. Therefore, with a high H_3PO_4 content, the pyrolysis of surface carbon atoms became predominant, leading to an increase in the weight loss and a low carbon yield. The presence of phosphoric acid during activation promoted the depolymerization, dehydration and redistribution of samples and favored the conversion of aliphatic to aromatic

compounds, thus increasing the yield of activated carbon (Prahas et al., 2008). Under the experimental conditions, a carbonization temperature of 500°C and impregnation ratio of 1.5 were found to be suitable for the desired activated carbon yield. Nevertheless, it should be evaluated with the physical characterization of the activated carbon products.

The chemical recovery of activated carbon also decreased with increasing carbonization temperature at each impregnation ratio. The activated carbon samples with lower impregnation ratios had higher H₃PO₄ recovery values at the same carbonization temperature. Similar chemical recovery values have been previously reported in literature (Hayashi et al., 2000). At a carbonization temperature of 500°C and impregnation ratio of 1.5, the product was found to be suitable for the desired chemical recovery.

The carbon yield and chemical recovery values of activated carbon samples produced from PC, PW, FC, and FW residues show that the selection of H₃PO₄ as an activating agent is a good choice since the characterization of the produced activated carbon is very compliant with literature and the quality parameters have high values. In addition, the carbonization temperature had a very critical role with respect to the yield of the final product. The yield gradually declined with an increase in the carbonization temperature (Hayashi et al., 2000). This is an expected phenomenon because the amount of volatilization of volatile matter increases with the carbonization temperature, therefore the amount of final product is reduced.

4.4. pH of Produced Activated Carbon

The pH values of all produced activated carbon samples are given in Table 4.24. According to these results, the pH values of the products were influenced by the impregnation ratios.

Table 4.24. pH values of the activated carbon samples.

Temperature, °C	H ₃ PO ₄ conc., %	PC	FC	PW	FW
400	40	5.29	5.80	5.7	5.44
	50	5.07	5.89	5.32	5.61
500	30	5.23	5.45	5.91	5.57
	40	4.92	5.24	5.55	5.44
	50	4.88	5.67	5.27	5.89
600	30	4.86	5.24	5.84	5.06
	40	4.77	5.37	5.08	5.42
	50	4.85	5.44	5.11	5.32
700	30	4.70	5.21	5.24	5.00
	40	5.02	5.00	4.96	5.19

The effects of impregnation ratio and carbonization temperature on pH values for the various prepared activated carbon samples are represented in four figures below – Figure 4.12 through Figure 4.15. All pH values were found to be between 4.70 and 5.80. It was noted that for each type of feedstock, the pH values were not in the acidic range, as they are higher than 5, with the exception of the pretreated samples that have pH values lower than 5. This could be explained by the higher ash content of these feedstocks used for the preparation of activated carbon. Montane et al. (2005) showed that the carbonization of lignin produces a very small quantity of ash, and thus, this pH value was due to the rather high ash content of pretreated feedstocks. In Figure 4.13, it was observed that the pH ratios of PC-based products decreased with increasing I.R. because the quantity of H₃PO₄ used for the activation was influenced slightly by the pH of the activated carbon. In contrast, the weak ash content of fermented feedstocks explains their pH values, which are higher than that of the others (Figures 4.15 and 4.16). As a result, the activated carbon resulting from the precursors having low ash contents have higher pH values, and thus, the activated carbon of selected feedstocks cannot be considered hazardous waste materials and are not corrosive (Ketcha et al., 2012).

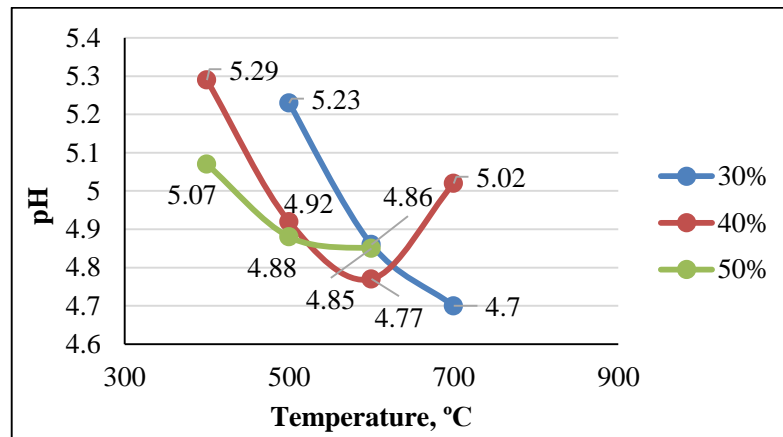


Figure 4.13. The effect of process conditions on pH ratio for PC-based product.

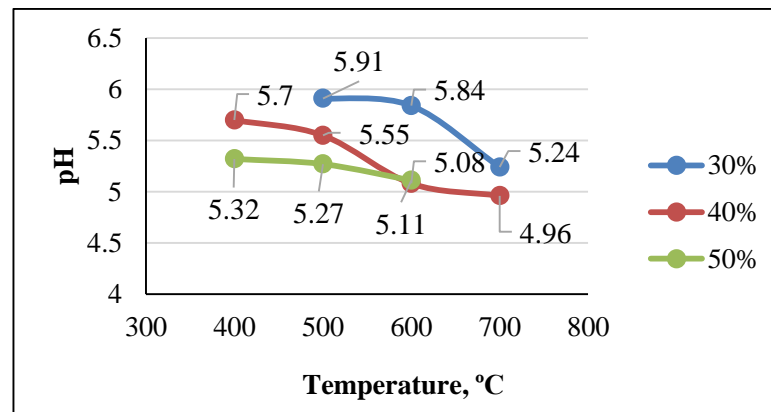


Figure 4.14. The effect of process conditions on pH ratio for PW-based product.

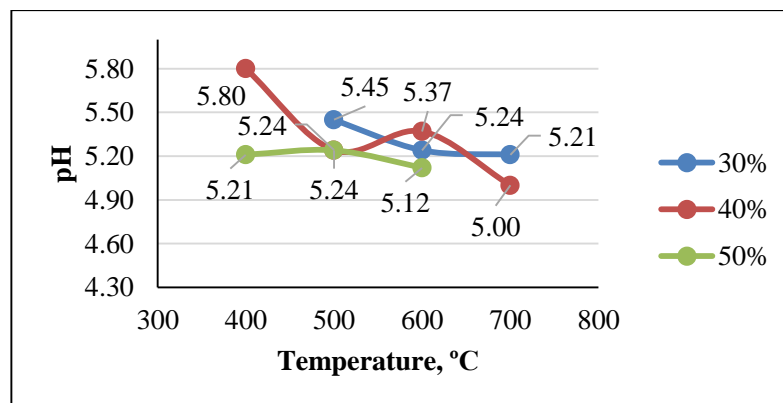


Figure 4.15. The effect of process conditions on pH ratio for FC-based product.

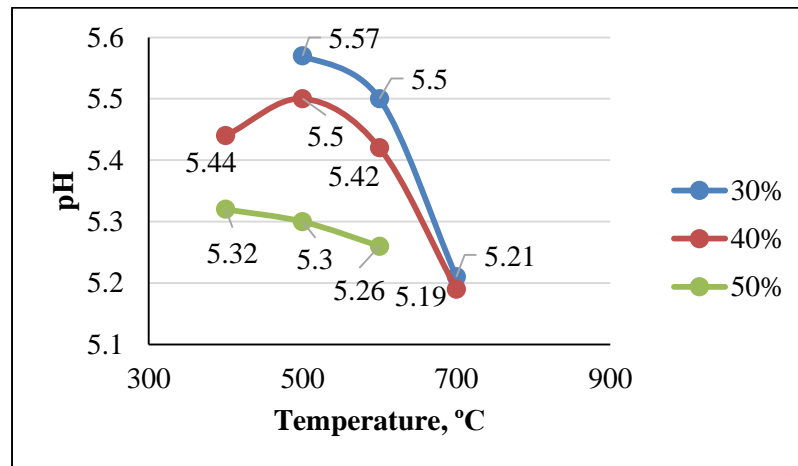


Figure 4.16. The effect of process conditions on pH ratio for FW-based product.

4.5. Ash Content of Produced Activated Carbon

The ash content of activated carbon varies in the range of 1–12% and is mainly composed of silica, alumina, iron, alkaline and alkaline earth metals (Çeçen, 2014). Generally, a good activated carbon must have low ash content because a small increase in ash content causes a decrease in the adsorptive properties of activated carbon. In this study, the PC, PW, FC, and FW samples have estimated ash contents of 10.12%, 9%, 10.35% and 7.34%, respectively (Table 4.15). However, the ash contents of the products were slightly higher than typical values given in Çeçen (2014). For the PC, PW, FC, and FW series, these values were in the range of 13.45-16.42%, 11.50-15.15%, 14.524-17.15% and 10.45-16.23%, respectively. When the carbonization temperature increased, the ash content of samples increased, as shown in Table 4.25. Moreover, a high amount of ash may be the result of the high impregnation ratios. Although H_3PO_4 restricted the formation of tar, high impregnation ratios increased the amount of tar. As a result, it was expected that with an increase in the ash content of the samples, the amount of tar formation would also increase. In order to decrease the ash content, low ratios should be selected for impregnation, which were taken as constant during the experiments. As a result, the optimum carbonization temperature for selected feedstocks could be 500°C.

Table 4.25. Ash content of produced activated carbon samples.

Temperature, °C	H ₃ PO ₄ conc., %	PC	FC	PW	FW
400	40	13.45	14.24	11.50	10.45
	50	14.07	15.40	12.94	12.73
500	30	14.86	15.65	12.48	13.44
	40	13.48	17.04	13.67	12.56
	50	14.25	16.55	14.43	13.28
600	30	13.76	14.72	14.92	14.40
	40	15.98	16.84	13.45	15.75
	50	16.42	17.95	14.26	16.42
700	30	14.26	17.83	14.85	16.23
	40	15.13	17.15	15.15	15.09

4.6. The Influence of Different Process Conditions on the BET Surface Area

Adsorption capacity related parameters are usually determined from gas adsorption measurements. In this study, the specific surface area was calculated by applying the BET equation. The BET surface areas of the samples can be obtained from the plot of $P/V (P_0 - P)$ versus P/P_0 plot, in the relative pressure range of 0-0.2, as shown in Figure 4.17 as an example.

Samples impregnated with 30% H₃PO₄ and carbonized at 400°C resulted in very low surface area values of 2.4 m²/g. In addition, a sample impregnated with 50% H₃PO₄ and carbonized at 700°C had relatively low results. It was also observed that the sample was not resistant to a 700°C carbonization temperature, resulting in only approximately a 10% yield. These preliminary results show that a sample impregnated with a low chemical concentration and with a low carbonization temperature does not have a high BET surface area. Similarly, the physical characteristic values of the sample with a high activation ratio and carbonization temperature, which is higher than the temperature range of TGA experiments, were not consistent with the literature values. In literature, activated carbon samples have a large internal surface area ranging from 500 to 2000 m²/g (Suhas and Carrot, 2007). As a result, a

700°C carbonization temperature with 50% H₃PO₄ and a 400°C carbonization temperature with 30% H₃PO₄ were not considered as potential experimental conditions.

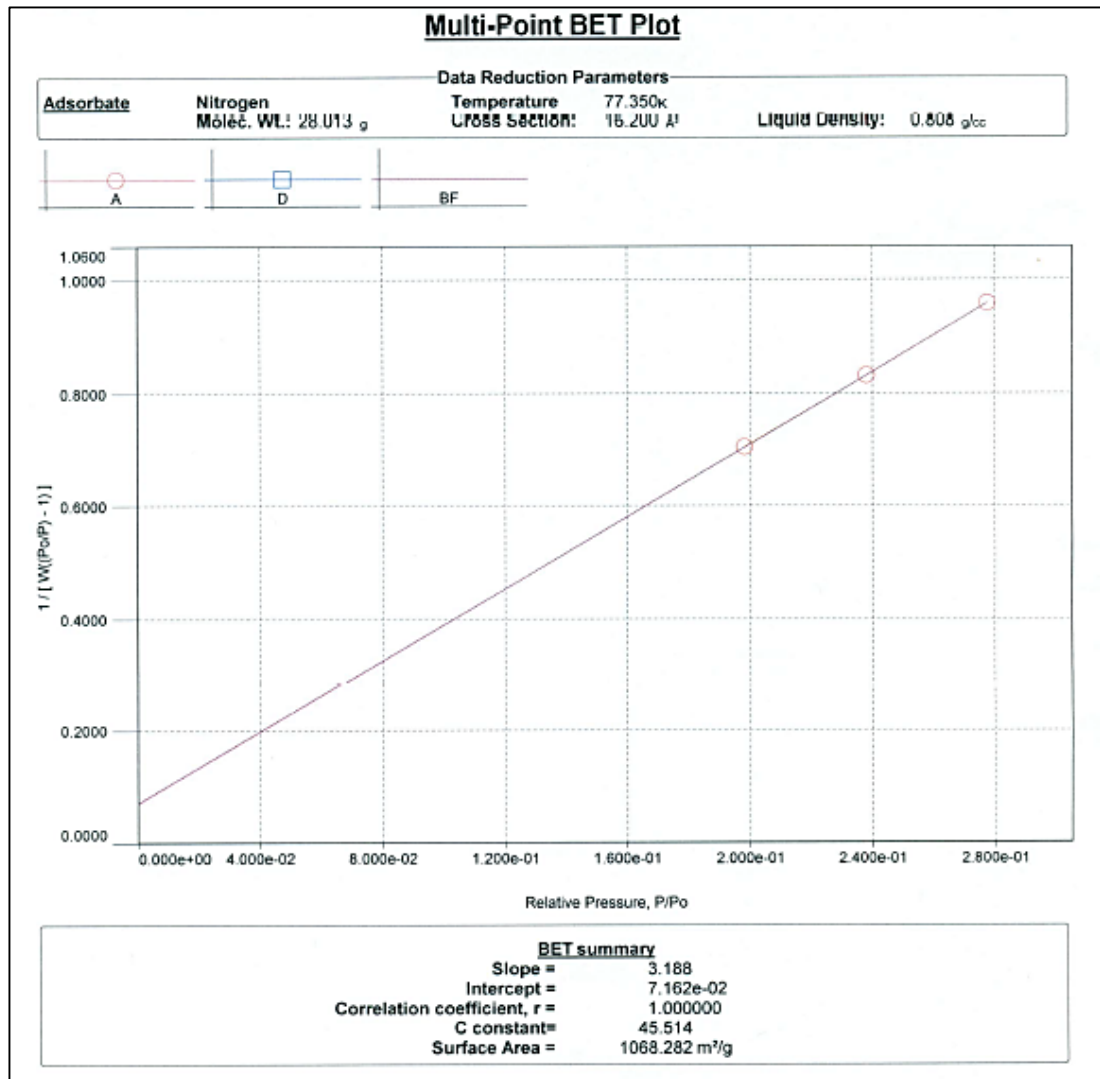


Figure 4.17. An example to multi-point BET of produced activated carbon.

4.6.1. PC-Based Activated Carbon

BET surface area values for PC-based activated carbon samples are shown in Table 4.26.

Table 4.26. BET surface areas for PC-based activated carbon samples.

Sample No	Temperature, °C	H ₃ PO ₄ conc., %	BET Surface Area, m ² /g
PC1	400	40	176
PC2		50	168
PC3	500	30	658
PC4		40	733
PC5		50	753
PC6	600	30	486
PC7		40	694
PC8		50	658
PC9	700	30	486
PC10		40	383

In PC-based activated carbon samples, the BET surface area values ranged from 168 to 753 m²/g. Activated carbon samples produced at 500°C with 40% and 50% H₃PO₄ concentrations had higher surface area values relative to the others. When the carbonization temperature reached to 600°C for 40% and 50% H₃PO₄ concentrations, the BET surface area values were in good agreement with literature. However, about 60% of H₃PO₄ still remained in the carbonized sample, and the yield decreased to 9.5% when the temperature was 700°C. In addition, the BET surface area dramatically decreased with an increase in temperature from 600°C to 700°C. Thus, the highest BET surface area (753 m²/g), the optimum product yield and chemical recovery were observed in sample PC5, which was impregnated with 50% H₃PO₄ and carbonized at 500°C. In Figure 4.18, the effect of carbonization temperature and H₃PO₄ concentration on the BET surface areas of PC-based products can be seen.

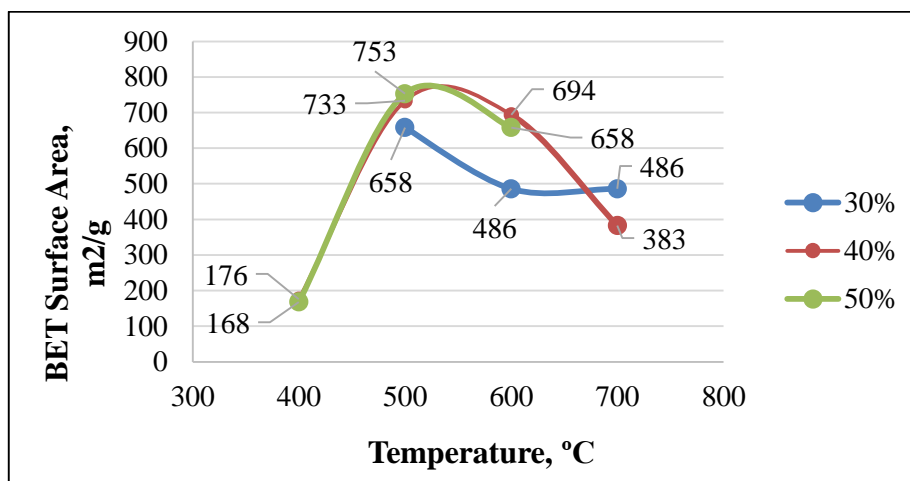


Figure 4.18. The effect of process conditions on BET surface area for PC-based product

4.6.2. PW-Based Activated Carbon

The BET surface area values of PW-based activated carbon samples are shown in Table 4.27. For PW-based products, BET surface area values varied from 327 to 1068 m²/g. As can be seen in Figure 4.19, BET surface area values increased as the temperature increased from 400°C to 700°C at all impregnation ratios. Sample PW10, impregnated with 40% H₃PO₄ and carbonized at 700°C, had the maximum BET surface area of 1068 m²/g, which is the highest value observed in this study. Activated carbon samples prepared from PW residue had the largest surface areas relative to those of other types of feedstocks used in this research. This indicated that PW samples were the most suitable feedstock to produce activated carbon, and the type of feedstock played a crucial role in determining the surface area. Generally, in products produced from other types of feedstock, H₃PO₄ recovery dramatically decreased from 65 to 30% when the carbonization temperature increased to 600-700°C. However, chemical recovery ratios ranging from 35% to 65% in activated carbon samples produced from PW residue were higher than that of the others. The effect of the impregnation ratio and carbonization temperature on BET surface areas for PW-based products is shown in Figure 4.19.

Table 4.27. BET surface areas of PW-based activated carbon.

Sample No.	Temperature, °C	H ₃ PO ₄ conc., %	BET Surface Area, m ² /g
FC1	400	40	327
FC2		50	604
FC3	500	30	820
FC4		40	782
FC5		50	872
FC6	600	30	867
FC7		40	931
FC8		50	862
FC9	700	30	1008
FC10		40	1068

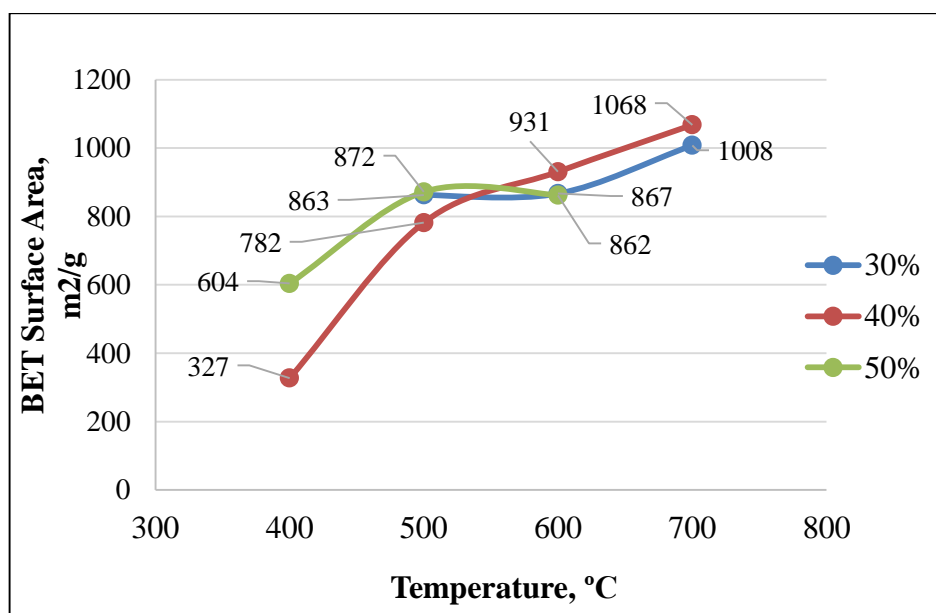


Figure 4.19. The effect of process conditions on BET surface area for PW-based product.

4.6.3. FC-Based Activated Carbon

The BET surface area values for fermented corn-based activated carbon samples are shown in Table 4.28.

Table 4.28. BET surface areas of FC-based samples.

Sample No.	Temperature, °C	H ₃ PO ₄ conc., %	BET Surface Area, m ² /g
FC1	400	40	24
FC2		50	34
FC3	500	30	77
FC4		40	109
FC5		50	19
FC6	600	30	348
FC7		40	143
FC8		50	402
FC9	700	30	10
FC10		40	15

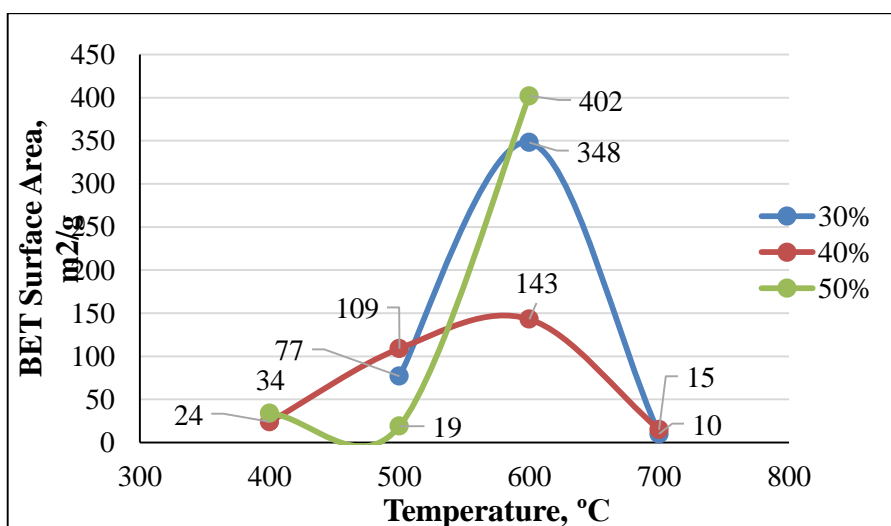


Figure 4.20. The effect of process conditions on BET surface area for FC-based product.

In activated carbon samples generated from FC-based samples, the surface areas increased at temperatures between 500°C to 600°C at all impregnation ratios, however, the maximum BET surface area of 402 m²/g was observed with sample FC8, which was impregnated with 50% H₃PO₄ and carbonized at 600°C. This value is not compatible with literature values. BET surface area results showed that FC-based activated carbon resulted in lower surface areas (10-402 m²/g) with respect to other types of feedstock under the same conditions. These preliminary results led to the conclusion that FC residue was not a proper precursor for activated carbon production by chemical activation with H₃PO₄. The effect of

carbonization temperature and H_3PO_4 concentration on BET surface areas for FC-based products is shown in Figure 4.20.

4.6.4. FW-Based Activated Carbon

BET surface area values for FW-based activated carbon samples are shown in Table 4.29.

Table 4.29. BET surface areas of FW-based samples.

Sample No.	Temperature, °C	H_3PO_4 conc., %	BET Surface Area, m^2/g
FW1	400	40	19
FW2		50	79
FW3	500	30	711
FW4		40	708
FW5		50	863
FW6	600	30	689
FW7		40	639
FW8		50	774
FW9	700	30	109
FW10		40	233

Sample FW5, which was impregnated with 50% H_3PO_4 and carbonized at 500°C, had the highest BET surface area of 863 m^2/g . After a temperature of 500°C, the BET surface area values showed a gradual three-fold decrease for all H_3PO_4 concentrations. These results indicate that at temperatures greater than 500°C, H_3PO_4 compounds did not work effectively as activating reagents for FW-based activated carbon processing. In Figure 4.21, the effect of carbonization temperature and H_3PO_4 concentration on BET surface area for FW-based products are shown. As a result, the best conditions to produce FW-based activated carbon with a very high specific surface area are an impregnation ratio of 1.8 and a carbonization temperature of 500°C.

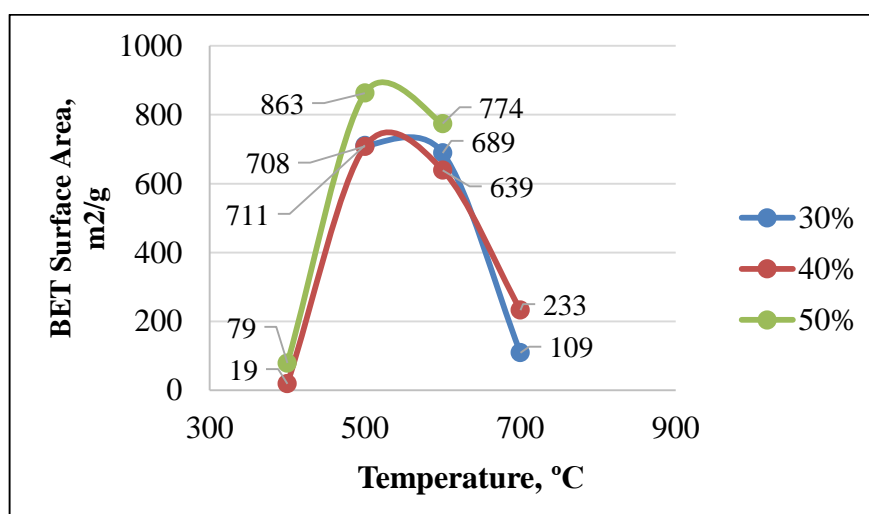


Figure 4.21. The effect of process conditions on BET surface area for FW-based product.

4.7. Influence of Different Process Conditions on Pore Volume

Three products – PC5, PW10, and FW5 – among a total of forty corn and wheat-based products were selected; and other physical characterization methods such as micropore area (S_{micro}), total pore volume (V_T), micropore volume (V_{micro}), mesopore volume (V_{meso}), and average pore diameter (D_p) were carried out. As the BET surface area results for FC-based products were not compatible with literature values, FC-based activated carbon was not chosen for applying other characterization methods. The porosity analysis for produced activated carbon is given in Table 4.30.

The N_2 adsorption/desorption isotherms of these three samples are shown in Figures 4.22, 4.23 and 4.24, which give information about the porous texture of the adsorbent. Isotherm shapes which were originally defined by Brunauer et al. (1943) and classified into five well-known groups (as it was shown in Figure 2.3), show that all products have similar isotherm to Type II. According to Brunauer, this type of isotherm is perhaps the most common isotherm for physical adsorption, and it is most frequently encountered when adsorption occurs on powders with pore diameters larger than micropores. Another way of obtaining information about the porous texture of the solids is to compare the shape of the hysteresis loop (Figure 3.17) with the shape of adsorption and desorption branches of the standard shapes that were originally classified by De Boer (1958). There was a distinct Type II hysteresis loop for adsorption/desorption isotherms, as it can be seen in the isotherm

figures of the samples. According to Gregg and Sign (1982), Type II hysteresis loops might be formed on the complex porous structure with different sizes and shapes.

Table 4.30. Porosity analysis for produced activated carbon.

Product	PC5	PW10	FW5
S_{BET}, m²/g	753	1068	863
S_{micropore}, m²/g	4.08	2.60	-
V_{total}, cm³/g	0.64	0.94	0.77
V_{micro}, mm³/g	4	6.83	-
V_{meso}, cm³/g	0.64	0.93	0.77
Dp, nm	3.66	3.66	3.76

In literature, activated carbon samples have pore volumes ranging from 0.5 to 1 cm³/g (Musatto et al., 2010). In Table 4.31, the pore volumes of PC5, PW10, and FW5 were observed as 0.64, 0.94 and 0.77 cm³/g, respectively. Among the samples, the FW-based sample, impregnated with a 50% H₃PO₄ solution and higher carbonization temperatures (700°C) had higher mesopore volume than that of the other samples. Also, all of the three activated carbon samples had a high amount of mesopore volume, whereas they included a trace amount of micropore volume. Micropore volume values were directly related with the micropore area values. The pore structure distribution in activated carbon is crucial for adsorption of organic molecules with different sizes. The relative proportions of micropores, mesopores, and macropores in activated carbon vary considerably according to the raw material. For example, micropores dominate in a coconut shell-based carbon and constitute 95% of the available internal surface area. In contrast, meso/macropore structures dominate in wood and peat-based carbon; therefore, such carbon types are ideal for the adsorption of large molecules. In accordance with this, they are often used in decolorization processes where the removal of large molecules is of interest. The pore structures of coal-based carbons are somewhere between the coconut shell and wood-derived carbon types. For instance, small organic molecules such as phenol can access micropores. On the other hand, natural organic matter (NOM) found in water supplies can access only mesopores. Bacteria typically have a diameter in the molecular range of 200-2000 nm, and they can access macropores only (Çeçen, 2014). In this context, the activated carbon produced from PC, PW, and FW-

based residue might be conveniently used for decolorization processes and the adsorption of large molecules like natural organic matter, as well as bacteria having large diameter molecules.

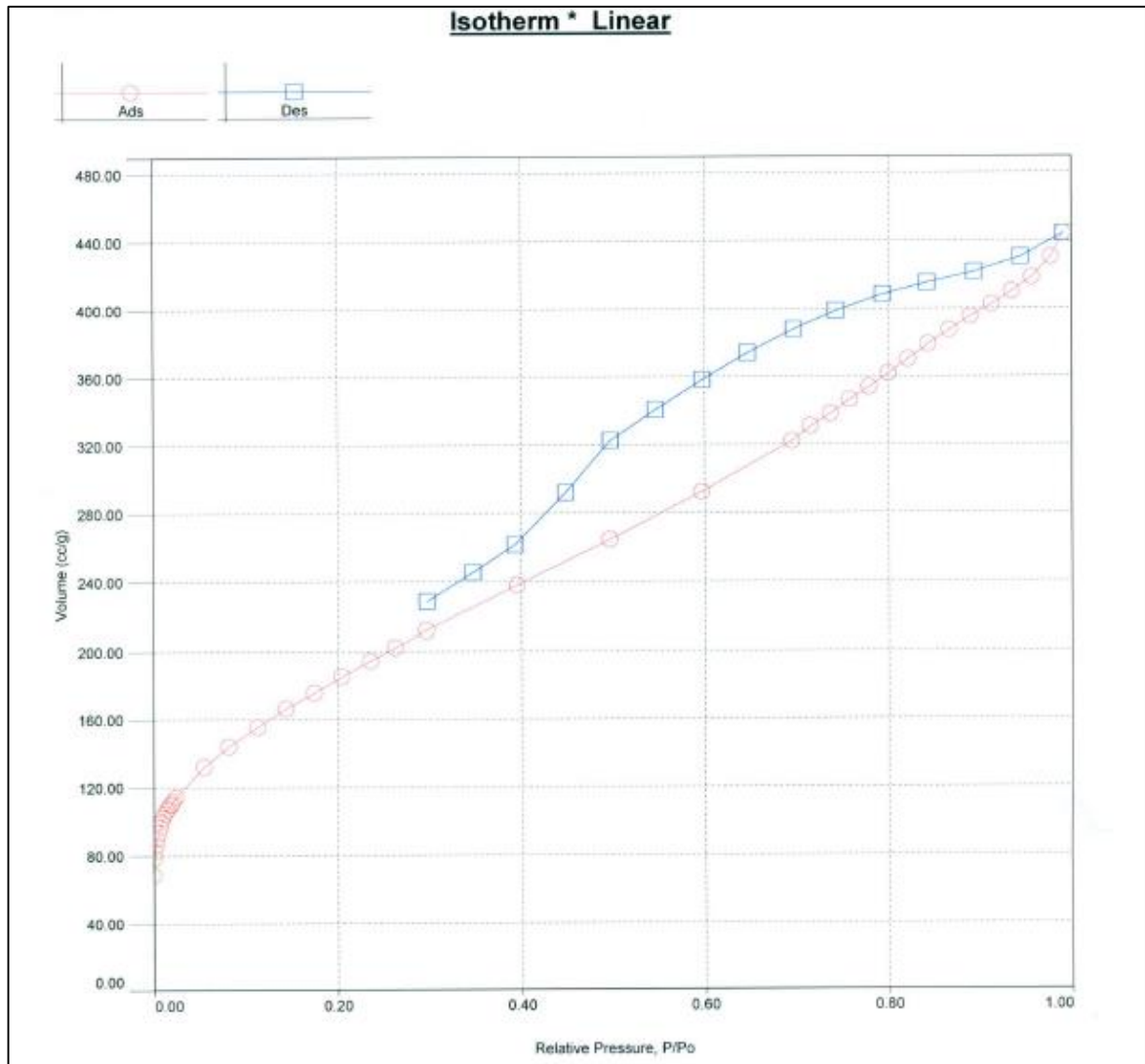


Figure 4.22. N₂ adsorption/desorption isotherms of sample PC5.

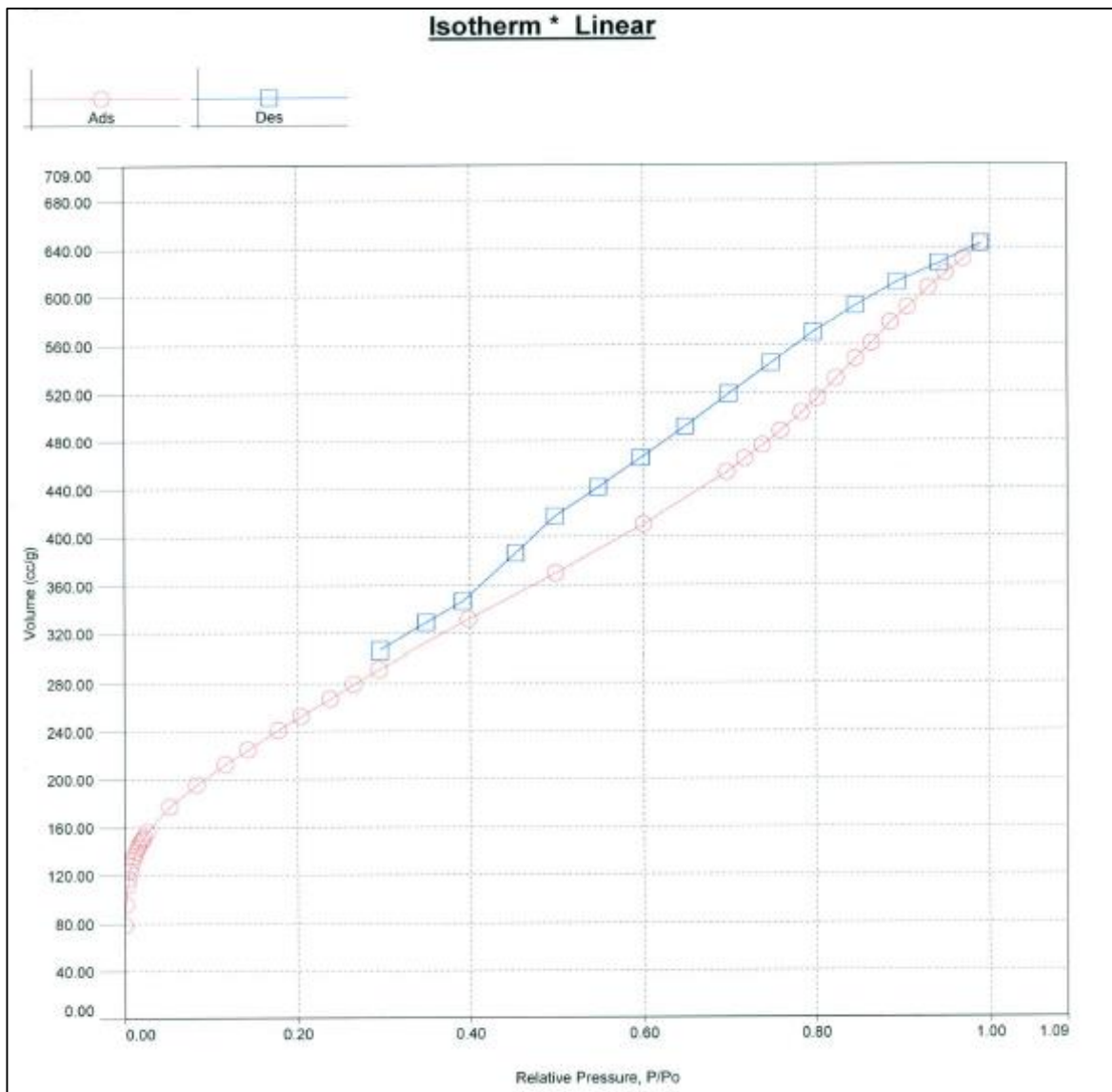


Figure 4.23. N₂ adsorption/desorption isotherms of sample PW10.

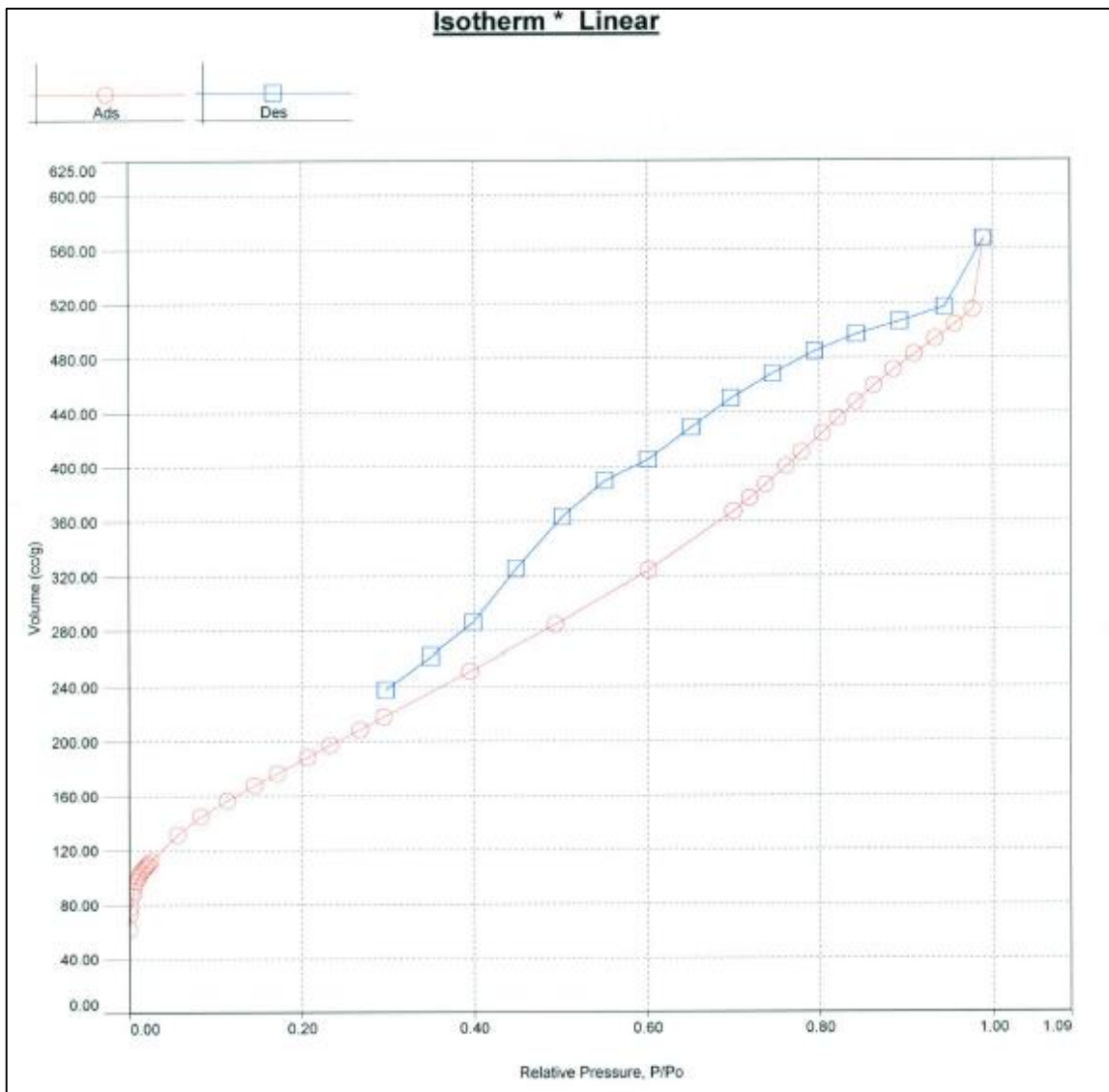


Figure 4.24. N₂ adsorption/desorption isotherms of sample FW5.

5. CONCLUSIONS

In this study, lignin-rich corn stover and wheat straw residues subjected to dilute acid/steam pretreatment processes, as well as saccharification and fermentation processes, were recovered for use as a precursor for activated carbon production. For this purpose, a laboratory-scale pyrolysis system was utilized, and the impacts of feedstock type, chemical impregnation ratio, and carbonization temperature on biochar properties were investigated. This is the first study that has investigated the production of activated carbon as a high value-added product from lignin-rich residues generated from bioethanol processes.

In the first step, different types of feedstock – pretreated corn stover residue (PC), pretreated wheat stover residue (PW), fermented corn stover residue (FC) and fermented wheat straw residue (FW) – were recovered by a dilute acid and alkali pretreatment process. The composition of selected samples was characterized to evaluate the suitability of these feedstocks for production of activated carbon via pyrolysis. In addition to the PC, PW, FC and FW, characterization of raw corn stover (RC) and raw wheat straw (RW) were also evaluated to understand the effects of the delignification process applied to the lignin residues generated from pretreatment and bioethanol fermentation processes. The total ash and volatile solids (VS) content of corn stover was determined as 8.5% and 84.05%, respectively. The RW samples had a lower ash content (4.9%) as compared to the corn stover samples, and the VS content was measured as 88.44%. The moisture content of pretreated and fermented lignin residues increased by 27% and 13% relative to the raw lignocellulosic materials, as the lignin flocs formed by the addition of acid solution had a more viscous structure compared to the raw material. FC and FW samples have high VS contents of 70.64% and 73.85%, respectively. The VS content plays a vital role in estimating the approximate tar content of feedstocks that are volatile and cause dramatic weight loss at carbonization temperatures, in turn decreasing the char yield. PC, PW, FC, and FW samples have high lignin contents – 72.84%, 73.14%, 47.99% and 57.79%, respectively. These results showed that the delignification process has been very effective for pretreated and fermented feedstocks.

In the production of activated carbon, the selected feedstocks were impregnated with 30%, 40% and 50% H_3PO_4 solutions (w/w) and then subjected to heat with a rate of $20^\circ\text{C}/\text{min}$ to the final carbonization temperatures of 400°C , 500°C , 600°C and 700°C at a gas flow rate of $200\text{ mL}/\text{min}$ N_2 . Ten activated carbon samples were obtained for each type of feedstock labelled as PC, PW, FC, and FW. The physical characterization of generated activated carbon samples was investigated according to the char yield, chemical recovery ratio, the pH value, the ash content, the BET surface area and the porosity.

The preliminary experiments showed that a sample impregnated with a low chemical concentration and carbonization temperature does not have a high BET surface area. Similarly, the physical characteristic values of the sample with a high activation ratio and carbonization temperature, which is higher than the temperature range of TGA experiments, was not consistent with the literature values.

In PC-based activated carbon, the yield of the char impregnated with H_3PO_4 dramatically decreased from 37.63% to 20.18% (w/w) with a rise in temperature from 400°C to 700°C . Chemical recovery ratios decreased with increasing temperature and impregnation ratio. The H_3PO_4 recovery rate decreased from 64.21% to 35.6% when the temperature increased from 400°C to 700°C at all impregnation ratios. However, the decline ratios of products impregnated with 50% H_3PO_4 were lower compared to other concentrations. Therefore, a 50% H_3PO_4 concentration was the most suitable activation ratio to produce PC-based activated carbon. In PC-based activated carbon samples, the BET surface area values ranged from 168 to $753\text{ m}^2/\text{g}$. Activated carbon produced at 500°C with 40% and 50% H_3PO_4 concentrations had higher surface area values relative to the others. The BET surface area dramatically decreased with an increase in temperature from 600°C to 700°C ; further, about 60% of H_3PO_4 remained in the carbonized sample, and the yield decreased to 9.5% under these conditions. As a result, the highest BET surface area ($753\text{ m}^2/\text{g}$) and the optimum product yield and chemical recovery were observed in sample PC5, which was impregnated with 50% H_3PO_4 and carbonized at 500°C .

In PW-based activated carbon, the effect of carbonization temperature and H_3PO_4 concentration on yield and chemical recovery was similar to the PC-based products. As the carbonization temperature increased from 400°C to 700°C , the char yield decreased from

51.44% to 28.5% with 50% H₃PO₄. The yield rates of activated carbon impregnated with 40% H₃PO₄ decreased from 41.91% to 29.40% (w/w). Products impregnated with 30% H₃PO₄ had the maximum yield rates. These results were consistent with the literature. Moreover, the H₃PO₄ recovery rate (ranging from 65% to 35%) dramatically decreased when the temperature increased from 400°C to 700°C at each impregnation ratio. However, in products produced from other types of feedstock, H₃PO₄ recovery decreased beyond that seen in the PW-based products. The BET surface area values, which varied from 327 to 1068 m²/g, increased as the temperature increased from 400°C to 700°C at all impregnation ratios. The sample PW10, impregnated with 40% H₃PO₄ and carbonized at 700°C, had the maximum BET surface area of 1068 m²/g, which is the highest amount observed in this study. Activated carbon samples prepared from PW residue had the largest surface areas relative to those of other types of feedstock used in this research. This indicated that PW samples were the most suitable feedstock to produce activated carbon, and the type of feedstock played a crucial role in determining the surface area.

In FC-based activated carbon, yield and C.R. ratios again decreased with increasing temperature. In addition, a lower impregnation ratio resulted in a higher amount of char yield and C.R. ratio. Products obtained from the FC-based residue resulted in a low specific BET surface area (10-402 m²/g) with respect to other types of feedstock under the same conditions. These preliminary results led to the conclusion that FC residue was not a proper precursor for activated carbon production by chemical activation with H₃PO₄.

In FW-based activated carbon, the percentage of the yield and chemical recovery were similar to other types of feedstock under the same experimental conditions. The BET surface area values ranged from 19 to 863 m²/g. Sample FW5, which was impregnated with 50% H₃PO₄ and carbonized at 500°C, had the highest BET surface area of 862.572m²/g. After a temperature of 500°C for all H₃PO₄ concentrations, the BET surface area values showed a gradual three-fold decrease. These results indicated that at temperatures greater than 500°C, H₃PO₄ compounds did not work effectively as activating reagents for FW-based activated carbon processing. As a result, the best conditions to produce FW-based activated carbon with a very high specific surface area are an impregnation ratio of 1.8 and a carbonization temperature of 500°C.

For all types of feedstock, the yield of activated carbon decreased with increasing activation temperature as the weight loss rate increased due to the large amount of volatiles, which can be easily released at a higher temperature. In addition, at each carbonization temperature, the activated carbon yields decreased with increasing impregnation ratio. The H_3PO_4 reacted with the char and volatile matter and diffused quickly out of the surfaces of particles during the process. Therefore, with a high H_3PO_4 content, the pyrolysis of surface carbon atoms became predominant, leading to an increase in weight loss and a low carbon yield. The presence of phosphoric acid during activation promoted the depolymerization, dehydration and redistribution of samples and favored the conversion of aliphatic to aromatic compounds, thus increasing the yield of activated carbon. The chemical recovery of activated carbon also decreased with an increase in carbonization temperature at each impregnation ratio. However, the carbon yield and chemical recovery values of activated carbon samples, produced from PC, PW, FC, and FW residues, show that the selection of H_3PO_4 as an activating agent is a good choice, since the characterization of produced activated carbon is very compatible with the literature and the quality parameters have high values. Nevertheless, the adsorption capacities of the products should be compared according to their specific surface areas and pore volumes.

The pH values of all products were found to be between 4.70 and 5.80; as a result, for each type of feedstock, the pH values were not very acidic as they are higher than 5 with the exception of the pretreated samples which have a pH value lower than 5. This can be explained by the higher ash content of these feedstocks used for the preparation of activated carbon. The carbonization of lignin produces a very small quantity of ash, and thus, this pH value was due to the rather high ash content of pretreated feedstocks. In addition, the quantity of H_3PO_4 used for the activation was influenced slightly by the pH of the activated carbon; however, the results showed that selected H_3PO_4 concentrations for this study were a good choice since low pH values that affect the quality of products were not obtained. It was noted that the activated carbon of selected feedstocks cannot be considered a hazardous waste material and are not corrosive.

The ash contents of PC, PW, FC and FW-based products were in the range of 13.45-16.42%, 11.50-15.15%, 14.524-17.15% and 10.45-16.23%, respectively. However, the ash contents of the products were slightly higher than values of typical activated carbon (between

1% and 12%). In this study, when the carbonization temperature increased, the ash content of the samples increased. Moreover, high ash values may be caused by a high impregnation ratio. Although H_3PO_4 restricted the formation of tar, the high impregnation ratio increased the amount of tar. As a result, it was expected that an increase in the ash content of the samples resulted in higher amounts of tar formation.

The results showed that PC5, PW10, and FW5 carbon products, among a total of forty corn and wheat-based products, have quite high apparent surface areas and optimum yield, ash, and pH values. In the last step, other physical characterization methods such as micropore area (S_{micro}), total pore volume (V_{T}), micropore volume (V_{micro}), mesopore volume (V_{meso}) and average pore diameter (D_p) were carried out for these products. The pore volumes of PC5, PW10, and FW5 were observed as 0.64, 0.94, and 0.77 cm^3/g , respectively. In addition, all three activated carbon samples had a high amount of mesopore volume, whereas they included a trace amount of micropore volume. The same results were shown in the N_2 adsorption/desorption isotherms for these three samples, which were similar to the Type II isotherms defined by Brunauer (1945).

As a consequence, the best way to produce activated carbon from lignin-rich residue is using pretreated wheat-based lignin, impregnated with a 40% H_3PO_4 concentration and carbonized at 700°C. In addition, a pretreated corn-based product that is impregnated with 50% H_3PO_4 and carbonized at 500°C and a fermented corn-based product that is impregnated with 50% H_3PO_4 and carbonized at 500°C are also quite reproducible activated carbon types. Interestingly, mesoporous structures dominate in H_3PO_4 -impregnated lignocellulosic material-based activated carbon. Therefore, these carbons are ideal for the adsorption of large molecules and decolorization.

REFERENCES

Ahmadpour, A., Do, D., 1995. The preparation of active carbons from coal by chemical and physical activation. *Carbon*, 34, 471- 479.

Aktaş, Ö., 1999. Powdered Activated Carbon Addition to Activated Sludge in the Treatment of Landfill Leachate, M.S. Thesis, Boğaziçi University, Institute of Environmental Sciences.

Anaya, A. J. R., Molina, A., Garcia, P., Ruiz-Colorado, A. A., Linares-Solano, A., Salinas-Martinez, C., 2011. Phosphoric acid activation of recalcitrant biomass originated in ethanol production from banana plants. *Biomass and Bioenergy*, 35, 1196- 1204.

Agrawal, R. K., Mc Cluskey, R. J., 1983. The low-pressure pyrolysis of newsprint. *Journal of Applied Polymer Science*, 27, 367-382.

Azadi, P., Inderwildi, O. R., Farnood, R., King, D. A., 2013. Liquid fuels, hydrogen and chemicals from lignin: A critical review. *Renewable and Sustainable Energy Reviews*, 21, 506- 523.

Bagheri, N., Abedi, J., 2009. Preparation of high surface area activated carbon from corn by chemical activation using potassium hydroxide. *Chemical Engineering Research and Design*, 87, 1059- 1064.

Balcı, S., 1992. Kinetics of Activated Carbon Production from Almond Shell, Hazelnut Shell and Beech Wood and Characterization of Products, Ph.D. Thesis, Middle East Technical University, The Graduate School of Natural and Applied Sciences.

Bandsoz, T. J., 2006. *Activated Carbon Surfaces in Environmental Remediation*, Elsevier Inc., U.S.A.

Bansal, R. C., Goyal, M., 2005. *Activated Carbon Adsorption*, Taylor and Francis Imprint, U.S.A.

Başçetinçelik, A., Öztürk, H. H., Karaca, C., Kaçira, M., Ekinci, K., Kaya, D., Baban, A., Güneş, K., Komitti, N., Barnes, I., Nieminen, M., 2005. A guide on exploitation of agricultural residues in Turkey. Project No. LIFE03TCY/TR/000061. European Commission Life Programme, Europe.

Buranov, A. U., Mazza, G., 2008. Lignin in straw of herbaceous crops. *Industrial Crops and Products*, 28, 237- 259.

BP Statistical Review of World Energy Home Page.

<http://www.bp.com/statisticalreview>. (accessed June 2015).

Brunauer, S., 1945. *The Adsorption of Gases and Vapours*, Princeton University Press, U.S.A.

Cardona, C. A., Sanchez, O. J., 2007. Fuel ethanol production: process design trends and integration opportunities. *Bioresource Technology*, 98, 2415- 2457.

Chiou, C. T., 2002. *Partition and adsorption of organic contaminants in environmental systems*, Wiley-Interscience, U.S.A.

Ciliz, N., Daylan, B., Yildirim, H., 2015. Bioethanol production from agricultural wastes for waste minimization and carbon budget analysis. Project No. 110Y261. Scientific and Technical Research Council of Turkey.

Cotana, F., Cavalaglio, G., Nicolina, A., Gelosia, M., Coccia, V., Petrozzia, A., Brinchia, L., 2014. Lignin as co-product of second-generation bioethanol production from ligno-cellulosic biomass. *Energy Procedia*, 45, 52- 60.

Çeçen, F., Aktaş, Ö., 2011. *Activated Carbon for Water and Wastewater Treatment: Integration of Adsorption and Biological Treatment*, Wiley-VCH., ISBN: 978-3-527-32471-2.

Çeçen, F., 2014. Activated Carbon, Kirk-Othmer Encyclopedia of Chemical Technology, John Wiley and Sons, Inc., U.S.A.

Çuhadar, Ç., 2005. Production and Characterization of Activated Carbon from Hazelnut Shell and Hazelnut Husk, M.S. Thesis, Middle East Technical University, The Graduate School of Natural and Applied Sciences.

Dalla Martaa, A., Mancinib, B., Orlando, F., Capecchic, L., Orlandinia, S., 2014. Sweet sorghum for bioethanol production: Crop responses to different water stress levels. *Biomass and Bioenergy*, 64, 211- 219.

Daylan B., 2016. Carbon Balance Assessment for Bioethanol Production from Agricultural Residues, Ph.D. Thesis, Boğaziçi University, Institute of Environmental Sciences.

De Boer, J. H., 1958. *The Structure and Properties of Porous Materials*, Butterworths, U.K.

Dury, S. S. K., 2009. Removal of tar in biomass gasification process using carbon materials. *Chemical Engineering Transactions*, 18, 665- 670.

Fierro, V., Fernandez, T. V., Celzard, A., 2007. Methodical study of the chemical activation of Kraft lignin with KOH and NaOH. *Microporous and Mesoporous Materials*, 101, 419-431.

Foyle, T., Jennings, L., Mulcahy, P., 2007. Compositional analysis of lignocellulosic materials: Evaluation of methods used for sugar analysis of waste paper and straw. *Bioresource Technology*, 98, 3026- 3036.

Girgis, B. S., Daifullah, A. A., 1998. Removal of some substituted phenols by activated carbon obtained from agricultural waste. *Water Resource*, 32, 1169- 1177.

Girgis, B. S., El-Hendawy, A. A., 2002. Porosity development in activated carbons obtained from date pits under chemical activation with phosphoric acid. *Microporous and Mesoporous Materials*, 52, 105- 117.

Gonzalez-Serranoa, E., Corderoa, T., Rodriguez-Mirasola, T. J., Cotorueloa, L., Rodriguez, J. J., 2004. Removal of water pollutants with activated carbons prepared from H₃PO₄ activation of lignin from kraft black liquors. *Water Research*, 38, 3043- 3050.

Gosselink, R. J. A., Jong, E., Guran, B., Abacherli, A., 2004. Co-ordination network for lignin-standardization, production and applications adapted to market requirements (EUROLIGNIN). *Industrial Crops and Products*, 20, 121- 129.

Gosselink, R. J. A., 2011. Lignin as a Renewable Aromatic Resource for the Chemical Industry, Ph.D. Dissertation, Department of Food and Biobased Research, Wageningen University.

Gratiso, M. K. B., Panyathanmaporn, T., Chumnanklang, R. A., Sirinuntawittaya, N., Dutta, A., 2008. Production of activated carbon from coconut shell: Optimization using response surface methodology. *Bioresource Technology*, 99, 4887- 4895.

Gregg, S. J., Sign, K. S. W. (Eds), 1982. Adsorption, Surface and Porosity, Second Ed., New York Academic Press, U.S.A.

Guo, Y., Rockstraw, D. A., 2007. Physicochemical properties of carbons prepared from pecan shell by phosphoric acid activation. *Bioresource Technology*, 98, 1513- 1521.

Gupta, A., Verma, J. P., 2015. Sustainable bioethanol production from agro-residues: a review, *Renewable Sustainable Energy Reviews*, 41, 550- 567.

Hames, B., Ruiz, R., Scarlata, C., Sluiter, A., Sluiter, J., Templeton, D., 2008. Laboratory Analytical Procedure for Preparation of samples for compositional analysis Technical Report, National Renewable Energy Laboratory. NREL/TP-510-42620. Golden, CO. August.

Hayashi, J., Kazehaya, A., Muroyama, K., Watkinson, A. P., 2000. Preparation of activated carbon from lignin by chemical activation, *Carbon*, 38, 1873- 1878.

Holladay, J. E., Bozell, J. J., White, J. F., Johnson, D., 2007. Top Value-Added Chemicals from Biomass Volume II Results of Screening for Potential Candidates from Biorefinery Lignin Report. United States Department of Energy, Oak Ridge, TN. DE-AC05-76RL01830. October.

Hu, Z., Srinivasanb, M. P., Nia, Y., 2001. Novel activation process for preparing highly microporous and mesoporous activated carbons. *Carbon*, 39, 877- 886.

Huijgen, W. J. J., Smit, T., de Wild, P. J., den Uil, H., 2012. Fractionation of wheat straw by prehydrolysis, organosolv delignification and enzymatic hydrolysis for production of sugars and lignin. *Bioresource Technology*, 114, 389– 98.

Ioannidou, O., Zabaniotou, A., 2007. Agricultural residues as precursors for activated carbon production-a review. *Renewable and Sustainable Energy Reviews*, 11, 1966- 2005.

International Energy Agency World Energy Outlook 2013 Home Page.

<http://www.iea.org/>. (accessed March 2015).

Jin, X. J., Yu, M. Z., Wu, Y., 2010. Preparation of activated carbon from lignin obtained by straw pulping by KOH and K₂CO₃ chemical activation. *Cellulose Chemistry and Technology*, 46, 79- 85.

Jung, K. A., Woo, S. H., Lim, S., Park, J. M., 2015. Pyrolytic production of phenolic compounds from the lignin residues of bioethanol processes. *Chemical Engineering Journal*, 259, 107- 116.

Ketcha, J. M., Dina, D. J. D., Ngomo, H. M., Ndi, N. J., 2012. Preparation and characterization of activated carbons obtained from maize cobs by zinc chloride activation. *American Chemical Science Journal* 2, 136- 160.

Kim, S., Dale, B. E., 2004. Global potential bioethanol production from wasted crops and crop residues. *Biomass Bioenergy*, 26, 361- 375.

Kahr, H., Wimbergera, J., Schurza, D., Jagera, A., 2013. Evaluation of the biomass potential for the production of lignocellulosic bioethanol from various agricultural residues in Austria and Worldwide. *Energy Procedia*, 40, 146 - 155.

Liu, Z. S., Wu, X. L., Kida, K., Tang, Y. Q., 2012. Corn stover saccharification with concentrated sulfuric acid: effects of saccharification conditions on sugar recovery and by-product generation. *Bioresource Technology*, 119, 224- 33.

Lozano-Castello, D., 2001. Preparation of activated carbons from Spanish anthracite; Activation by KOH. *Carbon*, 30, 741- 749.

Mansouri, N. E., Yuan, Q., Huang, F., 2011. Alkaline lignins for resins. *BioResource*, 6, 2647- 2662.

Metcalf and Eddy, 1991. *Wastewater Engineering, Treatment, Disposal and Reuse*. McGraw Hill, New York.

Minu, K., Jiby, K., Kishore, V. V. N., 2012. Isolation and purification of lignin and silica from the black liquor generated during the production of bioethanol from rice straw. *Biomass and Bioenergy*, 39, 210- 217.

Montane, D., Torne-Fernandez, V., Fierro, V., 2005. Activated carbons from lignin: Kinetic modeling of the pyrolysis of Kraft lignin activated with phosphoric acid. *Chemical Engineering Journal*, 106, 1- 12.

Mussatto, S. I., Fernandes, M., Rocha, G. J. M., Orfao, J. J. M., Teixeira, J. A., Roberto, I. C., 2010. Production, characterization and application of activated carbon from brewers spent grain lignin. *Bioresource Technology* 101, 2450- 2457.

Nor, N. M., Chung, L. L., Teong, L. K., Mohamed, A. R., 2013. Synthesis of activated carbon from lignocellulosic biomass and its applications in air pollution control: A review. *Journal of Environmental Chemical Engineering*, 1, 658- 666.

Ohgren, K., Bura, R., Saddler, J., Zacchi, G., 2007. Effect of hemicellulose and lignin removal on enzymatic hydrolysis of steam pretreated corn stover. *Bioresource Technology*, 98, 2503- 2510.

Orfao, J. J. M., Antunes, F.J. A., Figueiredo, J. L., 1999. Pyrolysis kinetics of lignocellulosic materials-three independent reactions model. *Fuel*, 78, 349- 358.

Pontius, F. W., 1990. *Water Quality and Treatment*, McGraw-Hill Inc., U.S.A.

Prahas, D., Kartika, Y., Indraswati, N., Ismadji S., 2008. Activated carbon from jackfruit peel waste by H₃PO₄ chemical activation: Pore structure and surface chemistry characterization. *Chemical Engineering Journal*, 140, 32- 42.

Oubagaranadin J. U. K., Murthy, Z. V. P., 2011. Activated Carbons: Classifications, Properties and Applications. In Kwiatkowski, J. F. (Eds.), *Activated Carbon: Classifications, Properties and Applications*, 239- 266, Nova Press, Australia.

Beal, P. T., 1979. Application of Cell Biology to an Understanding of Biological Water. In Drost-Hansen W., Clegg J. S. (Eds.), *Cell Associated Water*, 271- 291, Academic Press, N.Y.

Sarkar, N., Ghosh, S. K., Bannerjee, S., Aikat, K., 2012. Bioethanol production from agricultural wastes: An overview, *Renewable Energy*, 37, 19- 27.

Singh, D., Zeng, J., Laskar, D. D., Deobald, L., Hiscox, W. C., Chen, S., 2011. Investigation of wheat straw biodegradation by *Phanerochaete chrysosporium*. *Biomass and Bioenergy* 35, 1030- 1040.

Sluiter, A., Hames, B., Hyman, D., Payne, C., Ruiz, R., Scarlata, C., Sluiter, J., Templeton, D., Wolfe, J., 2008. Laboratory Analytical Procedure for Determination of total solids in biomass and total dissolved solids in liquid process samples Technical Report. National Renewable Energy Laboratory. NREL/TP-510-42621. Golden, CO. March.

Sluiter, A., Hames, B., Ruiz, R., Scarlata, C., Sluiter, J., Templeton, D., 2008a. Laboratory Analytical Procedure for Determination of Ash in Biomass Technical Report. National Renewable Energy Laboratory. NREL/TP-510-42622. Golden, CO. January.

Sluiter, A., Ruiz, R., Scarlata, C., Sluiter, J., Templeton, D., 2008b. Laboratory Analytical Procedure for Determination of Extractives in Biomass Technical Report. National Renewable Energy Laboratory. NREL/TP-510-42619. Golden, CO. January.

Sluiter, A., Hames, B., Ruiz, R., Scarlata, C., Sluiter, J., Templeton, D., Crocker, D., 2011. Laboratory Analytical Procedure for Determination of Structural Carbohydrates and Lignin in Biomass Technical Report. National Renewable Energy Laboratory. NREL/TP-510-42618. Golden, CO. July.

Suhas, P. J. M., Ribeiro Carrott, M. M. L., 2007. Lignin-from natural adsorbent to activated carbon: A review. *Bioresource Technology*, 98, 2301- 2312.

Tay, T., Ucar, B., Karagöz, S., 2009. Preparation and characterization of activated carbon from waste biomass. *Journal of Hazardous Materials*, 165, 481- 485.

Templeton, D. W., Sluiter, A. D., Hayward, T. K., Hames, B. R., Thomas, S. R., 2009. Assessing corn stover composition and sources of variability via NIRS. *Cellulose*, 16, 621- 639.

Toles, C. A., Marshall, W. E., Johns, M. M., 1997. Granular activated carbons from nutshells for the uptake of metals and organic compounds. *Carbon*, 35, 1407- 1414.

Tsai, W. T., Chang, C. Y., Lee, S. L., 1998. A low cost adsorbent from agricultural waste corncob by $ZnCl_2$ activation. *Bioresource Technology*, 64, 211- 217.

Vishtal, A., Kraslawski, A., 2011. Challenges in industrial applications of technical lignins. *BioResources*, 6, 3547- 3568.

Weber, W. J., 1972. *Physicochemical Process for Water Quality Control*, Wiley-Interscience, New York.

Wolfrum, E. J., Sluiter, A. D., 2009. Improved multivariate calibration models for corn stover feedstock and dilute-acid pretreated corn stover. *Cellulose*, 16, 567- 576.

Wu, Q., Zhang, F., 2012. A clean process for activator recovery during activated carbon production from waste biomass. *Fuel*, 94, 426- 432.

Xu, F., Yu, J., Tesso, T., Dowel, F., Wang, D., 2013. Qualitative and quantitative analysis of lignocellulosic biomass using infrared techniques: A mini-review. *Applied Energy*, 104, 801- 809.

Yağşi, N. U., 2004. *Production and Characterization of Activated Carbon from Apricot Stones*, M.S. Thesis, Middle East Technical University, The Graduate School of Natural and Applied Sciences.

Yahya, M. A., Al-Qodah, Z., Zanariah, C. W., 2015. Agricultural bio-waste materials as potential sustainable precursors used for activated carbon production: A review. *Renewable and Sustainable Energy Reviews*, 46, 218- 235.

Yang, H., Yan, R., Chen, H., Lee, D., H., Zheng, C., 2007. Characteristics of hemicellulose, cellulose and lignin pyrolysis. *Fuel*, 86, 1781- 1788.

Yorgun, S., Yıldız, D., 2015. Preparation and characterization of activated carbons from paulownia wood by chemical activation with H₃PO₄. *Journal of the Taiwan Institute of Chemical Engineers*, 53, 122– 131.

Zanzi, R., Sjöström, K., Björnbom, E., 2002. Rapid pyrolysis of agricultural residues at high temperature. *Biomass Bioenergy*, 23, 357- 366.

Zhu, J., Wan, C., Li, Y., 2010. Enhanced solid-state anaerobic digestion of corn stover by alkaline pretreatment. *Bioresource Technology*, 101, 7523- 7528.